BMPRIA MIMETIC PEPTIDE TREATMENTS FOR BONE AND CARTILAGE FORMATION AND REPAIR

by

Hemanth Akkiraju

A dissertation submitted to the Faculty of the University of Delaware in partial fulfillment of the requirements for the degree of Doctor of Philosophy in Biological Sciences

Summer 2016

BMPRIA MIMETIC PEPTIDE TREATMENTS FOR BONE AND

CARTILAGE FORMATION AND REPAIR

by

Hemanth Akkiraju

Approved: _____

Robin W. Morgan, Ph.D.
Chair of the Department of Biological Sciences

Approved: _____

George H. Watson, Ph.D.
Dean of the College of Arts and Sciences

Approved: _____

Ann L. Ardis, Ph.D.
Senior Vice Provost for Graduate and Professional Education

I certify that I have read this dissertation and that in my opinion it meets the academic and professional standard required by the University as a dissertation for the degree of Doctor of Philosophy.

Signed: _____

Anja G. Nohe, Ph.D.
Professor in charge of dissertation

I certify that I have read this dissertation and that in my opinion it meets the academic and professional standard required by the University as a dissertation for the degree of Doctor of Philosophy.

Signed: _____

Randall L. Duncan, Ph.D.
Member of dissertation committee

I certify that I have read this dissertation and that in my opinion it meets the academic and professional standard required by the University as a dissertation for the degree of Doctor of Philosophy.

Signed: _____

Robert A. Sikes, Ph.D.
Member of dissertation committee

I certify that I have read this dissertation and that in my opinion it meets the academic and professional standard required by the University as a dissertation for the degree of Doctor of Philosophy.

Signed: _____

Catherine B. Kirn-Safran, Ph.D.
Member of dissertation committee

I certify that I have read this dissertation and that in my opinion it meets the academic and professional standard required by the University as a dissertation for the degree of Doctor of Philosophy.

Signed: _____

Xinqiao Jia, Ph.D.
Member of dissertation committee

ACKNOWLEDGMENTS

I would like to express my deepest gratitude to Dr. Anja Nohe for being my advisor and giving me this opportunity to work with her. I still remember as if it was yesterday. I walked into her room as a freshly graduated undergrad, looking for a place to grow my research skills. She took me in without reservation and nurtured my inner abilities, for this I cannot thank you enough. I want to express to my heartfelt gratitude to her for helping me grasp my potential. Her encouraging words really catapulted me to achieve the progress that I did. I thank her for giving me this project and the opportunity to work on others at the same time. That truly taught me the way of project managerial pressures. Thank you again for everything you have given me. It has been a pleasure working with you, and I have grown to be more confident under your guidance. Thank you for giving me the tools to carry the torch forward.

I would like to sincerely thank my committee members for their support and constructive suggestions that helped me prioritize my research goals and achieve them productively. I would like to thank my committee member, Dr. Catherine Kirn-Safran, and her former student Dr. Padma Srinivasan who helped me immensely, without which my project would not have progressed. I thank Dr.Safran, for constant suggestions that helped my project tremendously and also her help in providing me the materials I needed for my project. I would like to thank my committee member Dr. Xinqiao Jia, and her

former student Dr. Xian Xu for giving me the support and the materials that I needed at any time without hesitation to test for my project.

I would like to thank my committee member Dr. Robert Sikes, who is been there since the beginning pushing me the right way to ask the right questions for my project. I thank him for his constructive criticism and the support he has given me to the progression of my project. I really had fun from our talks. He is a true inspiration and my fitness role model.

I would like to thank my committee member Dr. Randall Duncan, for the motivation and inspiration he has given me to think like a researcher. His words of wisdom and comfort truly resonated throughout my journey as a graduate student. Thank you for making me ask the right questions. I truly enjoyed every conversation we had, and all the research talks. Your care for students like me is something that I cannot express lightly. His energy and enthusiasm is very inspiring.

I would like to thank Dr. Melinda Duncan, who from the get go kept an eye on me and pushed me to get my things done. I thank her for helping me through this process. Even though we did not have many conversations, everyone one of them made a difference in my life. Most of all I thank her for helping me finish what I have started. Thank you again for everything.

I would like to thank Dr. Liyun Wang and her lab members for assisting me with the instrumentation. I would like to thank Dr. Christopher Price, for providing me with all the protocols and sound advices for histological work. I would like to thank Michael Moore, and Dr. Jeffrey Caplan from the Delaware Biotechnology Institute for helping

me with the imaging setups. I would like to thank Mike for his support in setting up the imaging for SHG.

I would like to thank Dr. Deni Galileo, for allowing me to use his equipment whenever I needed them. Also, I would like to thank Dr.Sonali Barwe for allowing me to utilize the instruments in Nemours. Without them it would not have been possible to get the work done.

I would like to thank Betty Cowgill, who has been a pillar of support for all the administrative processes that I needed to do. She has really taken care of everything without a hitch, without I would have been lost. I would also like to thank her for being a very good friend that listened to my problems no matter what time it was. I would like to thank James Farmer and Jamie for all their work in setting up our lab. They have been crucial for my experimental setups.

I would like to thank my past and present lab members for giving me a wonderful time through out these years. I would like to thank Dr. Beth Bragdon from whom I learned a lot from. She has set the bar high and I can only hope I can reach those standards. I would like to thank Jeremy Bonor, who has been as a good friend over these years and helped me through the most critical times. I would also like to thank all the current lab members who gave constant support and joy to work with.

I would like to also thank Gina, for bringing so much joy into my life. Your curiosity for life and science is truly contagious and you have treated me as your own son. This is something I can never forget, I hope this continues for many more years.

I would like to thank Dr. Padma Srinivasan, who not only helped me with the animal surgeries, but also gave me the comfort in times when I needed motivation. Thank you for being a good friend and a well-wisher. Without your guidance I know I would not have achieved what I did today. It is a joy playing with Arya, and I hope to see him grow up.

I would like to thank Archana Siddam and her husband Lakshmi who has been like family. I like to thank Lakshmi for all the valuable words he has given me, that really helped me through tough times. I would like to thank Archana for all the good times we had, I can never forget our bickering and laughter and joy all in one conversation. You really are my big sister. From the day that we met, till now things have not changed and that is something I will cherish alot. I hope our friendship continues for many years to come. I would also like to thank Dr. Mallika Pathania for giving me sound advice when I need it the most. It was joy seeing Garv grow up.

I would like to thank my friends here at UD for whom I am extremely thankful to each and everyone one for making my life at UD memorable. I have grown personally and professionally with all your help along the way. The batch of friends I came in with be it “Batata warriors” or the “Guys Group” truly gave me a family away from my family. I am extremely grateful for having such close friends for all the good times and all of the support you all have given me when I needed it the most.

I will need to specially thank Dr. Aasma Khan and Dr. Sona Lakshme Balasubramaniam for their friendship. I thank you for being there professionally and personally when I needed you both the most. Being there through thick and thin it has

been a joy to have come to UD just to meet you two. If it is not for Sona and Aasma my professional growth would not have progressed. I need to thank Aasma for critically analyzing my work through these years, and I would like to thank Sona for helping me with all my trouble shootings and for the amount of work she put in for my research helping me every step of the way. I also need to thank them for being patient with me. Thank you, I hope this continues for life.

I would also need to thank Devesh Radhakrishnan who has been a confidant and also my mentor. I am very grateful for the life lessons I have learnt in your guidance. He has truly nurtured me professionally and brought out the best in me. I will miss all of the gym sessions. I would also need to thank Soma Dash. She has been a great inspiration for me, against all odds she taught me to run with the situations rather than fighting against them and helped me challenge my own abilities as a researcher. Thank you for always being there, your addition to the group had tremendously helped us, more than you know.

I cannot but thank Adithya boddu, Dr. Vimal Gangadharan, Dr. Praveen Chandar, Dr. Vignesh Viswanathan, Sai Siddharth, Dr. Pratima Patil, Srinivas Rao Chintala, for having been my closest of friends. I cannot imagine my graduate life without you guys in all good and bad times you guys have been there. I would like to thank Boddu for truly being there in times of need and for all the fun times we had. I would like to thank Vimal, your words “If you can think you can solve” I still follow today, thank you always giving me the advice I needed. Srinivas, I would like to thank you for making these past 4 years most pleasurable, I truly enjoyed every single day

with your presence. Thank you all for making me your family. I hope this continues forever.

I would like to thank Gautham Ravichandran, who is my closest friend, whom without I would not be here today. He has truly pulled me out of some real tough problems. I do not have the words to thank you for your compassion and your friendship. I would like to thank Avanti Challa for being my closest friend and also for putting up with me. I cannot imagine my days without you or Gautham. You two are my friends and family for life.

I would like to thank my family. I would like to thank my father and mother for making many sacrifices that allowed me and my brother to be where we are today. They are my pillars of support, and strength. I would not be here and I would not be me if it is not for you both. You both are my inspiration and your motivation is what drives my success in life. Thank you for nurturing my interest for science and for the liberty to choose my life as I wanted and supporting my every decision. I hope I will keep making you proud. I would like to thank my new family member Anusha. Thank you for being a part of my life. I hope I will make you proud as well, and I thank you for giving me a family, for which I am forever happy for.

TABLE OF CONTENTS

LIST OF FIGURES

ABSTRACT

Osteoporosis and osteoarthritis, are two most common skeletal disorders that are idiopathic in nature. Osteoporosis is characterized by excessive bone resorption and inadequate formation of bone resulting in skeletal fragility. Osteoarthritis (OA) is characterized by degradation of articular cartilage (AC) that surrounds the diarthrodial joints followed by the formation of osteophytes that calcification of cartilaginous tissue. While there are pharmacotherapeutics today that can slow the progress of bone loss due to osteoporosis induced bone loss, the long term effects are not effective and atypical fractures are commonly observed (Schilcher et al., 2014). In OA there is no drug today that can slow the progression of the disease nor help regenerate the lost cartilage. Therefore, there is a dire need for research to find effective targets for pharmacological development that can slow the process of disease progression and also regenerate the lost tissue. It is beneficial to exploit the basic molecular mechanisms that control the overall tissue generation to identify therapeutic targets. Growth factors greatly influence the process of bone and cartilage formation. Among the growth factors Bone Morphogenetic Proteins (BMPs) are essential for formation and maintenance of long bones and AC.

Among BMPs, BMP2 is important for embryogenesis, development, and maintenance of adult tissue homeostasis (Wang et al., 2014). BMP2 is a potent growth

factor that is essential for limb patterning and proper bone and cartilage formation. BMP2 is present in all stages of chondrocyte development and also regulates osteoblastogenesis and indirectly osteoclastogenesis. BMP2 is pleiotropic in nature and influence many bodily functions. In musculoskeletal disorders such as osteoporosis or OA, BMP2 plays varied roles contributing to the progression of the diseases. In osteoporosis, the BMP2 effect of osteoblastogenesis is reduced but increases osteoclastogenesis and adipogenesis (Donoso et al., 2015; Itoh et al., 2001). In OA increased physiological levels of BMP2 induce chondrocyte hypertrophy and cartilage degradation followed by subchondral bone alterations and osteophyte formation (van der Kraan et al., 2010). BMP2 and BMP7 are approved by the FDA for bone fracture healing and are also in consideration for osteoporotic and osteoarthritic therapy. However, as mentioned earlier BMP2 can elicit both anabolic and catabolic activities. Therefore, by targeting these specific signaling mechanisms can help us in therapeutic development.

Nohe has demonstrated previously a novel Bone Morphogenetic Protein Receptor Type Ia (BMPRIa) interaction with Casein Kinase 2 (CK2) (Bragdon et al., 2010). It is demonstrated that upon BMP2 binding to the serine/threonine kinase receptor complex CK2 dissociates from BMPRIa allowing the phosphorylation of downstream signals (Bragdon et al., 2010). Using prosite search Nohe lab has identified three potential BMPRIa CK2 interaction sites. Nohe lab has developed three mimetic peptides (CK2.3, CK2.2, and CK2.1) that encompass the site specific sequences that could block the interaction of CK2 with BMPRIa. In this study I investigated the

potential of the peptides CK2.3, and CK2.1 in activating BMPRIa downstream signaling for inducing bone and cartilage formation respectively. Nohe lab previously demonstrated the effect of CK2.3 in osteogenesis and bone formation in mice calvaria (Bragdon et al., 2011b). In this study I examined the effect of CK2.3 in trabecular bone formation (Akkiraju et al., 2015). Where CK2.3 induced trabecular bone growth by inducing osteoblastogenesis and inhibiting osteoclastogenesis and osteoclast activity as compared to BMP2 that activated both osteoblast and osteoclast activity.

Moreover, I demonstrated here CK2.1 induced chondrogenesis but not osteogenesis *in vitro* by activating the BMPRIa downstream signaling and cartilage formation and cartilage repair *in vivo*. Peptide CK2.1 induced chondrogenesis in mesenchymal stem cells (MSC) and demonstrated positive chondrogenic differentiation and extracellular matrix (ECM) secretion without the induction of chondrocyte hypertrophy both *in vitro* and *in vivo*. CK2.1 induced chondrogenic regulation resulted in positive secretion of collagen type II and collagen type IX formation without collagen type X (hypertrophic marker). In mice, CK2.1 systemic injections lead to increased cartilage formation in a similar capacity as BMP2. Furthermore, in an OA mice model that underwent Destabilization of Medial Meniscus (DMM) that AC damage through secondary injury was injected intra-articularly with slow release system of CK2.1 conjugated with hyaluronic acid based gels (HGPs). This HGP-CK2.1 intra-articular injections completely restored the lost cartilage comparable to SHAM treated mice. Moreover, both systemic treatments and DMM mice femurs injected with CK2.1 demonstrated proteoglycan secretion and collagen type II and collagen type IX but not

collagen type X. This is in sharp contrast with the systemic BMP2 injected group that demonstrated up regulation of collagen type II and also collagen type X thereby enhancing chondrocyte hypertrophy. Peptide CK2.3 specifically induced osteogenesis in MSCs and bone formation in similar capacity to BMP2 treatments in mice without activating osteoclastogenesis as did BMP2 treatment. Similarly, CK2.1 induced specifically chondrogenesis and cartilage formation and repair without inducing chondrocyte hypertrophy or cartilage degradation. Both peptides CK2.3 and CK2.1 may specifically regulate BMPRIa downstream signaling for bone and cartilage formation respectively. Understanding these signaling cascades can help identify the molecular targets necessary for inducing bone and cartilage growth. In this study I have successfully demonstrated the potential of peptide CK2.3 in bone formation and peptide CK2.1 in cartilage formation and cartilage repair. Taken together, these peptides present a unique opportunity for identifying the therapeutic targets that can used for treating bone and cartilage disorders like osteoporosis or OA.

Chapter 1

INTRODUCTION

1.1 Function and Structure of Bone

Bone is a dynamic tissue that is rigid and forms the skeleton of the body. Bones support and protect the various organs of the body. Bones play an important role in brain, heart and lung functions, locomotion, support of haematopoiesis in the bone marrow, storage of minerals (i.e. calcium, phosphate) and providing attachment to muscles (Proff and Romer, 2009). The tissue is largely comprised of organic and inorganic components. Organic components consist of collagen type I amounting to about 90% of total bone protein, the rest composing of non-structural proteins like growth factors, blood protein, osteonectin and osteocalcin. The inorganic components of bone are mainly composed of mineral hydroxyapatite ($Ca_{10}(PO_4)_6(OH)_2$). These organic and inorganic materials together form the flexible character as well as compressive strength (Proff and Romer, 2009).

1.1.1 Bone Formation

Bone formation is specially controlled by the bone cells namely; osteoblast (form the bone matrix), osteoclast (resorb the bone) and osteocytes (bones endocrine system that regulates bone formation). Skeleton is generated from three distinct lineages. Namely somites that generate the axial skeleton, lateral mesoderm that

generate the limb skeleton, and the cranial neural crest gives rise to the craniofacial bones and cartilage (Kobayashi and Kronenberg, 2014). There are two major modes of bone formation; intramembranous ossification that is the direct bone formation from mesenchymal tissue, a process that results in formation of the skull. Alternatively, long bones form through endochondral ossification; where the mesenchymal cells differentiate into chondrocytes that make the hyaline cartilage, later replaced by bone formed by the bone cell infiltration. In this study I focused on the long bones specifically the femurs that develop through endochondral ossification.

1.1.2 Endochondral Ossification

Multiple steps are involved in long bone formation through endochondral ossification. Starting with cartilage tissue is formation and later replaced by bone (Price et al., 1994). Initiated by mesenchymal cells commitment to chondrocytes. Mesenchymal cells condense into compact nodules in the presence of N-Cadherin and N-CAM and differentiate into the prechondrocytes (Hall and Miyake, 1995; Oberlender and Tuan, 1994). Transcriptional regulator *SOX9* gene is known to be highly expressed in these precartilagenous condensations. It is shown that mutations in *SOX9* gene cause camptomelic dysplasia, a rare skeletal disorder that results in the deformities of most skeletal bones in the body (Wright et al., 1995). Upon MSC differentiation to chondrocytes they proliferate and divide and secrete the cartilage specific extracellular matrix (ECM) Followed by terminal differentiation of chondrocytes (hypertrophic chondrocytes). These hypertrophic chondrocytes die and leave spaces for

vascularization and bone marrow formation. In this region MSCs differentiate into osteoblasts allowing for the formation of bone matrix and formation of the bone tissue (Bruder and Caplan, 1989; Hatori et al., 1995). Long bone formation through endochondral ossification starts with 1) collar formation: periosteum forms around a piece of hyaline cartilage, where differentiated osteoblasts lay bone matrix and mineralize the tissue forming a bony collar. 2) Cavity formation: A primary ossification center is formed in the center of the cartilaginous tissue. Calcification and hardening of the center impedes nutrient supply to the cartilage leading cellular death and allow cavity formation. 3) Vascular invasion: inner cavity containing many hole is invaded by nutrient rich foramen. In this are many components enter through the nutrient foramen such as nerves, lymphatics, osteoclasts, osteoblasts etc. Remaining cartilage is broken down by osteoclasts and the osteoblasts secrete their osteoid forming trabeculae (spongy bone). 4) Elongation: Continual invasion of osteoclasts, and osteocytes allow for the elongation of the bone shaft (diaphysis). Therefore, the hollow inner cavity or medullary cavity is formed as the diaphysis elongates. Elongation ends into the epiphysis where the vasculature ends and the hyaline cartilage begins called the secondary ossification center. 5) Epiphyseal ossification: formation of spongy bone is done in this region same as previously explained. Here the hyaline cartilage is left on the ends of the bones (Articular cartilage) and the epiphyseal growth plates are formed (figure 1.1).

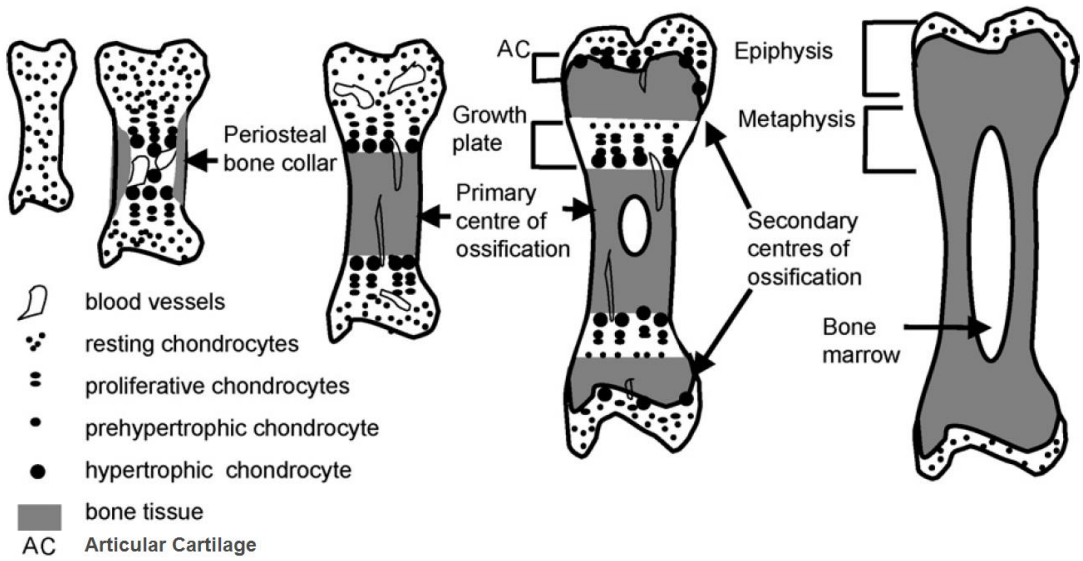

Figure 1.1 **Development of long bones through Endochondral ossification.** Endochondral ossification is one of the two essential processes during fetal development of the mammalian skeletal system. Cartilage is replaced by cancellous bone forming the primary ossification center. Followed by vascularization of the medullary cavity forming the secondary ossification center separating diaphysis and the growth plate. Image was modified from (Mackie et al., 2008)

1.1.3 Osteoblast and bone formation

Osteoblasts are bone forming cells that are known to form bone tissue by secreting alkaline phosphatase (ALP), Osteocalcin, collagen type I, proteoglycans, bone sialoprotein (BSP), and osteopontin other matrix proteins. Osteoblasts are found in clusters along the bone surface where they produce bone matrix by depositing collagen type I. Subsequently, collagen matrix becomes mineralized, presumably through the ALP activity. Although ALP activity in bone formation is less clear, it is commonly involved in bone mineralization process (Wennberg et al., 2000). Osteoblasts, besides their role in bone formation are also involved in osteoclast differentiation as they produce receptor activator of nuclear factor κ-B ligand (RANKL) or Osteoprotegerin

(OPG) to modulate osteoclast activity (Takahashi et al., 1999; Udagawa et al., 1999). Osteoblast cells originate from pluripotent MSCs of the bone marrow (Katagiri and Takahashi, 2002). A number of transcription factors and biochemical factors tightly regulate osteoblast recruitment, function and maturation. Osteoblast differentiation is controlled by the secretion of lipid-modified glycoproteins of the wingless (Wnt) family, BMP2 and several other transcription factors. BMP signaling is among the many important signaling pathways that induce osteoblastogenesis and produce essential transcription factors such as runt-related transcription factor 2 (RUNX2) and Osterix. BMPs found in bone influence MSCs commitment to osteoblasts that express specific proteins, such as ALP, Osteocalcin, and the osteogenic transcription factor RUNX2 (Katagiri and Takahashi, 2002; Katagiri et al., 1994).

1.1.4 Osteoclasts and bone resorption

Osteoclasts are multi-nucleated cells specialized in bone resorption. Osteoclast differentiation involves recruitment and dissemination of osteoclast progenitors from hematopoietic monocyte-macrophage lineage (Kurihara et al., 1989; Proff and Romer, 2009). This osteoclast activity is dependent on two cytokines; macrophage colony stimulation factor (M-CSF) and RANKL and calciotropic hormones (Katagiri and Takahashi, 2002; Teitelbaum, 2000). M-CSF binds to the receptor c-fms on the surface of the osteoclast progenitor and thereby provides the signals required for proliferation (Teitelbaum, 2000). Furthermore, M-CSF enhances osteoclast activity and osteoclast survival by preventing apoptosis (Glantschnig et al., 2003; Roodman, 2006). RANKL

is expressed on the surface of osteoblast stromal cells. Differentiation of osteoclasts by RANKL is achieved by cell-cell interaction between osteoblasts and osteoclasts (Datta et al., 2008; Kostenuik, 2005; Teitelbaum, 2000). Membrane bound RANKL is taken by the osteoclast surface RANK receptor as a crucial factor for osteoclast differentiation. Another cytokine that is expressed by osteoblasts is osteoprotegrin (OPG). OPG competes with RANKL binding to RANK receptor to inhibit osteoclastogenesis (Simonet et al., 1997; Yasuda et al., 1998). It is thus assumed that the concentration differences between RANKL and OPG regulate bone resorption and bone strength (Kostenuik, 2005).

Bone resorption is initiated with the migration of osteoclasts onto the bone surface and this adhering to the area of the bone to be remodeled. Osteoclast contact of the bone matrix is polarized with plasma membrane forming three distinct areas: the basolateral membrane, which is not in contact with bone matrix, the zone sealed and tightly attached to the bone, and finally the ruffled border which is ring-shaped and surrounded by the sealing zone. The ruffled border is in direct contact with the bone sealing the areas thereby forming a diffusion barrier to ensure defined proton and protease concentration secreted by the ruffled border in the evolving resorption lacunae underneath the osteoclast (Vaananen and Laitala-Leinonen, 2008). Osteoclasts are capable of dissolving bone material like hydroxyapatite, by secretion of hydrochloric acid. A V-type ATPase pump present in the ruffled membrane of osteoclasts, translocates protons into the resorption lacuna acidifying the environment below pH 4.5

and a carbonic anhydrase II is present in osteoclasts to supply protons. Once the bone material is demineralized the organic phase of bone is more accessible. Bone turnover is a complex process influenced by mutual actions of the osteoblasts and osteoclasts that provide the strength to withstand mechanical forces. An imbalance between these processes leads to bone diseases like osteopetrosis or osteoporosis to name a few. These imbalances can be caused by myriad of reasons and the differences in the signaling pathways can alter the course of bone remodeling. Understanding these molecular and biochemical mechanisms in bone maintenance, stability and integrity ensures and proper strategies for therapeutic development for bone metabolic disorders.

1.1.5 Bone remodeling

Bone is a metabolically active tissue that undergoes continuous remodeling to maintain its stability and integrity. About 10% of bone is renewed each year (Lerner, 2006). Bone remodeling is a complex process that involves bone resorption performed by osteoclasts, followed by bone formation carried out by osteoblasts. This remodeling cycle involves in these sequential steps; resorption, reversal and formation (Hadjidakis and Androulakis, 2006; Hill, 1998) (figure 1.2). Osteoclasts activity occurs in small cortical and trabecular bone covering areas, where the remodeling process occurs. In these sites, osteoclastogenesis comes first with the expression of nuclear factor κ B ligand (RANKL) by bone lining cells, binding to RANK that exists as a surface receptor on the membrane of pre-osteoclasts. Binding of RANK to RANKL initiates the activation of signaling cascades for the osteoclast commitment (Wada et al., 2006). In

the resorption stage, several chemokines or chemotactic cytokines are secreted by stromal cells or bone lining cells that attract and stimulate the recruitment of osteoclast precursors and allow for bone resorption. Along with the osteoblasts, osteocytes also influence bone remodeling. Osteocytes, in bone embedded are proposed to sense microcracks and microfractures triggering the subsequent osteoclast differentiation and bone resorption (Bonewald, 2007a; Bonewald, 2007b; Matsuo and Irie, 2008). Further resorption is carried out by the fully differentiated osteoclasts that resorb bone forming pits, during this process allows proteins like Bone Morphogenetic Proteins (BMP) and insulin-like growth factor-1 (IGF-1) to influence mesenchymal stem cells (MSCs) commitment to osteoblasts that reverse the process of bone resorption to bone formation (Matsuo and Irie, 2008). Osteoblasts lay down new bone in the pits formed by the osteoclasts, by mineral deposition on the newly formed matrix replacing the old bone completely (Figure 1.2) (Hill, 1998). An imbalance in this process can lead to progressive disorders as osteoporosis, where bone loss exceeds bone formation for various reasons that are otherwise idiopathic in nature.

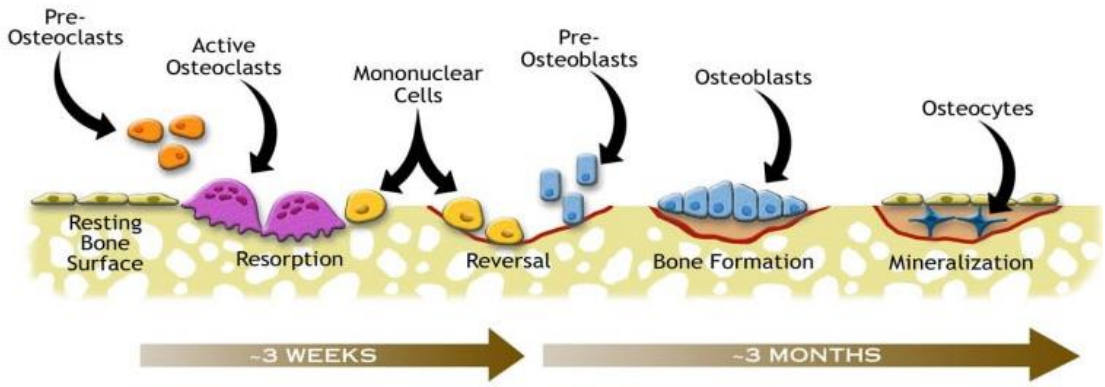

Figure 1.2 **Bone remodeling. Cycles consists of three phases.** 1) Bone resorption phases taking place is short and occurs in about 3 weeks, where pre-osteoclasts differentiate in the presence of M-CSF and RANKL to become active osteoclast releasing hydrolytic enzymes that resorb the bone. 2) Reversal, where pre-osteoblasts differentiation into osteoblast and lay new bone matrix in the pits where osteoclasts resorbed. 3) Bone formation phase could take up to 3 months, where the new matrix is mineralized and resulting osteoblasts terminally differentiate and are embedded into the matrix as osteocytes. Image adapted from (http://ns.umich.edu/Releases/2005/Feb05/bone.html)

1.2 Osteoporosis

Osteoporosis is an idiopathic degenerative bone disease that leads to the loss of bone. Imbalance between osteoblast and osteoclast activity cause osteoporosis. Bone matrix remodeling is a dynamic process where 10% of all bone mass is replaced per year. This process of takes place in multicellular units (BMUs) was first describes by Frost & others in 1963 (Hattner and Frost, 1963). Osteoclasts assist the bone degradation, while osteoblasts rebuild the bone matrix. Low bone density usually occurs when their osteoclasts degrade the bone matrix faster than osteoblast can mineralize the matrix making the tissue brittle and susceptible for fractures. Osteoporosis can be

caused due to either of these factors; type 1 osteoporosis the more common type is due to age-related loss of bone, commonly observed in postmenopausal women due to estrogen deficiency. Type 2 or senile osteoporosis occurs in women and men due to vitamin D_3 deficiency resulting in excessive bone resorption but not bone formation, and type 3 or secondary osteoporosis caused by product of long term progression of other diseases or drug therapy.

1.2.1 Pathogenesis of osteoporosis

Excessive bone resorption and inadequate formation of bone results in skeletal fragility. Therefore, it is essential to understand this process in order to isolate the underlying mechanisms for controlling the processes necessary for bone growth. Trabecular bone, in comparison to cortical, undergoes larger remodeling when considering number of BMUs per square centimeter. However, in cortical bone the process is slower as this bone resorption has to consider large structural entities such as the Haversian canal systems on cortical structures (Raisz, 2005). Resorption phase of bone is short. However, the period required for osteoblast mediated bone formation or replacement of the bone is a long process. Any increase in the rate of bone remodeling will results in loss of bone mass (Raisz, 2005). Excessive resorption can result in a complete loss of trabecular structures. There are many ways that invigorates osteoclastic resorption. However, also to note that high rates of resorption may not always associate with bone loss; like pubertal growth that usually includes excess bone turnover.

Therefore, an inadequate formation response during remodeling is a critical component of the pathogenesis of osteoporosis.

Postmenopausal women who suffer from lowered estrogen levels are at the greatest risk of developing osteoporosis. In mechanical loading studies it has been shown that estrogen deficient bone had the least bone formation (Lee et al., 2003). . Also to be considered is the rate of osteoblast induced RANKL and OPG production inducing osteoclast activity (Suda et al., 1999). It is shown that OPG knockout in mice lead to increased bone loss and severe osteoporosis, conversely RANKL knockout mice suffered from osteopetrosis (Bucay et al., 1998). Previous study confirmed an increase in RANKL levels in estrogen deficient postmenopausal women (Bekker et al., 2004). While OPG deficiency has not been linked to pathogenesis of osteoporosis, it has been shown that T cell production may play a role in the increase in RANKL levels in pathologic states thereby contributing to osteoporosis related bone loss (Weitzmann et al., 2001). Many possible factors including abnormalities of cytokine and growth factor signaling such as that of Wnt, BMP, TGFβ, IGF-1 and FGF signaling cascades have been shown to induce accelerated bone loss in osteoporosis (Canalis, 2013; Chung et al., 2003; Fromigue et al., 2004; Lodewyckx and Lories, 2009; Miyazono et al., 2001; Moerman et al., 2004).

1.2.2 Osteoporosis therapeutics

Osteoporosis is a serious public health concern being a worldwide epidemic. Currently it is estimated that 200 million people worldwide suffer from the disease.

Approximately 30% of all postmenopausal women have osteoporosis in the United State and in Europe. At least 40% of these women and 15-30% of men will sustain osteoporosis induced fracture in their lifetime (http://www.iofbonehealth.org/epidemiology). Patients with a history of fractures have a 2-3-fold increased risk of hip fracture. By 2050, there is an estimated 240% increase of fractures in women and 310% in men worldwide. Many therapies have been introduced into the market ranging from bisphosphonates, Selective Estrogen Receptor Modulators (SERMS) and intermittent PTH therapy combined with bisphosphonates (Marie and Kassem, 2011). However, along with being expensive these drugs can cause side effects like osteonecrosis or osteosarcoma that are life threatening in the long term (Bilezikian, 2006). Bisphosphonates inhibit osteoclasts that accelerate bone loss; however, long term use has been shown to cause negative osteonecrosis and further accelerates the process of bone loss (Bilezikian, 2006). SERMS target estrogen receptors, by binding with high affinity to the estrogen receptor prevents osteoclast maturation and inhibiting overall bone loss. Intermittent PTH dosing was shown to increase bone formation within a two-year period, however long term dosing has proven to be ineffective and also a potential cause of osteosarcoma (Broadhead et al., 2011; Yamaguchi et al., 1987). Over the years BMP2 and BMP7 have been studied in preclinical trials for their effectiveness in bone formation (Rosen, 2008) and have been successfully approved by the FDA for spinal fusions and long bone fracture repair (Marcus R, 2008) (www.FDA.gov). The possibilities of BMP2 treatments for osteoporosis related bone fracture are in consideration due to its efficacy in long bone

fracture healing and are being researched in animal studies showing elevated levels for osteoblast activity for overall bone formation (Falahati-Nini et al., 2000; Khosla et al., 2008; Li, 2008; Marcus R, 2008; Rosen, 2008). A major drawback however is the large dosages (1.5mg/ml) required for the treatment. It has been shown that BMP2 directly enhances osteoclast differentiation and osteoclast activity (Jensen et al., 2010). Therefore, BMP2 treatments in the long run may lead to the accelerated bone loss due to BMP2 induced osteoclast activity (Itoh et al., 2001). Therefore, there is a great necessity to identify the underlying signaling factors that contribute to osteoblast differentiation and activation and also the mechanisms underlying osteoclast differentiation and activity.

1.3 Cartilage

Cartilage is an avascular strong flexible connective tissue that surrounds the joints between the bones, rib cage, ear, nose and also the intervertebral discs. Cartilage contains a gelatinous substance called chondroitin sulfate. There are three types of cartilage; hyaline, elastic, and fibrocartilage (http://www.ivyroses.com/HumanBody/Tissue/Tissue_Cartilage-Tissue.php). Elastic cartilage is the cartilaginous tissue that is found in the pharyngotympanic tubes, epiglottis, and ear lobes. Fibrocartilage is the type of cartilaginous tissue that is spongy in nature with collagen bundles providing elasticity and flexibility and serves as an excellent shock absorber, commonly found in pubic symphysis and intervertebral disks. The most abundant cartilage is hyaline cartilage that is found as the main substance in

nose, ears, trachea, larynx, and surrounding the diarthrodial joints as well as intervertebral discs. Hyaline cartilage that surrounds the Articular Cartilage (AC) serves to reduce the friction by creating a smooth viscoelastic surface between the joints (Poole, 1997). This particular type of cartilage is formed by chondroblasts that differentiate from MSCs. Found along the edges of cartilage plates under the perichondrium where appositional growth occurs. In this study I focus on AC and the cartilaginous structures formed by the chondrocytes and the ECM associated with it.

1.3.1 Chondrocyte Function and Regulation

Chondrocytes of the AC perform different functions compared to chondrocytes of the epiphyseal growth plates. Chondrocytes of the AC aid in joint articulation, while chondrocytes of the growth plate regulate the growth of the epiphyseal plates. Since this review focuses on OA, we will relate only to chondrocytes of the AC. Chondrocytes are metabolically active cells that synthesize and turnover a large volume of extra cellular matrix (ECM) components such as collagen, glycoproteins, proteoglycans, and hyaluronan (Archer and Francis-West, 2003). The metabolic activities of chondrocytes are altered by many factors that are present within their chemical and mechanical environment. Most important among these factors are the pro-inflammatory cytokines and growth factors that have anabolic and catabolic effects. These factors play a role in the degradation and synthesis of matrix macromolecules (Fortier et al., 2011; Goldring et al., 2008; Kapoor et al., 2011). However, little is known about the molecular mechanism by which these growth factors and peptides elicit their effects on ECM

metabolism. Chondrocytes are derived from MSCs and occupy only 1%–5% of the total cartilage tissue (Bhosale and Richardson, 2008). This low density is due to the high matrix to cell volume ratio (Bhosale and Richardson, 2008; Poole, 1997). Furthermore, the life span of the chondrocyte is controlled by the areas of its residence. Since AC is an avascular tissue, chondrocytes rely on diffusion of nutrients and metabolites from the articular

surface (Poole, 1997). Moreover, these cells function in a low oxygen environment with low metabolic turnover. They inherently contain low mitochondrial numbers (Archer and Francis-West, 2003). The mechanosensitive chondrocytes are major contributors for ECM production and they provide the functional and mechanical ability to withstand compressional, tensile, and shear forces across the diarthrodial joints.

1.3.2 ECM Production and Its Regulation by Chondrocytes

The main function of chondrocytes in the superficial and mid zone of AC is to synthesize ECM composed of collagen type II, IX, and XI and proteoglycans. This ECM facilitates compressional and tensile forces across the diarthrodial joint (Eyre, 2002; Sophia Fox et al., 2009). Collagens are the most abundant macromolecules of the ECM, and make up 60% of the dry weight of the cartilage and provide tensile and shear strength to the tissue. Collagen also stabilizes the matrix. Collagen type II makes up 90%–95% of the collagen in ECM and forms fibrils and fibers interwoven with proteoglycan like aggrecans (Eyre, 2002). Collagens type IX and XI represent 5%–10% of the AC collagenous network and offer support for the collagen fibrilar crosslinking.

Chondrocytes of the deep zone are terminally differentiated and actively synthesize collagen type X. Proteoglycans represent the second largest group of macromolecules and are heavily glycosylated protein monomers that resist compressional forces across the articular joint (Sophia Fox et al., 2009). These proteoglycans include aggrecan, decorin, biglycan, and fibromodulin. Aggrecans are the largest among the group (Roughley and Lee, 1994; Sophia Fox et al., 2009). Growth factors play a crucial role in controlling chondrogenesis by affecting MSCs differentiation to chondrocytes. They also influence chondrocytes to synthesize specific ECM proteins (Figure 1). The shift in expression of collagen type X by the chondrocytes also marks the regulation of proteolytic enzymes production. These enzymes aid in the clearing of the cartilage ECM and allow vascularization and calcification of tissue (Eyre, 2002; Poole et al., 2002).

In order to maintain the homeostasis of the ECM, the synthesis and degradation of the ECM must be fine-tuned. Damage to AC tissue leads to loss of its ECM, followed by chondrocytes secreting new ECM to repair the damage. Although, chondrocytes are the primary contributors of AC ECM secretion, their turnover rates are not balanced. Proteoglycan turnover is estimated to take up to 25 years, while the collagen half-life is estimated to range from several decades to 400 years (Sophia Fox et al., 2009; Verzijl et al., 2000). Therefore, damage to the tissue can further play a role in the progression of slow degeneration of the tissue and elevate OA like conditions.

The composition of the ECM as well as the organization of chondrocytes and their response to external factors such as cytokines is dependent on the age of the tissue,

however chondrocyte numbers remain unchanged (Hardingham and Bayliss, 1990). In the course of aging, dissipation of chondrocytes in the superficial region is followed by an increase in the number of chondrocytes in the deep layers. Consequently, the decrease in the hydration of the matrix results in an increased compressive stiffness. The age related decrease in the proteoglycan aggregate numbers within the ECM may be a result of proteolytic damage to the link proteins and glycosaminoglycan chains and increase in partially degraded hyaluronan without newly synthesized molecules (Martin and Buckwalter, 2001a; Martin and Buckwalter, 2001b; Martin et al., 1997). Thus, increased mechanical forces exerted on the tissue further lead to subchondral tissue calcification (Hwang et al., 2008; Sharma et al., 2013). These overall structural changes seen in the aging cartilage may just be another factor for the development of diseases, such as OA.

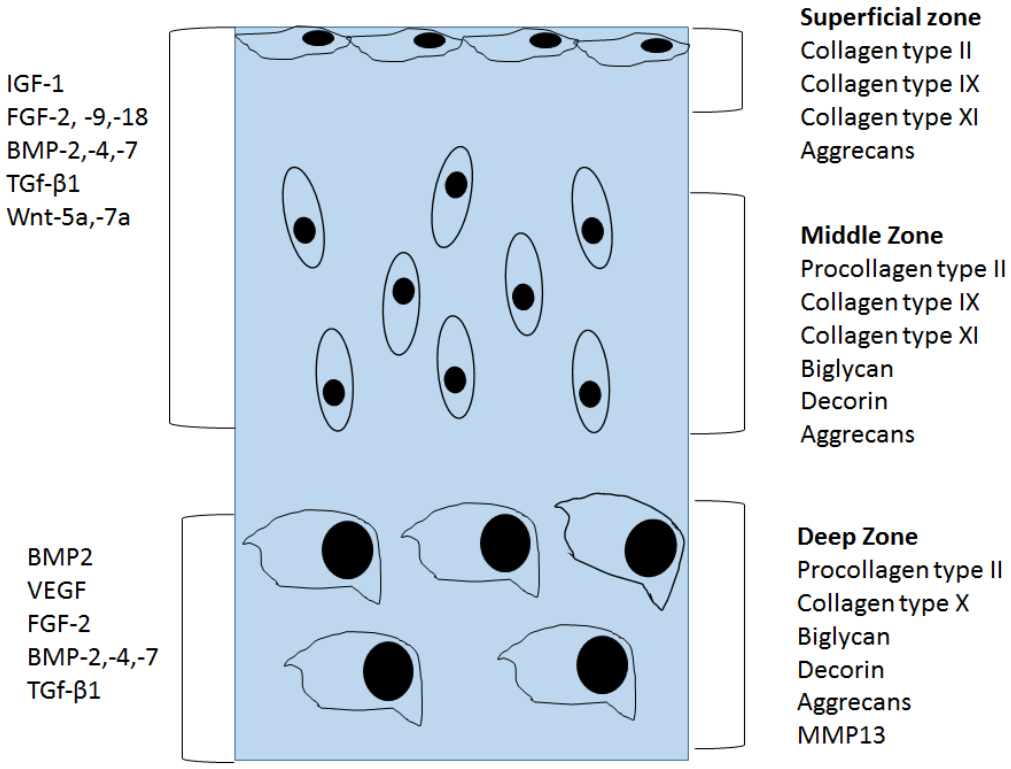

Figure 1.3. **Organization of normal articular cartilage.** Superficial, middle, and deep zones and their extracellular matrix according to zonal sections. Growth factors that control the chondrocyte function are divided based on the stage of chondrocyte lineage.

1.4 Structural Changes in OA Cartilage

OA is the most prevalent type of cartilage degenerative disease, the other being rheumatoid arthritis. OA results in progressive cartilage degradation characterized by the softening, fibrillation and erosions of the articular surface (Sandell and Aigner, 2001). Breakdown of proteoglycans leads to a reduction in the compressive stiffness of the tissue that accelerates the rate of collagen loss (Falah et al., 2010). In OA, besides cartilage erosion in subchondral bone, synovial fluid, and the synovial membrane also play a role in the progression of OA. Osteophyte formations, subchondral bone

remodeling, and synovial membrane inflammation may further aid in cartilage tissue degradation. In early stages of OA, hypertrophic chondrocytes express collagen type X. This production marks the terminal differentiation of chondrocytes that regulates the expression of proteolytic enzymes like MMPs, and ADAMTS that degrade the proteoglycan and collagen network. Simultaneously, activation of transcriptional regulators such as Runt-Related Transcription Factor 2 (RUNX2) are known to induce terminal differentiation and enhance the expression of collagen type X and proteolytic enzymes that digest the AC ECM (van der Kraan and van den Berg, 2012; Wang et al., 2004; Zheng et al., 2003). MMP-1 (Collagenase-1) and MMP-13 (Collagenase-3) are the primary factors that lead to overall degradation of collagenous framework. MMP-3 (Stromelysin-1) and ADAMTS-4 (aggrecanase-1) degrade proteoglycans (Troeberg and Nagase, 2012; Wu et al., 1991). It is shown that MMP activities are controlled by physiologic activators such as cathepsin B and tissue inhibitors of MMPs (TIMPs) (Kostoulas et al., 1999). An imbalance between these factors is commonly observed in OA tissue. Repeated mechanical insult to AC enhances MMP production and enhances cartilage matrix breakdown, (Blain, 2007; Buckwalter et al., 2013). These deleterious effects are pronounced in the superficial region of AC (Lin et al., 2004). However, the process that regulates the production of proteolytic enzymes still remains unclear (Lin et al., 2004).

Inflammatory cytokines, such as IL-1β, TNF-α, and IL-6, are known to be upregulated during OA progression (Kapoor et al., 2011). These inflammatory cytokines are secreted by chondrocytes and synoviocytes. They play an important role

in the disruption of cartilage homeostasis, and MMP mediated cartilage degradation (Choy et al., 2002; Kapoor et al., 2011). This is done by modulating the hypertrophic chondrocyte activity by increasing MMP expression and inhibiting the production of MMP inhibitors (Kostoulas et al., 1999). IL-1β mediated TNF-α expression has been shown to regulate IL-6 production and nuclear factor-κβ (NF-κβ) dependent transcriptional expression of Hypoxia-inducible factor 2α (HIF-2α) drive the processes that may further enhance AC destruction (Caron et al., 1996; Rigoglou and Papavassiliou, 2013; Saito et al., 2010; Stannus et al., 2010; van de Loo et al., 1995; Wehling et al., 2009). OA induced cartilage damage follows a myriad of cascades that once activated result in irreversible damage to the tissue. Chondrocytes recognize the loss of ECM and actively produce collagen type II and proteoglycans. However, the ratio between the ECM protein production to proteolytic enzyme production is imbalanced and results in complete loss of cartilaginous tissue overtime. Moreover, cellular attempts to repair the tissue results in aberrant osteoblast like differentiation forming osteophytes or fibroblastic differentiation inducing fibrosis or stiffening of the joints (Findlay and Atkins, 2014; Hashimoto et al., 2002; Remst et al., 2015).

1.4.1 OA Induced Osteophyte Formation and Fibrosis

Osteophyte formation of the AC and sclerosis of subchondral bone is commonly observed in OA development. In addition, synovitis is a common occurrence in OA, which involves osteophyte formation at the junction of periosteum and synovium (Blom et al., 2004; Gelse et al., 2003b; Matyas et al., 1997; Sandell and Aigner, 2001).

Commonly osteophyte development is caused by MSCs near the periosteum as a form of repair mechanism to help stabilize the joints (Matyas et al., 1997; Sandell and Aigner, 2001). The increase in endogenous MSCs recruitment and chondrogenic differentiation in the damaged cartilage can be seen as a form of tissue repair and regeneration (Wong et al., 2015). However, in this process aberrant expression of growth factors, such as Transforming Growth Factor β (TGF-β), BMP-2 and upregulation of other inflammatory responses, can lead to chondrocyte hypertrophy/apoptosis and osteophyte formation (Uchino et al., 2000; van Beuningen et al., 1998). The mechanisms that control this activity remain unknown. Macrophages from the synovial lining enhance the inflammatory response and the cartilage damage. These synovial macrophages induce both anabolic and catabolic processes. Macrophages initiate these processes by secreting growth factors such as TGF-β, and BMP-2 (Champagne et al., 2002; Cutolo et al., 1993). The development of osteophytes causes pain and loss of movement. Simultaneously, the production of spontaneous nitric oxide by chondrocytes and chondrocyte death allows osteophyte formation (Figure 1.4) (Hashimoto et al., 2002).

Another important hallmark of OA along with cartilage degeneration, and osteophyte formation is fibrosis that results in joint pain and stiffness. It results from the imbalance induced by the growth factor activity regulating matrix synthesis and degradation. Two main factors contribute to this, TGF-β and Connective Tissue Growth Factor (CTGF) (Leask and Abraham, 2004; Leask et al., 2004). Fibrosis results in fibrin deposition within the synovium. It causes joint stiffness that is another symptom in the progression of OA in combination with osteophyte formation and degradation of the

AC. The body's attempts at cellular repair include the recruitment of chondroprogenitors from the surrounding MSC niche. However, MSCs ability for multilineage differentiation makes this an arduous process. Moreover, MSC differentiation relies on the signaling factors that control the cell turnover. Signaling in OA cartilage may be a potential problem for treatments in the long term.

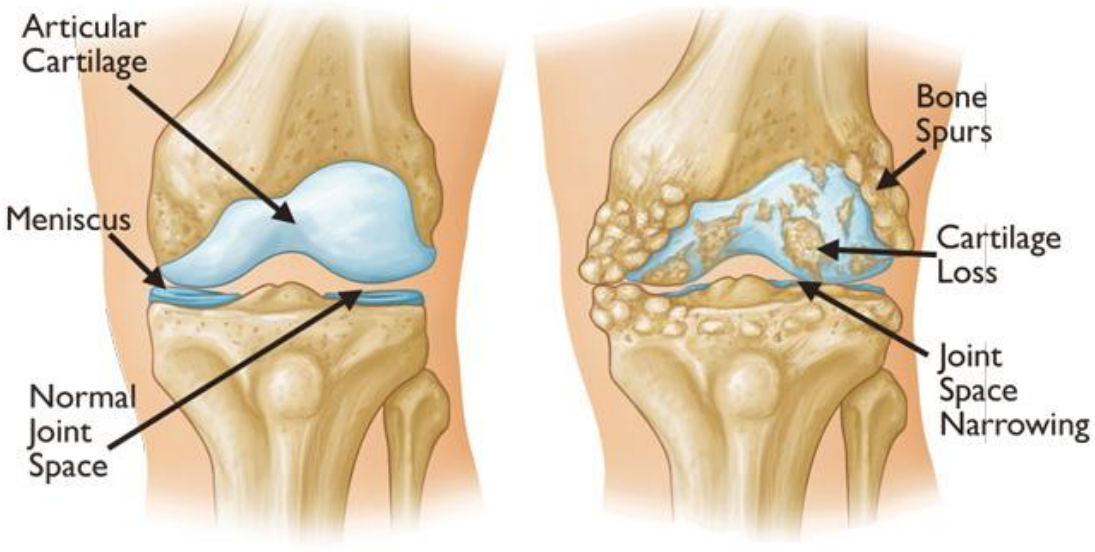

Figure 1.4. **OA of the knee.** Healthy cartilage with normal joint space between femur and tibia (Left). OA cartilage with decreased joint space due to cartilage degeneration and bone spur (osteophyte) formation (Right). Adopted and modified from (http://orthoinfo.aaos.org/topic.cfm?topic=a00212)

1.4.2 Signaling in OA Cartilage

AC development, growth, maintenance, and repair are controlled by several signaling factors that trigger multiple bioactive roles within the chondrocyte metabolism. The

regulatory mechanisms of the growth factors are responsible for cartilage homeostasis. An imbalance between them is often noticed in OA cartilage. The activated signaling cascades involved in OA progression are TGF-β1, BMP2/4/7, Wnt5a, Insulin Growth Factor 1 (IGF-1), and Fibroblast Growth Factor 2 (FGF-2) (Mariani et al., 2014; Shi et al., 2009; Wang et al., 2004; Yan et al., 2011). TGF-β1 together with BMP2/4/7, and IGF-1, contributes to cartilage formation and their mechanisms have been extensively studied (Fortier et al., 2011; Shintani et al., 2013). However, these anabolic growth factors are catabolic in OA (Blaney Davidson et al., 2007b; Goldring et al., 2006; Papathanasiou et al., 2012; van der Kraan and van den Berg, 2012). Similarly, HIF, NF-κβ pathway, Mitogen-Activation Protein Kinase (MAPK) pathways may contribute to OA progression (Olivotto et al., 2015; Saito et al., 2010). Representative schematic of the crosstalk between these signaling factors in the development of OA is shown in (Figure 1.5).

The effect of BMPs on chondrogenesis was demonstrated. BMPs function to promote differentiation, proliferation, and maturation throughout the chondrocytes lineage (van der Kraan et al., 2010). While BMP7 enhanced chondrogenic activity, BMP2 also induces chondrocyte hypertrophy. This is remarkable since both factors signal through the same receptors. The BMP canonical Smad 1/5/8 pathway is a potent inducer of chondrocyte hypertrophy and endochondral ossification (Retting et al., 2009). Therefore, other pathways within BMP signaling may be responsible for the diversity of effects. During OA, BMP2 mRNA levels are upregulated and followed by terminal differentiation of chondrocytes (Nakase et al., 2003). The terminal differentiation of

chondrocytes enhances the secretion of collagen type X and MMP-13. During progression of OA, several chondrocytes within the cartilage tissue express BMPs. Enhanced BMP production influence the acceleration of terminal differentiation of chondrocytes present in the OA cartilage that lead to enhanced MMP production. BMPs may potentiate chondrogenic differentiation but may also initiate aberrant osteophyte formation as well as enhance proteolytic enzyme production for the acceleration of cartilage degradation (Zoricic et al., 2003). Crosstalk between BMP, TGF-β and Wnt signaling pathways is known to regulate terminal differentiation of chondrocytes and the differential modulation between these signaling pathways could accelerate OA (Chan and Little, 2012; van der Kraan et al., 2009). BMP2-induced Wnt/β-catenin signaling enhances the low-density-lipoprotein receptor-related protein 5 catabolic activity, followed by promoting hypertrophy in osteoarthritic chondrocytes. Wnt/β-catenin negatively regulate NF-κβ and drive TGF-β/BMP signaling. This leads to enhanced expression of RUNX2 that enhances the expression of MMP-13, MMP3, and collagen type X (Mariani et al., 2014; Papathanasiou et al., 2012). This process drives chondrocyte hypertrophy and accelerates OA induced cartilage damage. Figure 1.5 summarizes the pathways involved in OA progression. How or what causes these imbalances in these signaling cascades is not known. Moreover, the regulation of the crosstalk between the factors is not completely understood.

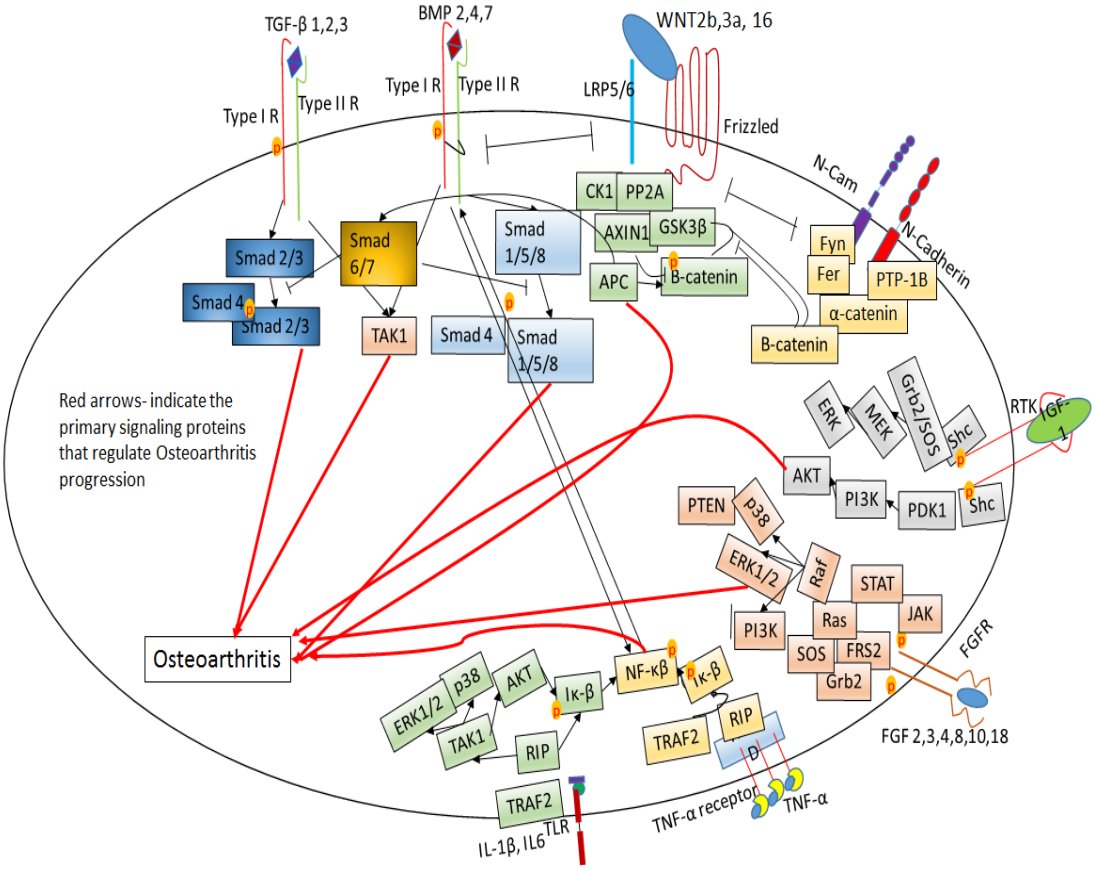

Figure 1.5 **Signaling cascades involved in Osteoarthritis**. Red arrows indicate the primary signaling protein that regulate OA progression. The black arrows signify the activation of the proteins. The bars indicate inhibition of the proteins.

1.4.3 OA Pharmacotherapy

OA pathophysiology features loss of AC through the loss of cartilaginous ECM and the cells that are embedded in it. Chondrocytes are relatively inert cells with insufficient regenerative capacity. Overexpression of proteolytic enzymes including MMPs, ADAMTS further degrade the diseased cartilage. Common practice for mild OA treatments include using physiotherapy and pharmacologic agents to reduce pain

and inflammation. As the disease progresses intra-articular steroids or hyaluronic acid administration is the common practice (Chevalier, 2010). However, while the patients experience temporary relief, it is short lived and its effectiveness is debatable. In advanced cases of OA progression knee replacements are common (Buckwalter et al., 2004; Gupta et al., 2012). However, these patients suffer from joint stiffness and limited mobility.

Current pharmacological intervention addresses only chronic pain in OA but insufficiently, and there is no proven method today that provides structure modifying therapy (Goldring and Goldring, 2007). Common recommendations include analgesics nonsteroidal anti-inflammatory drugs (NSAIDs) (Vane and Botting, 1997). Another approach that is being adopted is the usage of bisphosphonates and strontium ranelate, a rationale used to delay bone turnover to prevent osteophyte formation and cartilage calcification (Richette and Roux, 2012). Other therapies include; inhibitors of inducible nitric oxide synthase (iNOS), believed to suppress the production of inflammatory cytokines that produce of Nitric Oxide (NO) as an inflammatory response enhancing production of catabolic agents that breakdown cartilage (Clutterbuck et al., 2009). There is also anti-MMP therapy, which aims to stop the MMP activity in collagen degradation. However, it has proven to be ineffective and no new development in this area was made (Mobasheri, 2013). Over the last decade many compounds have been tested and while some are now in the phase II and phase III trials, there

is yet to be a concrete disease modifying osteoarthritic drug (DMOAD). An alternative to pharmacotherapy is the more invasive approach; are arthroplasty, and MSC therapy.

Although, the causes for the degenerative disorders like OA are still unknown. Signaling cascades of TGFβ, BMP, Wnts, and FGF that help in cartilage formation should be determined and utilized to delay or reverse the progression of OA. Therefore, a great deal of work is still needed to understand this degenerative disease, and for the development of therapeutics to stop the progression of OA and regenerate lost cartilage.

1.5 Overview of Bone Morphogenetic Proteins (BMPs)

BMP are group of potent growth factors belonging to the TGFβ superfamily. BMPs are important morphogens necessary for embryogenesis, development, and maintenance of adult tissue homeostasis (Wang et al., 2014). Among BMPs BMP2 is essential for limb patterning and proper bone formation. BMPs also control MSCs to differentiate osteoblasts and BMP activity influences bone formation (Retting et al., 2009; Yoon and Lyons, 2004). BMP2 is also important in maintaining joint integrity, fracture repair, and vascular remodeling (Blaney Davidson et al., 2007b). Over half a century of research has demonstrated the importance of BMPs in the formation of skeletal framework. Though their functions have been extensively studied, less known of their activity at the ECM, cell membrane surface, and receptor activation (Bragdon et al., 2011a). BMPs form either homo or heterodimers, with the only exception being BMP15 monomers. Divided into the subgroups where heterodimers of; BMP2/5,

BMP2/6, BMP2/7, and BMP4/7 were observed *in vitro* and *in vivo*. Also these heterodimers signal more effectively than homodimers (Israel et al., 1996; Little and Mullins, 2009; Sieber et al., 2009). BMPs are grouped based on sequence similarities, typically subdivided among four groups: BMP2/4, BMP5/6/7/8a/8b, BMP9/10, and BMP12/13/14 (Bragdon et al., 2011a; Mazerbourg and Hsueh, 2006; von Bubnoff and Cho, 2001). Studies have demonstrated among BMPs, BMP4, 7, 9, 10, 11 and BMP14 form complex dimers with their prodomains following cleavage, while BMP2 prodomain fails to form complex homodimers with itself (Sengle et al., 2008). These protein complexes play an important role in a vast number processes including development of lung, skin, brain, eye, liver, and kidney (Reddi, 2005; Wagner et al., 2010).

In this study I focus on BMP signaling with a special focus on BMP2 as the model protein among the vast number of BMP family members. BMP2 is a potent inducer of cartilage and bone development (Retting et al., 2009; Yoon and Lyons, 2004). Studies also have demonstrated BMP2 induced signaling cascades are essential for the stimulation MSC differentiation to osteoblasts *in vitro* and plays a central role in bone formation and bone turnover *in vivo* (Chen et al., 2012; Jun et al., 2010; Katagiri and Takahashi, 2002). However, more recent evidence suggests that it is BMPs role in the activation of osteoclasts through their pathophysiological pathways that may play a key role in the progression of bone metabolic disorders like osteoporosis (Kanakaris et al., 2009). Although, studies confirm lowered expression of BMP2 in osteoporotic patients,

rhBMP2 treatments of bone marrow stromal cells (BMSCs) did not restore their osteogenic potential in aged populations to the degree they were in younger populations (Varkey et al., 2006). Interestingly, BMP2 presence in the osteoporotic population lead to an increased adipocyte differentiation of BMSCs and accumulation in areas where bone was lost (Donoso et al., 2015). Therefore, to consider BMP2 or BMP7 as treatment options for osteoporosis we need to understand their underlying mechanisms that are involved in the process of bone formation.

Another reason for BMP2 as a model choice is due to its critical role in the development of AC and cartilaginous tissue (Shu et al., 2011). However, BMP2 among other growth factors is known to accelerate overall progression of OA (van der Kraan et al., 2010). BMP2 mediated signaling is necessary for the modulation of cartilaginous template formation and AC development and are present throughout the chondrocyte lineage (van der Kraan et al., 2010). Although the physiological levels of BMP2 are low in normal AC they are elevated in times of damage for repair of the tissue. Also true during the progression of OA, where the physiological levels of BMP2 are elevated in the patellar capsule and the AC leading to the destruction of AC and osteophyte formation (Chan and Little, 2012; Nakase et al., 2003; van der Kraan et al., 2009; Zoricic et al., 2003). Therefore, it is quintessential to understand the signaling mechanisms to find potential therapeutic targets.

1.5.1 BMP receptors and signaling

BMP receptors are transmembrane bound serine/threonine kinase receptors. BMP receptors are composed of 10-12 cysteine residues at the extracellular domain, a single transmembrane domain and an intracellular domain with serine/threonine kinase region (Yamashita et al., 1996). BMP signaling occurs upon the ligand binding to the receptor complex of at least one type I and one type II receptor that forms a heteromeric complexes to signal downstream. However, these receptors form specific heteromeric complexes to signal downstream. There are five known receptors: ALK1 (ACVRL1), ALK2 (ActRI), ALK3 (BMPRIa), ALK4 (ActR1b) and ALK6 (BMPRIb); and three type II receptors: BMPRII, ActRIIa, and ActRIIb (Bragdon et al., 2011a). BMP ligands bind to the specific receptor complexes with varying affinities (Liu et al., 1995).

Type II receptors are constitutively active kinases, upon binding to BMP they form heteromeric complexes with the type I receptor and transphosphorylate it at the glycine/serine rich juxtamembrane region, called the GS-box. Upon phosphorylation by type II receptor, the type I serine/threonine kinase becomes activated and transduces the signal downstream (Itoh et al., 2000). As a result, BMP2 binds to the receptor complexes of at least one BMPR type I (ACVRI, BMPRIa, BMPRIb) and one BMPR type II (BMPRII, ActRIIa, ActRIIb) to signal downstream (Bragdon et al., 2011a). BMP2 binds to the BMPRIa and this interaction recruits BMPRII to signal downstream (figure 1.6). This binding affinity may change depending on the receptor complex that BMP2 binds

to form the signaling events that follow (Gilboa et al., 2000; Hartung et al., 2006; Nohe et al., 2002).

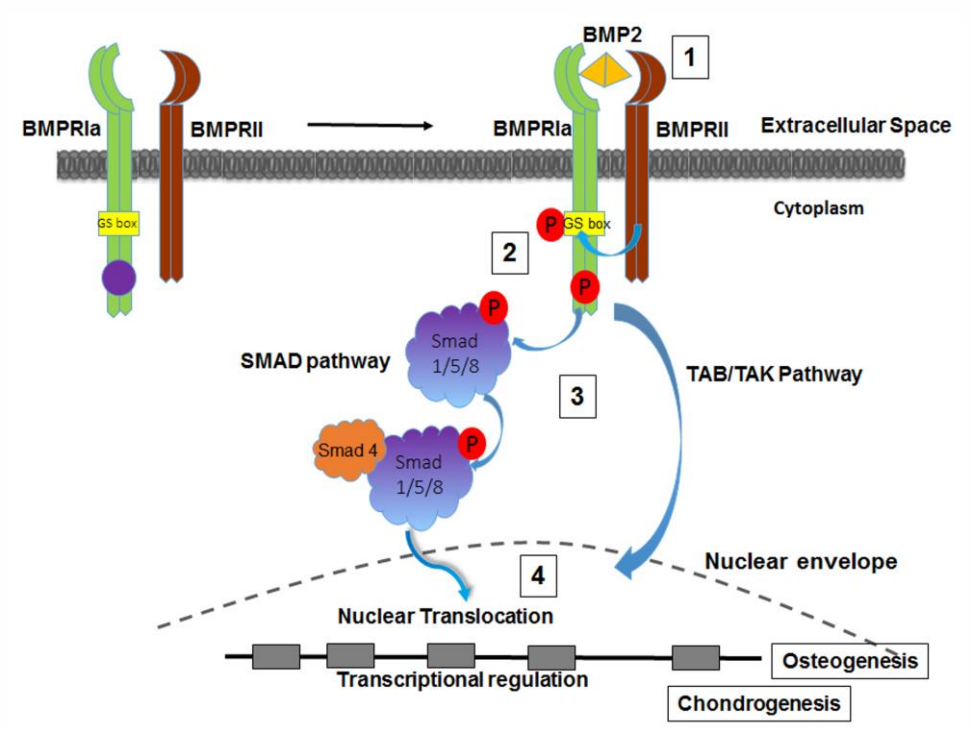

Figure 1.6 **BMP2 receptor signaling.** 1) Ligand binding to BMPRIa and BMPRII results in 2) phosphorylation of BMPRIa by the constitutively active BMPRII leading to the downstream signaling 3) via Smad 1/5/8 and Smad4 or via the TAB/TAK pathway that 4) induces either osteogenesis or chondrogenesis through gene regulation.

1.5.2 BMP2 induced signaling pathways

BMP2 ligand binding to its receptors initiates BMPRII receptor phosphorylation of BMPRIa that signals downstream via either Smad dependent signaling or through Smad independent pathways such as TAB/TAK pathway (Hassel et al., 2003). Smad dependent signaling pathways are the most studied among BMP signaling pathways.

There are eight members of the Smad family of proteins, grouped by their functional signaling, consisting of regulatory smads or Smad 1/5/8 for BMP signaling, and Smad2 and Smad3 for TGFβ signaling. They also consists of I-Smads or the inhibitory Smads consisting of Smad 6 (BMP pathways), Smad 7 (TGFβ pathway) and common Smad (Co-Smad) Smad 4 (Bragdon et al., 2011a). In BMP signaling through the Smad pathway, phosphorylated Smad 1/5/8 bind to and activate Smad 4 that translocates to the nucleus where they activate the expression of targeted genes (Massague, 1998). Smad 1/5/8 signaling has been demonstrated to be involved in cell growth, morphogenesis, apoptosis, development and immune responses. Smad signaling also plays a crucial role in chondrogenesis, osteoblastogenesis and adipocyte differentiation.

Smad independent pathways include but are not limited to Mitogen Activated Protein Kinase (MAPK) like p38, or C-Jun N-terminal Kinase (JNK), extracellular signal-regulated kinase (ERK), phosphoinositide 3-kinase (PI3K) and nuclear factor Kappaβ (NF-κβ) (Bragdon et al., 2011a). Smad independent signaling is activated by the ligand binding to the receptor complex that initiates the downstream activation of TAK1-TAB1 complex. This complex activates the downstream MAPK or MEK pathway involving p38, ERK1/2, AKT-mTOR, JNK pathways (Hata et al., 2003; Lu et al., 2007; Nohe et al., 2004a). It has been shown that activation of p38, ERK1/2 and JNK regulate gene transcription affecting osteoblast differentiation, adipocyte differentiation via p38 mediated ATF-2 activation and apoptosis (Guicheux et al., 2003; Hata et al., 2003). BMP2 stimulations can lead to the activation of PI3K, but this

particular mechanism remains poorly understood. Activated PI3K phosphorylated downstream AKT and mTOR pathways (Sugimori et al., 2005). Similarly, BMP2 mediates ERK1/2 activation that further activates MEK1/2 (Jun et al., 2010; Lou et al., 2000). These pleiotropic functions that BMP2 elicits can be understood due to its activation of various signaling cascades. BMP receptor signaling and interacting proteins

1.5.3 BMP receptor signaling and interacting proteins

BMPRIa and BMPRII are primarily found in caveolae and clathrin coated pits (CCPs) at the cell membrane. Caveolae flask shaped invaginations present at the plasma membrane are made of the scaffolding protein Cav1 that forms the shape (Fujimoto et al., 2000; Nohe et al., 2004b). It is demonstrated that BMP signal was regulated by Cav1 phosphorylation of BMPRII in the vascular smooth muscle cells (Wertz and Bauer, 2008). Also shown that BMP signaling occurs favorably through the caveolae while CCP being the favorable for the endocytosis function of the BMP receptors (Bragdon et al., 2009). More recently, another set of proteins were discovered that interact with BMP receptors to regulate their localization and signaling downstream. Proteins that interact with BMPRIa and BMPRII are; Adapter protein 2 (AP2), Caveolin-1(Cav1), Protein Phosphatase 2A (PP2A), and X linked Inhibitor of Apoptosis Protein (XIAP) (Bengtsson et al., 2009; Bragdon et al., 2009; Liu et al., 2009; Nohe et al., 2004b; Nohe et al., 2005; Yamaguchi et al., 1999). Those that interact only with BMPRII are; Cyclic

Guanosine 3',5' Monophosphate dependent Kinase (cGKI), c-src, related to EPS15 (Epidermal Growth Factor Receptor Path Substrate 15 (EPS15R) and inhibin (Schwappacher et al., 2009; Wiater et al., 2006; Wong et al., 2005). Proteins interacting only with BMPRIa are BMP associated molecule (BRAM1), Endofin, Smad1/5/8, Tab1 (Tak1 binding protein), Tak1 (TGFβ activate kinase 1), spliceosome associated protein subunit 4 (SAP49), and Casein kinase II (CK2) (Kurozumi et al., 1998; Lu et al., 2007; Sapkota et al., 2007; Shibuya et al., 1998; Yamaguchi et al., 1999; Zhang et al., 2009).

In this study I focus on CK2 and its implication in the development of novel mimetic peptides that block the interaction with BMPRIa inducing the downstream signaling.

1.5.4 Casein Kinase 2

Casein Kinase 2 (CK2) a serine/threonine selective protein kinase is ubiquitously expressed with over 300 substrates that affect cell growth, proliferation, differentiation, apoptosis and tumorigenesis (Duncan and Litchfield, 2008). Primarily detected in the nucleus, a fraction of CK2 also have been isolated from the plasma membrane, golgi apparatus, endoplasmic reticulum (ER) and ribosomes (Litchfield et al., 1996). CK2 Activity however, is localized to the membrane associated cell fractions (Litchfield et al., 1996). It has been demonstrated that the pleckstrin homology domain CK2 interacting protein-1 (CKIP-1) is responsible for the recruitment of CK2 to the plasma membrane. CK2 is a tetramer complex that consists of two catalytic subunits (α or α') and two regulatory β subunits (Litchfield, 2003; Olsten et al., 2004). The two β

subunits are inactive but is essential for the assembly of CK2 complex as well as recruitment and docking of CK2 subunits. CK2β recruits and enhances the catalytic activity of CK2α (Litchfield et al., 1990). This active complex is responsible for the phosphorylation of targeted substrates at serine, threonine and tyrosine residues surrounded by the acidic sequence of the proteins. These CK2 enzyme complex is also essential for the transcription and translation of various proteins necessary for the activation of gene transcription, signal transduction, protein synthesis, and cytoskeleton and structural protein formation (Allende and Allende, 1995; Yamaguchi et al., 1998). Therefore, CK2 is an important kinase in a variety of cellular processes including control of cell cycle, cell motility, embryogenesis, cell differentiation and apoptosis.

Nohe lab previously demonstrated a novel interaction between BMPRIa and CK2. Upon BMP2 binding to the BMP receptor complex BMPRII phosphorylates BMPRIa at the GS box (glycine/serine rich region of the type I receptor), which leads to the release of CK2 from the receptor to activate the downstream signaling (Bragdon et al., 2010). A representative schematic is shown in (figure 1.7). It was shown through immunoprecipitation assays that CK2 interaction with BMPRIa was lost upon ligand binding to the receptor to signal downstream. Therefore, based on this we performed an in depth prosite search across the BMP receptor complexes that included pattern of high probability of CK2 binding sites and yielded three possible CK2 phosphorylation sites on the type I receptors. These sites were located at the amino acid residues of 213-217

(SLKD), 324-328 (SLYD) and 466-469 (SYED) (Bragdon et al., 2011b; Bragdon et al., 2010).

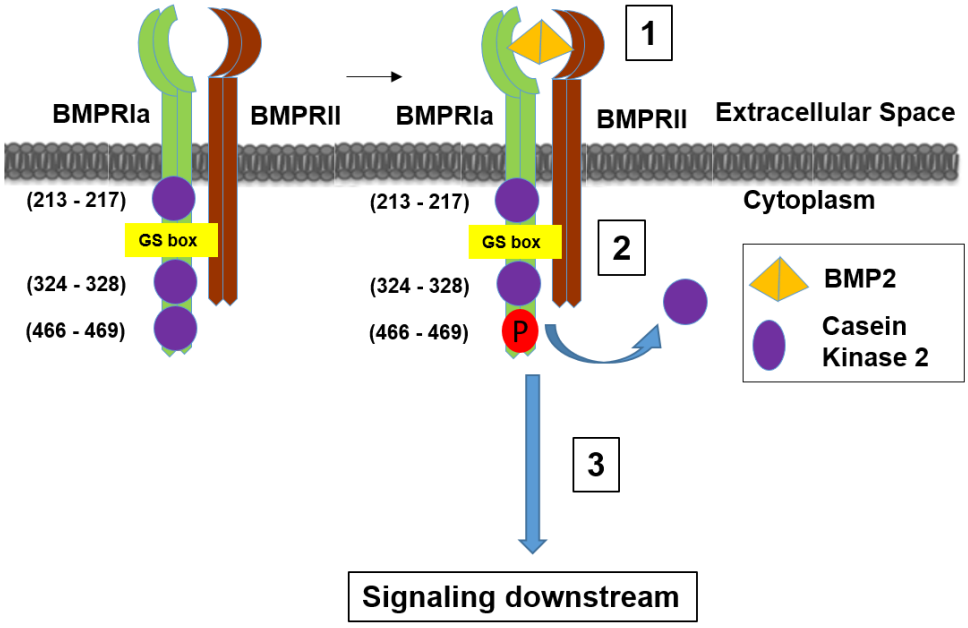

Figure 1.7 **BMP2 ligand receptor complex releases CK2**. 1) Upon BMP2 binding to BMPRIa and BMPRII receptor complex, 2) CK2 is released from BMPRIa interaction sites allowing for the constitutively active BMPRII to phosphorylate BMPRIa 3) to signal downstream.

1.5.5 Design of the CK2 peptides

We designed peptides that would stop the interaction of CK2 to the BMPRIa by mimicking the CK2 binding sequence on the BMPRIa receptor, peptides include an Antennapedia homeodomain signal sequence for the cellular uptake and incorporated one of the following CK2 binding site sequences labeling them as; CK2.1 (SYED), CK2.2 (SLYD), CK2.3 (SLKD). These peptides also included several amino acid

residues flanking each side, creating a total length of 27 amino acids (CK2.1) and 29 amino acids for CK2.2 and CK2.3 (Bragdon et al., 2011b). These blocking peptides successfully activate the BMP signaling pathway in absence of BMP2 ligand (Bragdon et al., 2011b). Nohe lab has also demonstrated the effect of CK2.3 in calvarial bone formation of mice *in vivo* and CK2.2 in adipogenic regulation *in vitro* in C2C12 cells (Bragdon et al., 2011c; Moseychuk et al., 2013). This study looks at the effect of peptides CK2.3 (Akkiraju et al., 2015) and CK2.1 and their activity in activating the BMPRIa downstream signaling and their consequential effects on MSC differentiation discussed in chapters 2,3, and 4. This study provides us a unique opportunity to observe the various responses induced by the BMP signaling that is responsible for the physiological outcome. It also gives us a window of opportunity in the designing of new age therapeutics for targeting musculoskeletal disorders as osteoporosis and osteoarthritis.

Chapter 2

SYSTEMIC INJECTION OF CK2.3, A NOVEL PEPTIDE ACTING DOWNSTREAM OF BONE MORPHOGENETIC PROTEIN RECEPTOR BMPRIA, LEADS TO INCREASED TRABECULAR BONE MASS.

2.1 Background

Bone is a dynamic tissue that is remodeled through the action of osteoblasts that form bone and osteoclasts that resorb bone. However, the action of these cells must be balanced to maintain skeletal integrity. Continued increase in osteoclast activity over decreased osteoblast activity leads to decreased bone mass and metabolic bone diseases such as osteoporosis (Boyle et al., 2003; Ferguson et al., 2003; Marie and Kassem, 2011). Most of the therapeutic agents that protect the skeleton block osteoclastogenesis and osteoclast activity while only a few drugs promote bone formation. Among these are growth factors like bone morphogenetic proteins (BMPs). BMP2 is a potent stimulator of bone formation that enhances osteoblastogenesis and is approved for clinical use in healing of long bone fractures (Marie and Kassem, 2011). However, long term BMP2 usage has been shown to increase osteoclastogenesis and osteoclast activity, reducing the anabolic effects of BMP2 and raising concerns that bone loss could increase due to this catabolic action (Jensen et al., 2010). We recently identified a novel

BMP type I receptor (BMPRIa) interacting protein, Casein Kinase 2 (CK2), that is released upon BMP2 stimulation (Bragdon et al., 2009). CK2 is a highly conserved, constitutively active, ubiquitously expressed enzyme with more than 300 substrates that regulates cell growth, proliferation, differentiation, apoptosis, and tumorigenesis (Litchfield, 2003).

We have designed a peptide, CK2.3 that blocks the interaction of CK2 with BMPRIa and contains an Antennapedia Homeodomain (HD) signal sequence for cellular uptake and localization to their respective binding sites (Bragdon et al., 2011b; Bragdon et al., 2010). We previously reported that subcutaneous injections of the CK2.3 peptide induces bone formation and increases the Mineral Apposition Rate (MAR) in mice calvaria (Bragdon et al., 2011b). CK2.3 stimulations also resulted in decreased osteoclast activity *in vitro* (Bragdon et al., 2010). Mutation of the CK2.3 site (MCK2.3) on BMPRIa in C2C12 cells increased mineralization by these cells through the ERK pathway (Moseychuk et al., 2013). In this study I investigate the effect of CK2.3 on bone formation by systemic injection *in vivo* and its potential mechanism *in vitro* and *in vivo*.

2.2 Materials and Methods

2.2.1 Mouse injections

C57BL/6J mice were obtained from The Jackson Laboratory (Bar Harbor, ME). At eight weeks of age, female C57BL/6J mice (n=7/group) were injected in the tail vein

once a day for five consecutive days with CK2.3 (2.3µg/kg per mouse), BMP2 (5µg/kg per mouse) or 50µl of PBS as a vehicle control. The dosage equal to the 1:2.5 molar ratio of BMP2:CK2.3 concentrations was based on previous experiments. The Nohe lab found that 100nM CK2.3 responded similarly to 40nM BMP2 (Bragdon et al., 2011b; Bragdon et al., 2010) . Three weeks after the initial injections, new bone formation was labeled by 100µl of calcein green (12mg/ml) via intraperitoneal injections. Five days later, second label of 100µl calcein green (12mg/ml) was injected intraperitoneally. Mice were euthanized by CO_2 two days later and the femurs were isolated and fixed using 10% neutral buffered formalin. Blood from all animals of each group was collected through the peri-orbital sinus of the mouse at 2^{nd} and 4^{th} week after the last injection for anabolic and catabolic bone marker analysis.

2.2.2 Alkaline phosphatase activity

Serum ALP activity was measured as described (Dimai et al., 1998). Briefly, 5 µl of the serum was mixed with 295 µl of assay solution (1mM magnesium chloride, 10mM PNPP, 150mM sodium carbonate buffer (pH 10.3), and 10mM L-phenylalanine to inhibit circulating intestinal ALP activity). Serum samples were pooled and loaded onto one plate. The plate was protected from light and incubated at 37ºC for 15-30 min and read in triplicate at 405/410nm. Results were normalized to time 0 (Dimai et al., 1998; Ferguson et al., 2003).

2.2.3 TRACP-5b assay

Serum TRACP-5b levels were quantified using the Mouse TRACP-5b ELISA kit from TSZ ELISA (Framingham MA) and followed the provided manufactures procedure. All samples were run on one plate in triplicate.

2.2.4 Osteocalcin assay

Serum osteocalcin levels were quantified using Mouse osteocalcin ELISA kit from Biomedical Technologies Inc. (Stoughton MA) as per manufacturer's protocol. Serum and cell samples were run in triplicates. For cells three different experiments were performed.

2.2.5 Von Kossa Staining

Bone Marrow Stromal Cells (BMSCs) were extracted (Liao et al., 2008) and were plated at cell density of $1X10^6$ cells/cm^2 in 35mm dishes using plating media for 7 days (Bragdon et al., 2011b). Cells were grown to 90% confluence in plates and serum starved overnight before treatment. The next day cells were treated as noted per individual experiment with CK2.3 (100nM) or BMP2 (40nM). After 7 days the cells were washed with cold PBS pH7.4, fixed using 4% (w/v) paraformaldehyde for 10 minutes, and washed with cold PBS pH7.4 again to remove remnants of fixative. Von Kossa stain; (5% (w/v) silver nitrate was diluted in dH2O and treated to the fixed layer of cells under UV light for 30 minutes as previously described (Bragdon et al., 2010). These areas were analyzed by taking at least 10 random high magnification images of

each well of treatment with a Nikon TMS automatic mode with phase 1 with a 20 x objective. Data was then quantified with the use of ImageJ (NIH, Bethesda), where images were converted to 8 bit and the threshold was set to the positive control. The same threshold was used for all treatments in an individual experiment. The surface area of the stain was quantified by using the "analyzing particles function" a function of ImageJ that can be used to calculate areas of black which represented mineralization. Samples were run in triplicates and at least 5 images per well were obtained for analysis.

2.2.6 Isolation of BMSCs

Mice were obtained from Charles River. BMSCs were collected from tibias and femurs of age matched female mice. At eight weeks, mice were sacrificed by CO_2 and the hind limbs were removed. In sterile conditions, tibia and femur were cleaned and the bone marrow was isolated by flushing the marrow with MEM alpha supplemented with 1% penicillin/streptomycin and 10% FBS. Cells were counted and plated at $10x10^5$ cells. Primary cultures were grown in MEM alpha (Gibco, Carlsbad, California) supplemented with 1% penicillin/streptomycin and with 10% FBS for seven days at 5% CO_2 and 37°C. Serum starvation started at 7 days in culture. The media was changed on day 3 and then every other day after that. Samples were run in triplicates and at least 5 images per well were obtained for analysis.

2.2.7 Calvarial Osteoblast Isolation

Calvaria were dissected from newborn mice (6-9 days old) and maintained in sterile conditions. Sutures were removed and the calvaria were subjected to four sequential 15 minute digestions in an enzyme mixture of collagenase P 1.5U/ml (Sigma-Aldrich) and 0.05% trypsin at 37°C. The cell fraction from the first digestion was discarded and the fractions 2-4 were collected and chilled using equal volumes of cold media (DMEM, 10% FBS, 1% penicillin/ streptomycin). The remaining fractions were pooled, centrifuged, and resuspended in media and filtered through a 70mm cell strainer. Cells were plated at a density of $1.5x10^4$ cells/cm^2 in 35-mm culture plates in DMEM containing 10% FBS. Twenty-four hours later medium was exchanged and 3 days later cultures were changed again. At 7 days of culture, the medium was changed and serum starved for 12 hours before being put in to differentiation medium (α-MEM containing 10% FBS, 25 mg/ml ascorbic acid, and 4 mM ß-glycerophosphate) as well as the appropriate stimulation BMP2 (40nM) or CK2.3 (100nM) or PBS (Bragdon et al., 2011b). Samples were run in triplicates and at least 5 images per well were obtained for analysis.

2.2.8 Osteoclasts Isolation

Primary pre-osteoclasts were isolated from the spleens of five female C57BL/6J mice as described in (Bragdon et al., 2011b). Briefly, three cuts were made in the spleens in order to remove cells using a 26-gauge needle with plating media (alpha-MEM, 10% FBS, and 1% penicillin/streptomycin). Cells were centrifuged at 1000 rpm for five

minutes at 4°C. The pellet was resuspended in osteoclast media (50mL plating media, 10µl RANKL (0.25µg/µl) and 6µl m-CSF (0.25µg/µl) from Pepro Tech, NJ, USA) and plated at $1X10^6$ cells/cm^2 on bone chips in 48 well plate. On day seven media was changed and cells were stimulated with peptide CK2.3 (100nM) or BMP2 (40nM) for 7 days. Samples were run in triplicates and at least 5 images per well were obtained for analysis.

2.2.9 TRAP Staining

Cells were fixed with 4% paraformaldehyde and stained using the Sigma-Aldrich kit, 387A, following the manufacture's procedure. Once cells were dried images were taken using a NikonTMS (model TMS-F #211153). Three random images per well per treatment were taken and images were quantified using ImageJ to calculate the number of osteoclasts per cell. The treatments were then normalized to the control. Osteoclasts were identified as multinucleated cells. Samples were run in triplicates and at least 5 images per well were obtained for analysis.

2.2.10 Osteoclast Resorption Activity

Cells plated on bone slices were removed using hypoxic conditions followed by staining for 10 seconds with hematoxylin solution Gill No 3 from the 387A kit from Sigma-Aldrich. Images were taken using a Nikon TMS (model TMS-F #211153) at a 10x magnification. For each bone chip, the number of pits was counted as described

previously (Bragdon et al., 2011b). Samples were run in triplicates and at least 5 images per well were obtained for analysis.

2.2.11 MicroCT40 and pQCT

Analyses of volumetric bone mineral density (vBMD) and trabecular bone volume (BV), tissue volume (TV), trabecular number (Tb.N), and trabecular thickness (Trab.th) were measured using MicroCT40 and pQCT as described. Tb.N is the average number of trabeculae Tb.Th is the average thickness between each trabeculi and Tb.Sp is the space between the trabeculae themselves as described in (Beamer et al., 2012; Bouxsein et al., 2004)[,](Bouxsein et al., 2010).

2.2.12 Histology

Femurs collected from mice (n= 7/group) were embedded in MMA as described (Bragdon et al., 2011b; O'Brien et al., 2000). Chemicals used for embedding are as follows; Methyl Methacrylate (MMA) (Acros, New Jersey, USA), N- Butyl Phthalate, and Benzoyl Peroxide (Wet) (Fisher Scientific, Fair Lawn, New Jersey, USA) that is dried carefully. All bones extracted from mice were fixed in 10% Neutral Buffered Formalin (NBF) for 24-48 hrs at 4^{o}C. Subsequently, bones were washed with PBS and dehydrated using serial changes of ethanol gradients at 70% (8 to 16 hours), 70% (8 to 16 hours), 90% (8 to 16 hours), 95% (8 to 16 hours), 100% (8 to 16 hours), 100% (8 to 16 hours), 2 changes of 2-propanol (8 to 16 hours each rinse), and 2 changes of methyl salicylate (4 hours each). Samples were infiltrated in order, first with MMA I (765ml

MMA + 140ml n-Butyl Phthalate) at room temperature for 48 hours, next MMA II (765ml MMA + 140ml n-Butyl Phthalate + 9.0g Dry Benzoyl Peroxide) at 4C for 48 hours, and last in MMA III (765ml MMA + 140ml n-Butyl Phthalate + 17.75g Dry Benzoyl Peroxide) at 4^{o}C for 48 hours. Polymerized blocks were trimmed and sectioned at 200µm using (10.2cm X 0.3mm) Beuhler diamond watering blade and sanded down to even the surface. All samples were bisected longitudinally through the interchondular notch to separate medial and lateral condyles making sagittal plane cuts, with 3 or 4 slices per femur.

2.2.13 Immunostaining

Sectioned (n=7 per group) samples were imaged for Calcein using Zeiss LSM 780; plan Apochromat 20X (0.75NA, Main Beam Splitter (MBS) 488, 7% laser power). Calcein labelled sections were used to quantify Mineral Apposition Rate (distance between the labels/time between labels). Immunostaining of plastic embedded samples (n=3 per group) was performed by modification and optimization of this protocol (O'Brien et al., 2000). Samples were pretreated in testicular hyaluronidase for 30 minutes at 37^{o}C followed by blocking with 3% BSA for one hour. Samples were labeled for 2 hours at room temperature with 2µg/ml of Antennapedia homeodomain antibody (Genetex, Irvin, CA, USA) followed by 4 µg/ml of Alexa 546 goat anti rabbit (Invitrogen, Eugene, OR, USA). Samples were imaged using Zeiss 510 NLO; Plan Apochromat 20X (0.8NA), Filters Long Pass (LP) 560, laser excitation of 543 nm, 10.9% laser power along with DIC filter. Smad1,5, and 8 and p-ERK labelling, samples

were incubated for 2 hours at room temperature with either 40ng/ml of Rabbit Polyclonal Smad 1/5/8 IgG (Santa Cruz Biotech, CA, USA) followed by 4 µg/ml Alexa 546 goat anti-rabbit (Invitrogen, Eugene, OR, USA) or 2µg/ml mouse monoclonal p44/p42 MAPK (ERK1/2) antibody (cell signaling, MA, USA) preconjugated with 4 µg/ml of Alexa 633 goat anti-mouse IgG (Invitrogen, Eugene, OR, USA) for 1 hour and counterstained with Hoechst stain for 10 minutes. Samples were imaged using Zeiss LSM 510 NLO; with Plan Apochromat 20X/0.8, two photon excitation with Titanium: Sapphire ($Ti:Al_2O_3$) laser at wavelength 790 nm and Helium Neon ($HeNe_2$) laser set at excitation 633 nm; both set to 35% power. Filters LP 560, LP 650, Band Pass (BP) 500 – 550IR and BP 390-465IR. Femurs were bleached to identify marrow cavities using auto fluorescence. Images were processed using ImageJ. Samples were run in triplicates and at least 8 images per well were obtained for analysis.

2.2.14 Statistical Analysis

Data were analyzed by ANOVA, followed by Tukey-Kramer post-hoc analysis. Maximum of three outliers were removed using the Chauvenets Criterion, but minimum number of samples required for statistical significance were used for the following analysis. Error bars represent standard error of the mean (SEM), where * denotes ($p<0.05$) and ** denotes ($p<0.01$) statistical significance.

2.3 Results

2.3.1 CK2.3 induces osteogenesis in primary calvaria as well as in BMSCs isolated from 8 week old mice

Nohe has previously shown that CK2.3 induces mineralization in C2C12 cells, a myogenic cell line (Bragdon et al., 2011b; Bragdon et al., 2010). However, I still needed to determine the effect of CK2.3 on primary bone cells such as calvarial osteoblasts and BMSCs. First I measured osteocalcin, a marker for osteogenesis secreted by osteoblasts. Osteocalcin levels were increased in CK2.3 and BMP2 treated cells compared to control (Fig 2.1 A, B). Next I determined the effect of CK2.3 on mineralization of isolated calvarial cells and BMSCs by von Kossa staining (Fig 2.2). Both BMP2 and CK2.3 significantly increased mineralization above that of vehicle and HD controls. CK2.3 significantly increased mineralization over that of BMP2 treatment in isolated calvarial cells

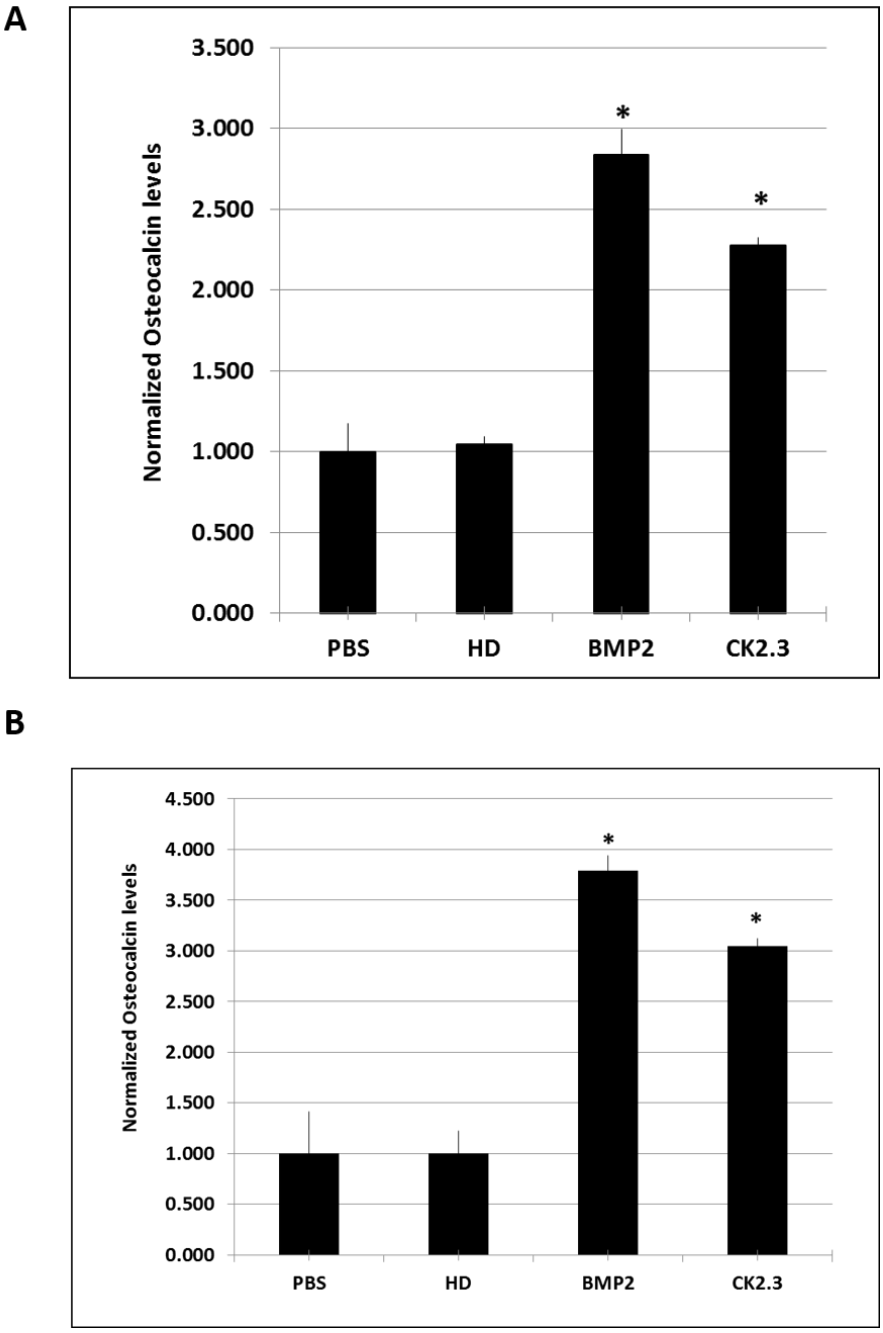

Figure 2.1 **CK2.3 stimulation of primary cells led to increased Osteoclacin levels**. Osteocalcin levels are increased in the supernatant of A) calvaria cells and B) BMSCs stimulated with PBS, HD (Antennapedia Homeodomain), 40nM BMP2, and 100nM CK2.3. At least 3 independent experiments were performed. Error bars represent SEM (* $p < 0.05$).

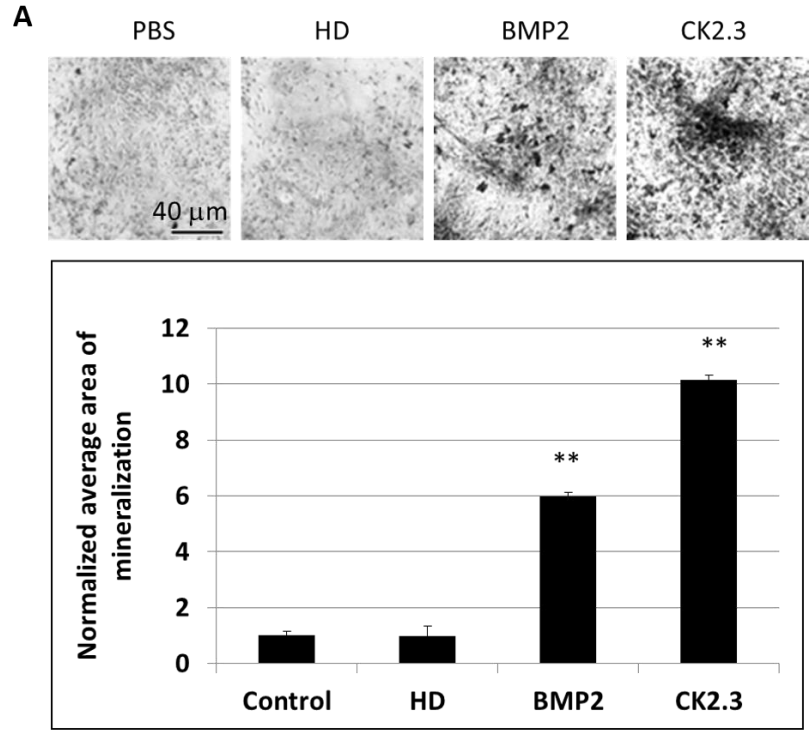
A
PBS
HD
BMP2
CK2.3
40 μm
Normalized average area of mineralization
12
10
8
6
4
2
0
**
**
Control
HD
BMP2
CK2.3

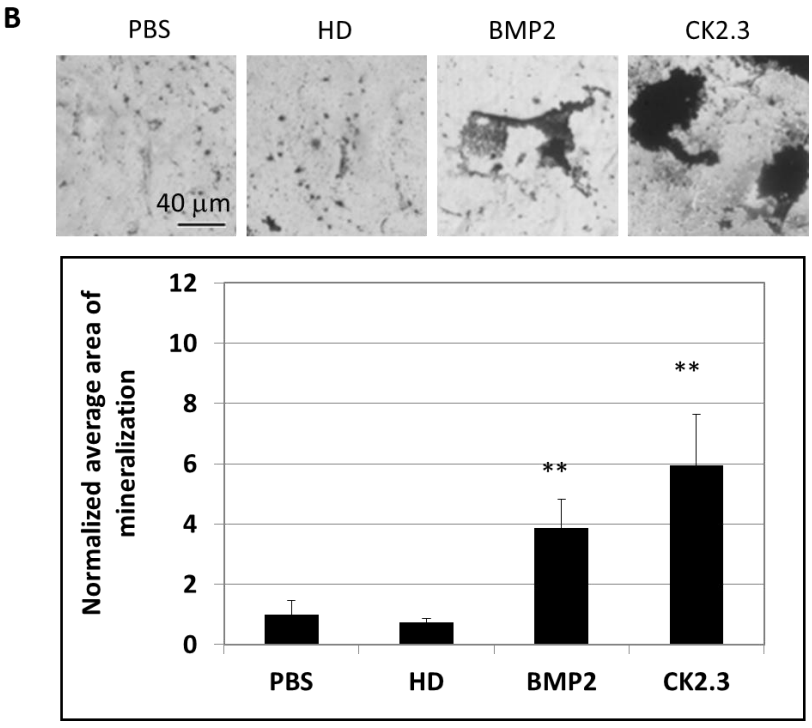
B
PBS
HD
BMP2
CK2.3
40 μm
Normalized average area of mineralization
12
10
8
6
4
2
0
**
**
PBS
HD
BMP2
CK2.3

Figure 2.2 **CK2.3 stimulation of primary calvarial and BMSCs led to increased mineralization.** A) Primary calvarial cells and B) BMSCs stimulated with PBS, HD (Antennapedia Homeodomain), 40nM BMP2, and 100nM CK2.3. 3 independent experiments were performed. Error bars represent SEM (** $p < 0.01$).

2.3.2 In vivo effects of CK2.3 on serum bone specific markers

To determine if bone remodeling was altered in mice systemically injected with CK2.3, I first examined changes in the serum levels of the osteoblast activity markers, alkaline phosphatase (ALP) and osteocalcin, and the osteoclast activity marker, TRACP 5b. ALP (Figure 2.3A) and osteocalcin (Figure 2.3B) were significantly increased in CK2.3 injected mice, but were not significantly elevated in BMP2 treated or PBS control mice. Further, only the CK2.3 injected mice showed significant reduction in TRACP 5b levels (Figure 2.3C). Interestingly, BMP2 showed increase levels of TRACP 5b even 4 weeks after injection. These studies suggest that CK2.3 increases bone formation without the subsequent increase in osteoclast activity seen in BMP2 treated animals.

A

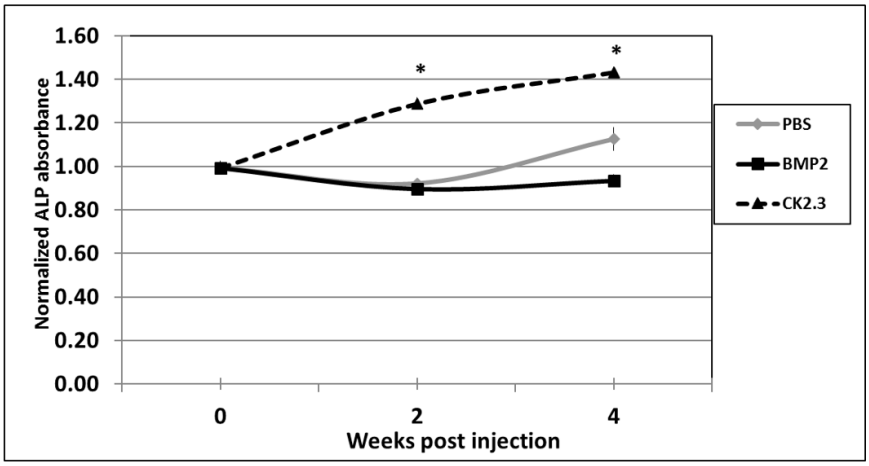
1.60
1.40
1.20
1.00
0.80
0.60
0.40
0.20
0.00
Normalized ALP absorbance
*
*
0
2
4
Weeks post injection
PBS
BMP2
CK2.3

B

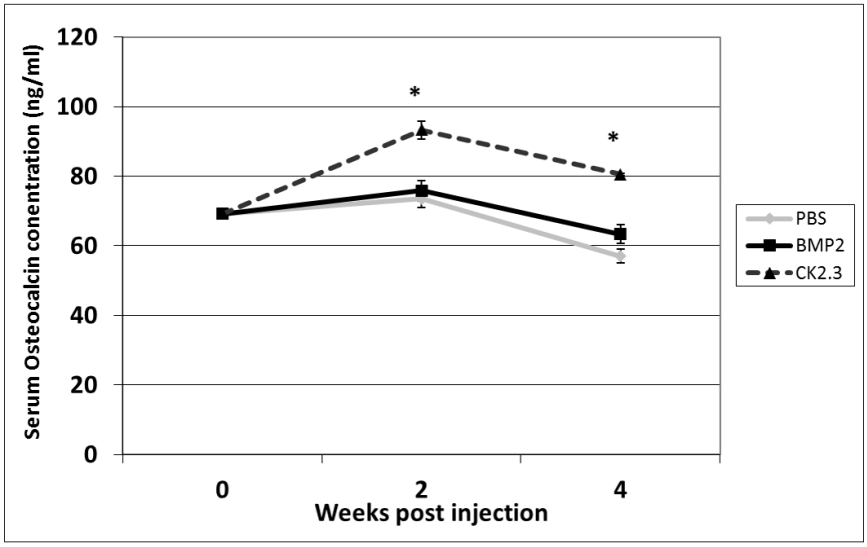
120
100
80
60
40
20
0
Serum Osteocalcin conentration (ng/ml)
*
*
0
2
4
Weeks post injection
PBS
BMP2
CK2.3

C

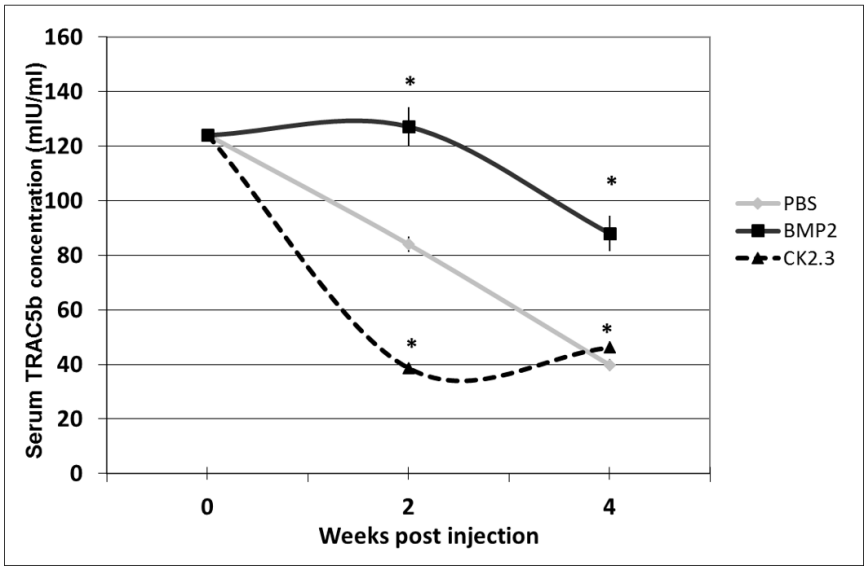
160
140
120
100
80
60
40
20
0
Serum TRAC5b concentration (mIU/ml)
*
*
*
*
0
2
4
Weeks post injection
PBS
BMP2
CK2.3

Figure 2.3 **Systemic injection of CK2.3 led to increased ALP and Osteocalcin serum levels, while TRACP 5b serum level was decreased**. Serum analysis of mice injected with CK2.3, BMP2, and PBS at weeks 0, 2 and 4 for A) ALP, B) osteocalcin, C), TRACP5b. Blood from mice (n=7/group) were pooled and analysis was performed. Error bars represent SEM (* $p < 0.05$).

2.3.3 Altered bone architecture and density in mice treated with CK2.3

To determine changes in trabecular and cortical bone structure and density in mice treated with CK2.3, I imaged mice treated with CK2.3, BMP2, or PBS control using pQCT and MicroCT. Mice injected with either BMP2 or CK2.3 demonstrated a significant increase in trabecular BMD (Figure 2.4A.), but no change in cortical BMD was detected (Figure 2.4B). MicroCT measurements revealed increases in bone volume fraction, the number of trabeculi (Tb.N), trabecular thickness (Tb.Th), and decreases in trabecular spacing (Tb.Sp) (Figure 2.4C). These data were supported by histological measurements of bone formation using Calcein labeling measurements in femurs of CK2.3, BMP2, and PBS injected mice (Figure 2.4C). These histological measurements also revealed higher MAR in CK2.3 injected mice compared to PBS injected mice (Figure 2.4C).

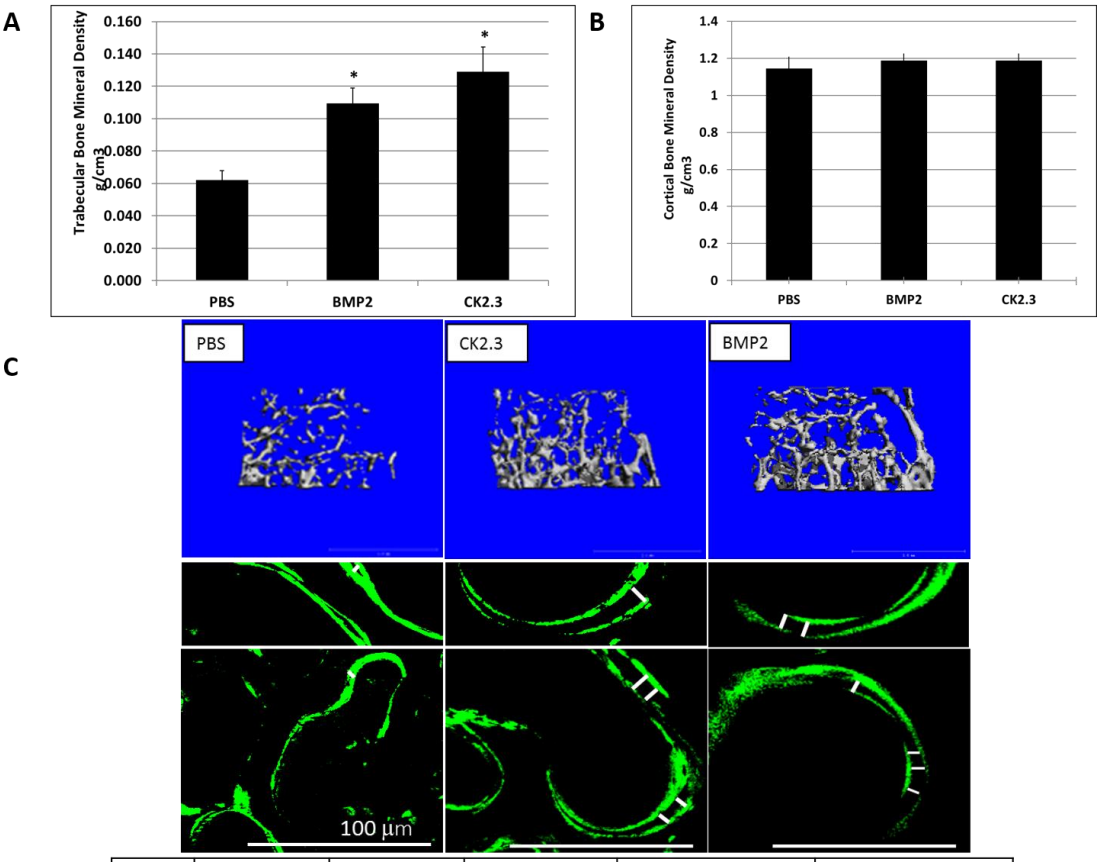

	BV/TV in %	TB.N (1/mm)	Tb.Th (mm)	Tb.Sp (mm)	MAR µm/day
PBS	23.3+/- 3.8	2.67+/-0.16	0.042+/-0.004	0.38+/-0.026	0.6+/-0.3
CK2.3	38.9+/-0.35*	3.19+/-0.13*	0.048+/-0.003	0.32+/-0.010*	2.2+/-0.3*
BMP2	37.9+/-0.46*	2.85/-0.12	0.048+/-0.001	034.+/-0.007	1.5+/-0.3*

Figure 2.4 **CK2.3 increased trabecular BMD as measured by pQCT and MicroCT.** pQCT and MicroCT analysis of femurs from mice injected with PBS, CK2.3 and BMP2 (n=7/group). A) Trabecular Bone Mineral Density, B) Cortical Bone Mineral Density C) MicroCT analysis and Calcein labelling of bone to determine MAR. (Top panel) Representative rendering of trabecular bone architecture (middle panel) calcein labeling. The white bar in middle panel represents bone growth over time. Error bars represent SEM (* $p < 0.05$).

2.3.4 SMAD and ERK in vivo signaling with CK2.3 treatment

BMPs mediate their actions through both Smad and Smad-independent signaling pathways to enhance osteogenesis (Ryoo et al., 2006). In order to identify CK2.3 induced signaling in bone formation I stained MMA embedded femur slices for Smad 1,5,8 and p-ERK to determine which pathway was prevalent in CK2.3 signaling. Osteoblasts lining the marrow cavity (MC), known as the lining cells (LC) aid in mineralization of the trabecular bone (TB). Osteoblasts and osteocytes (OT) actively expressed p-ERK in CK2.3 injected mice post 4 weeks (Fig 2.5). However, I did not observe p-ERK expression in femur samples of BMP2 and PBS injected mice (Fig 2.5). These data suggest that ERK is activated in CK2.3 injected mice 4 weeks after the final injection.

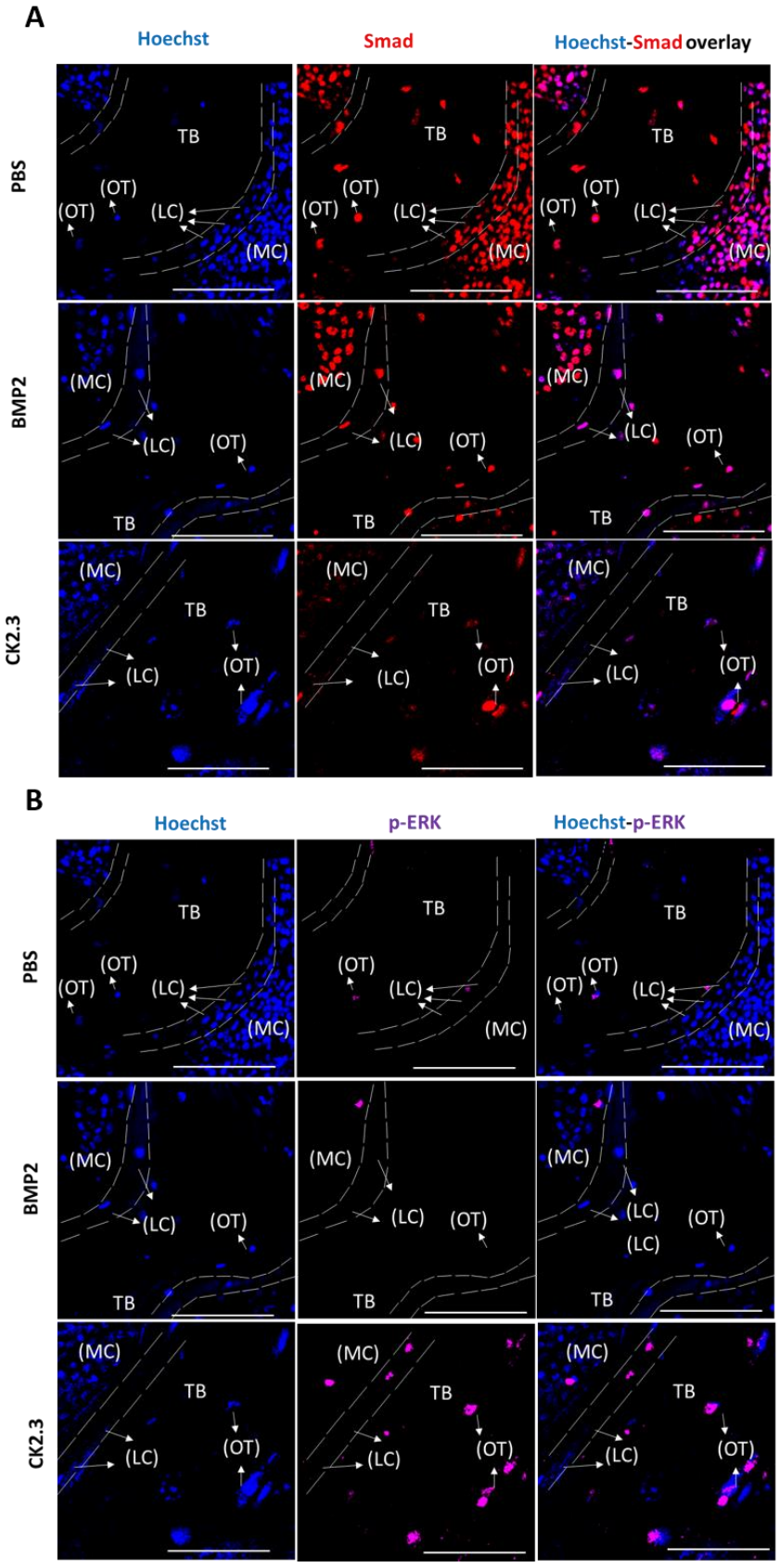
A
Hoechst
Smad
Hoechst-Smad overlay
PBS
BMP2
CK2.3
TB
(OT)
(LC)
(MC)
B
Hoechst
p-ERK
Hoechst-p-ERK
PBS
BMP2
CK2.3
TB
(OT)
(LC)
(MC)

Figure 2.5 **Injection of CK2.3 into mice led to an increase in p-ERK.** Bone in combination with a nuclear stain was used to determine the cell type (LC=Lining Cells, OT=Osteocytes) and location (MC= Marrow Cavity, TB=Trabecular Bone) within the bone (green, blue). A) Femurs from PBS, BMP2, CK2.3 injected mice (n=3 per group) fluorescently labelled for the nucleus in blue, Smad in red followed by the overlay. B) Femurs from PBS, BMP2, CK2.3 injected mice (n=3 out of 7/group) fluorescently labelled for the nucleus in blue, p-ERK in magenta followed by the overlay. Sections were imaged in the Trabecular Bone (TB) around Marrow cavity where the Lining cells (LC) or the active osteoblasts reside alongside of osteocytes (OT) indicated by arrows. Immunostaining shows increased p-ERK in CK2.3 injected as indicated by the arrows but not Smad1,5 and 8. p-ERK was not observed in PBS, and BMP2 injected mice. Scale bar representing 50μm.

2.3.5 CK2.3 decreases osteoclastogenesis and osteoclast activity

Next I determined if CK2.3 injected mice exhibit decreased osteoclastogenesis and osteoclast activity (Fig 2.6A, B). While increased osteoclast activity was observed in PBS and BMP2 injected mice, it was decreased in mice injected with CK2.3. This was correlative to the TRAC5b levels. These data are in accordance to previously shown data demonstrating reduced osteoclastogenesis and osteoclast activity in CK2.3 stimulated cultures (Bragdon et al., 2011b).

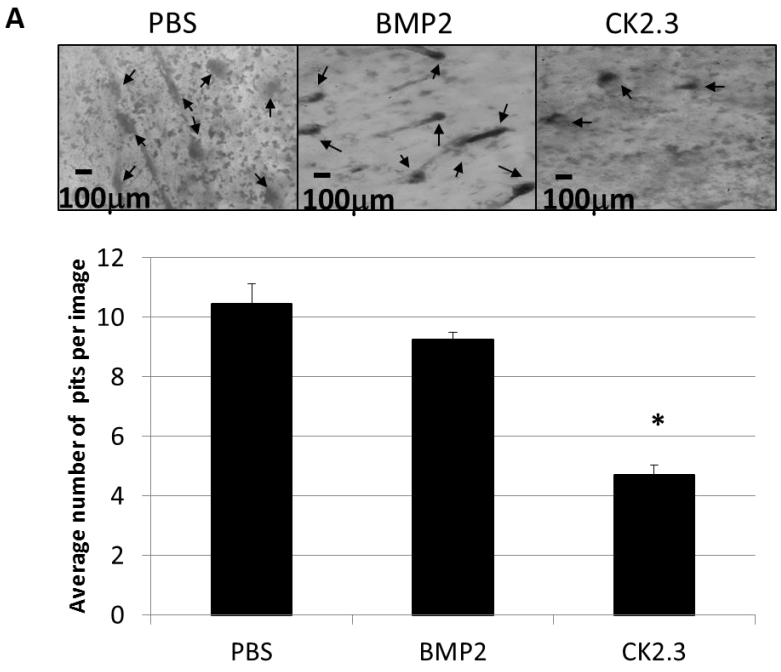
A
PBS
BMP2
CK2.3
100μm
100μm
100μm
Average number of pits per image
12
10
8
6
4
2
0
*
PBS
BMP2
CK2.3

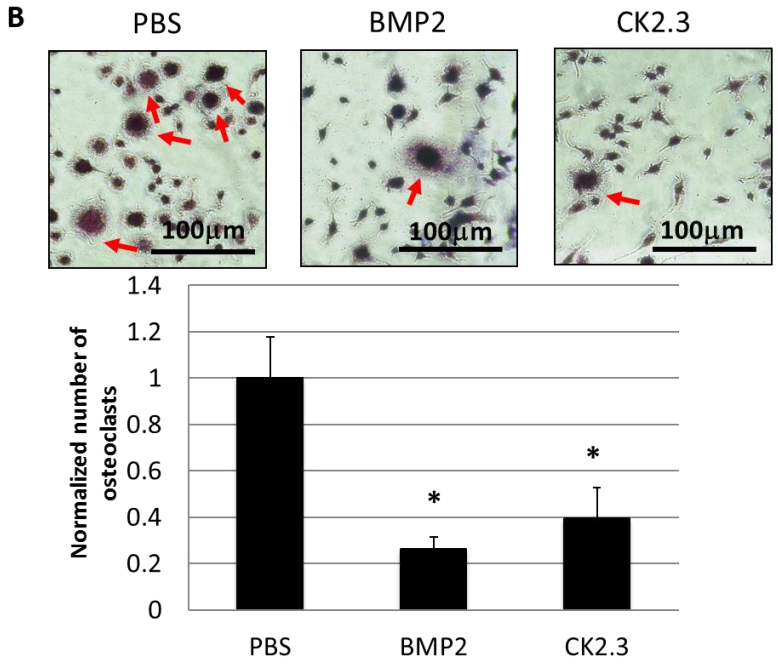
B
PBS
BMP2
CK2.3
100μm
100μm
100μm
Normalized number of osteoclasts
1.4
1.2
1
0.8
0.6
0.4
0.2
0
*
*
PBS
BMP2
CK2.3

Figure 2.6 **Injection of CK2.3 into B6 mice caused decreased osteoclast activity** (A) and osteoclastogenesis (B) in osteoclasts isolated from the spleen. Spleen cells isolated from CK2.3, BMP2, and PBS injected mice are seeded on (A) Bovine femoral bone chips (n = 6 per treatment) and (B) cultured in 1.9cm2 dishes (n = 6 per treatment) using osteoclast differentiation media. Measured for (A) osteoclast activity in pit formations, and (B) number of differentiated osteoclasts and were normalized to the control. At least three independent experiments were performed from spleen cells isolated from mice (n=7/group). Error bars represent SEM (* $p < 0.05$).

2.3.6 Peptide CK2.3 localized to marrow cavities

Post 4 weeks of CK2.3 injections in mice via the tail vein, mice femurs were extracted and embedded in MMA. These femur samples were bisected longitudinally across the sagittal plane for analysis of the trabecular architecture between PBS, BMP2, and CK2.3 injected mice. Here I wanted to know whether the CK2.3 localization affects the overall bone growth. What I discovered upon immunostaining for the antennapedia homeodomain as system to detect the peptide, is peptide CK2.3 is localized to the marrow cavities. This may explain how the peptide could have been trafficked through the blood to the marrow cavity to enhance osteoblastogenesis through the MSCs of the marrow cavity (Fig 2.7). This also an important aspect to be noted as I was able to pick up the peptide homing signal post 4 weeks of the injections.

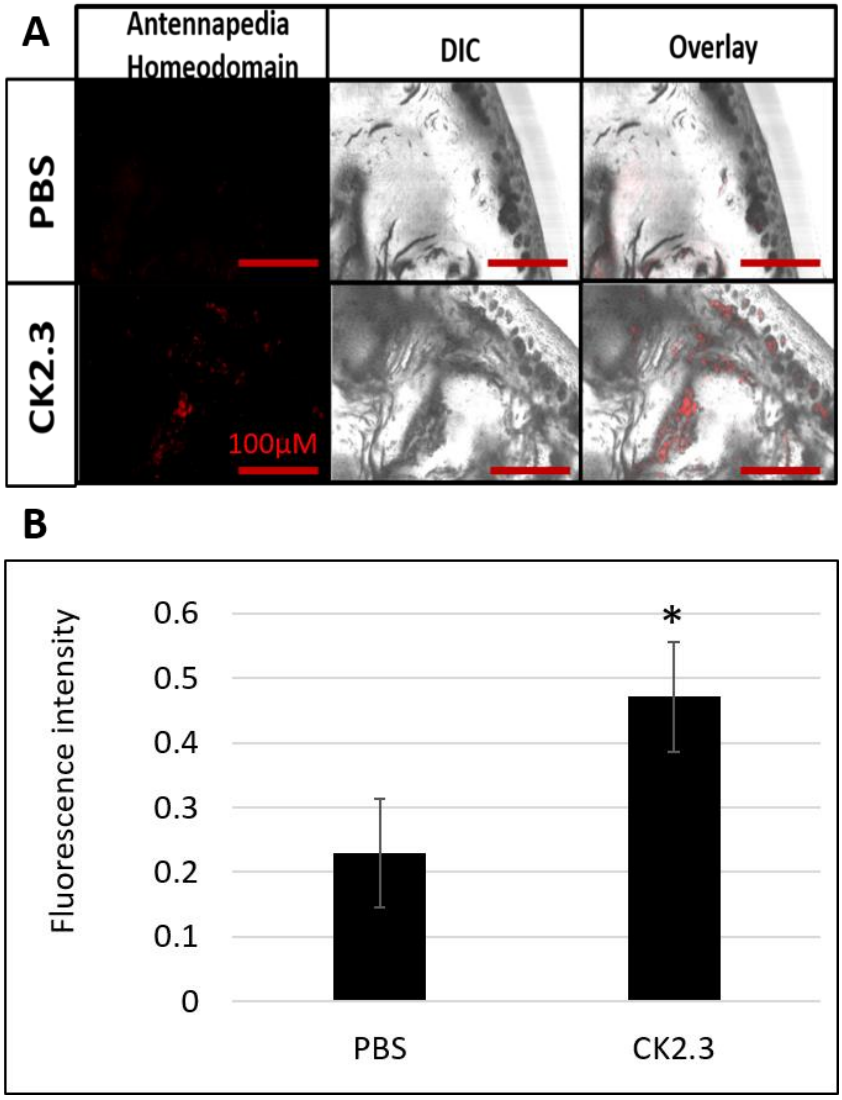

Figure 2.7 **Peptide CK2.3 is detectable in the mice femurs.** A) Sections of femurs from PBS and CK2.3 injected mice were stained with antibody recognizing the antennapedia homeodomain (HD) (n =3 per group). To determine whether CK2.3 was delivered to the femur, femur samples were fixed, embedded and sectioned on the sagittal plane as described previously. Sections from three separate CK2.3 injected or PBS control (n = 3 per group) mice were then fluorescently stained with an antibody against HD sequence located at the N-terminus of the CK2.3 peptide. Left immunostained bone sample for the HD (Sequence at N-Terminus of CK2.3), right DIC image of bone area. B) Fluorescent intensity quantified using ImageJ. Error Bars are SEM. * $p<0.05$.

2.4 Discussion

The discovery of Bone Morphogenetic Proteins revolutionized orthopaedic treatment of non-union fractures and bone loss. Injection of BMP2 significantly increases osteogenesis through increasing osteoblast production and stimulating these osteoblasts to increase bone formation. Previous work also showed that systemic delivery of 5μg/kg BMP2 resulted in increased bone formation in mice after 20 days (Turgeman et al., 2002). However, there are drawbacks to BMP2 treatment. Including the limited half-life of BMP2 and its role in osteoclastogenesis and bone resorption. Recent data suggested that BMP2 induces osteoclast activity (Jensen et al., 2010) and may cause increased bone turnover in the long term (Canalis et al., 2012). Here, I studied the effects of a novel mimetic peptide, CK2.3. CK2.3 acts downstream of BMPRIa and activates BMP2 signaling by releasing CK2 from BMPRIa. Although CK2.3 activates the Smad signaling pathway we previously showed that ERK activation is crucial for its function (Moseychuk et al., 2013). In this study I found significant differences between BMP2 and CK2.3 treatments both in vitro and in vivo. Injection of BMP2 and CK2.3 resulted in an increase in BMD and bone formation. This was shown by a decrease in trabecular spacing and a slight increase trabecular thickness though not significant to controls. Also the number of trabeculi was increased. Calcein injections demonstrated that within the last week of injection the MAR of CK2.3 and BMP2 were increased. However, my data suggest the mechanism of action may be different. CK2.3 but not BMP2 injection led to increase ALP and osteocalcin serum levels. These data suggest that osteoblast activity is increased in the CK2.3 injected mice after two weeks. Since BMP2 mice also showed increased BMD the increase in ALP and osteocalcin may have taken place at a different time point. This is correlative of non-systemic adenoviral infections of BMP2 resulting in increased ALP and osteocalcin (Tsuda et al., 2003).

Moreover, CK2.3 injection decreased TRACP 5b serum levels, suggesting a decrease in osteoclastogenesis. Interestingly, at 4 weeks TRACP 5C levels are similar to control, while BMP2 still showed high TRACP 5b level. This data was supported by the *in vitro* studies showing that CK2.3 treatment reduced osteoclast differentiation and decreased activity. While BMP2 decreased osteoclast differentiation, there was an increase in osteoclast activity. Previous research showed that BMP2 increases osteoclastogenesis in cultures (Itoh et al., 2001). I did not observe this increase. This effect may be caused by using spleen cultures instead of BMSCs to differentiate osteoclasts. My data further demonstrated that CK2.3 was delivered to the femur and could be detected at the end of the study (Fig 2.7). This indicates the effects of CK2.3 were not caused by a breakdown of the peptide and suggests a longer half-life than that of BMP2.

My study also uncovered the possible mechanism of bone formation induced by CK2.3. Immunostaining of femurs of CK2.3, but not BMP2 or PBS injected mice resulted in increased p-ERK levels in osteoblasts and osteocytes. This effect was confirmed by previous *in vitro* data. Overexpression of a mutant lacking the CK2.3 phosphorylation site lead to increased mineralization in vitro (Moseychuk et al., 2013). Using an ERK inhibitor this effect was negated. Taken together my immunostaining data suggest that activation of ERK is important for CK2.3 signaling. ERK signaling was shown to play an important role in Runx2 regulation, osteoblast differentiation, and skeletal development (Ge et al., 2007). However, little is known of BMP induced ERK signaling in bone formation in vivo. Mechanisms regulating these BMP induced pathways in bone formation remain unidentified. Furthermore, organ and blood analysis from mice did not demonstrate any signs of toxicity maintaining similar weights throughout these injected groups. All serum marker levels were within the normal

ranges as explained (Akkiraju et al., 2015; Boehm et al., 2007; CharlesRiver, 2012; Mazzaccara et al., 2008). In summary, I demonstrated the effect of the novel mimetic peptide of BMPRIa, CK2.3, as a mediator of osteogenesis and potent inducer of bone formation, without the secondary effects of osteoclastogenesis. This is in sharp contrast to BMP2 that enhanced both osteogenesis and osteoclast activity.

Chapter 3

CK2.1, A NOVEL PEPTIDE, INDUCES ARTICULAR CARTILAGE FORMATION IN VIVO

3.1 Background

Growth factors greatly influence the development and behavior of articular chondrocytes. Among these growth factors Bone Morphogenetic Proteins (BMPs), especially Bone Morphogenetic Protein 2 (BMP2), drives the development and maintenance of articular chondrocytes (Schmitt et al., 2003). BMP2 is a potent growth factor consisting of many pleiotropic functions, and plays a crucial role in the formation of the articular cartilage (AC) (Shu et al., 2011; van der Kraan et al., 2010). It drives the development of cartilage and induces the differentiation of mesenchymal progenitor cells (MPCs) into chondrocytes (Bragdon et al., 2010; Senta et al., 2009). It also plays a role in the maintenance of mature articular chondrocytes (Schmitt et al., 2003). One of the major drawbacks for the use of BMP2 as a therapeutic is that BMP2 affects all stages of chondrocyte differentiation. As a result, its known to induce chondrocyte hypertrophy followed by cartilage calcification (van der Kraan et al., 2010). Therefore, BMP2 may not be valuable as a therapeutic for cartilage formation or for cartilage restoration in degenerative diseases such as osteoarthritis (OA).

BMP2 signals through binding to type I and type II serine/threonine kinase receptors. Upon ligand binding type I receptor is phosphorylated by the constitutively active type II receptor at the GS box (glycine/Serine rich region) to initiate downstream signaling (Bragdon et al., 2010). Nohe lab previously reported that the protein Casein Kinase II (CK2) interacts with the Bone Morphogenetic Protein Receptor type Ia (BMPRIa) (Bragdon et al., 2010). Binding of BMP2 to BMPRIa releases CK2 and activates the Smad 1/5/8 pathway (Bragdon et al., 2010) (fig 3.1). Nohe lab has designed three peptides CK2.1, CK2.2, CK2.3 that inhibit the binding of CK2 to BMPRIa and activate the BMP signaling pathway in the absence of BMP ligand (Bragdon et al., 2010). Treatment of C2C12 cells with the peptide CK2.3 resulted in osteogenesis, while stimulation of C2C12 cells with CK2.2 resulted in adipogenesis and osteogenesis (Akkiraju et al., 2015; Bragdon et al., 2011b). Mutation of the CK2 phosphorylation sites on BMPRIa confirmed these effects (Moseychuk et al., 2013). Moreover, CK2.3 and CK2.2 activate the Smad and ERK1/2 signaling pathway (Bragdon et al., 2011b). Recent work also showed that CK2.3 induced bone formation in C57BL/6J mice, leads to increased Bone Mineral Density (BMD) and mineral apposition rate (Akkiraju et al., 2015). However, current data also show that the peptides CK2.3 and CK2.2 are more specific in the activation of the non-canonical BMP signaling pathways (Moseychuk et al., 2013). Since BMP2 signaling is also a major pathway activated during cartilage formation and growth, I evaluated the potential of the peptides to induce chondrogenesis and articular cartilage formation *in vitro* and *in vivo*. I found that one of the peptides CK2.1 is a potent inducer of chondrogenesis.

Stimulation of C3H10T1/2 cells and adult bovine chondrocytes with CK2.1 led to increased proteoglycan synthesis and collagen type II expression. At the end of 3 weeks CK2.1 treatments of adult bovine chondrocytes, greatly enhanced collagen type IX expression but not BMP2. In sharp contrast to BMP2 treatments enhanced collagen type X production in C3H10T1/2 and bovine chondrocytes and osteocalcin expression in C3H10T1/2 cells. Furthermore, 3week mRNA profiles of bovine chondrocytes treated with CK2.1 demonstrated a positive chondrogenic mRNA production shown by enhancing as SOX9, CREB, and ACAN. However, BMP2 treatments enhanced MEF2C marker of chondrocyte hypertrophy. Systemic injection of CK2.1 led to increased articular cartilage formation. Again in contrast to BMP2 CK2.1 did not induce collagen type X expression, however it led to increased collagen type IX expression *in vivo*. Moreover, injection of CK2.1 into the tail vein of mice did not lead to an increase in Bone Mineral Density as measured by pQCT. Taken together these data suggest that CK2.1 induces articular cartilage formation without induction of hypertrophy.

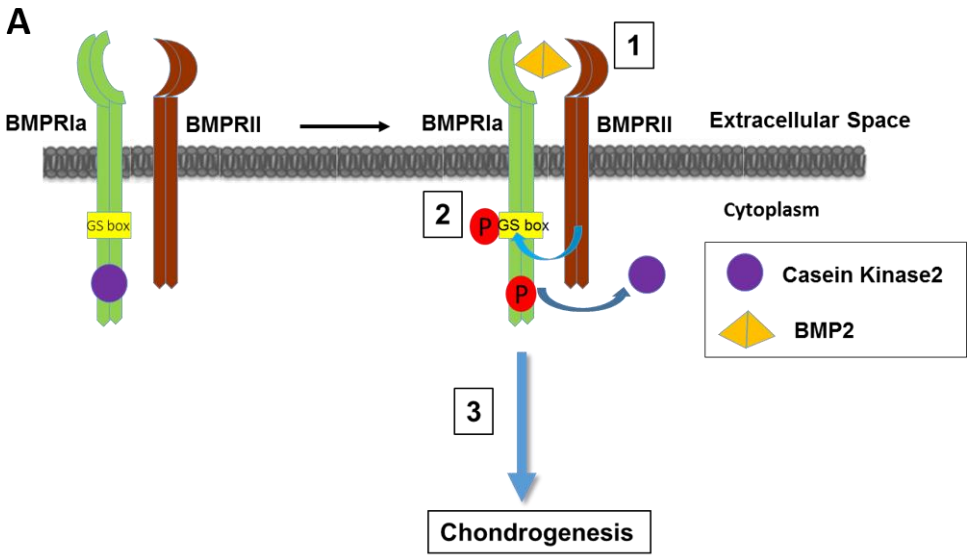
A
BMPRIa
BMPRII
BMPRIa
BMPRII
Extracellular Space
Cytoplasm
GS box
GS box
P
P
1
2
3
Casein Kinase2
BMP2
Chondrogenesis

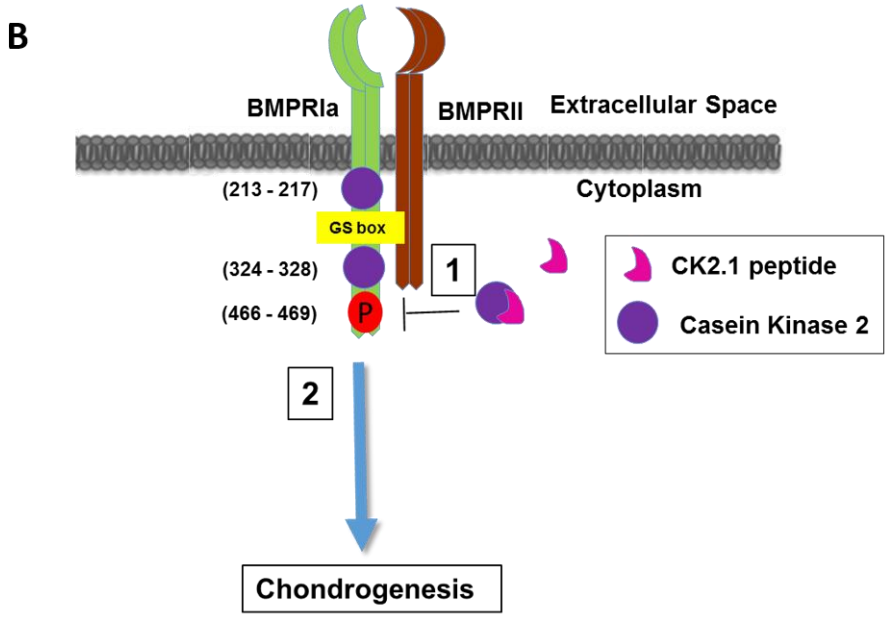
B
BMPRIa
BMPRII
Extracellular Space
Cytoplasm
(213 - 217)
GS box
(324 - 328)
(466 - 469)
P
1
2
CK2.1 peptide
Casein Kinase 2
Chondrogenesis

Figure 3.1 **Proposed mechanism of action of the peptide CK2.1**. A) Demonstrates the known mechanism of BMP2 mediated BMPRIa activation described according to the literature as follows: 1) Ligand binding to the BMPRIa and BMPRII receptor complex leads to the 2) release of CK2 allowing for phosphorylation of 3) downstream signaling to induce chondrogenesis. B) Schematic illustrates the possible mechanism of peptide through the activation BMPRIa downstream signaling as follows: 1) Peptide CK2.1 blocking of CK2 interaction to BMPRIa leads to 2) downstream signaling to induce chondrogenesis.

3.2 Materials and Method

3.2.1 Mouse injections

C57BL/6J mice were obtained from The Jackson Laboratory (Bar Harbor, ME) and maintained under conventional conditions. The animal protocol was approved by IUCAC at the University of Delaware. Eight week old female mice (C57BL/6J) were injected with peptides diluted in PBS via the tail vein at eight weeks of age (n=7 per group). A volume of 50 µl was injected for 5 consecutive days. CK2.1 injections were performed at a concentration of 1.7µg/kg. As a positive control BMP2 was injected at a concentration of 5µg/kg. Systemic delivery of 5µg/kg BMP2 for 20 days was shown previously to increase bone formation in mice (Turgeman et al., 2002). The ratio of BMP2 to CK2.1 peptide is based on the fact that 40nM BMP2 showed similar effects as 100nM CK2.1 *in vitro* (Bragdon et al., 2011b). As a negative control PBS was injected into mice.

3.2.2 Cell Culture

C3H10T1/2 cells were used as they are a well-established model for chondrogenesis and are responsive to BMP2 (Denker et al., 1999; Shea et al., 2003). These cells were purchased from American Type Culture Collection (CCL-26) (Manassas, VA) and monolayer cultures were maintained in T-75 flasks grown in Dulbecco's Modified Eagle's Medium (DMEM) (Mediatech, Manassas, VA) supplemented with 10% (v/v) Fetal Bovine Serum (FBS) (Gemini Bioproducts, West Sacramento, CA), 0.5% (v/v) L-Glutamine (Mediatech, Manassas, VA), and 1% (v/v) penicillin/streptomycin (100IU/ml penicillin, 100 µg/ml streptomycin (Fisher Scientific, Pittsburg, PA). Cultures were incubated at 37°C and 5% CO2, and cells were passaged at 90% confluency with 0.05% Trypsin-EDTA (Gemini Bioproducts, West Sacramento, CA).

3.2.3 Isolation of primary bovine articular chondrocytes

Chondrocytes were isolated from articular cartilage of immature calf knees obtained from the local butcher shop within 48 hrs of slaughter. Articular cartilage was shaved from the articular surface carefully and washed with serum free DMEM medium, then minced and digested using collagenase treatment (300units/10ml) (Gemini Bioproducts, West Sacramento, CA) in DMEM containing 10%FBS at 37ºC (Bhardwaj et al., 2011; Kuettner et al., 1982). Cartilage cells digested in DMEM containing collagenase were strained with 70µm cell strainer (Corning, Durham, NC) to minimize clumps, cells were suspended in DMEM with 10% FBS, spun down and

seeded on 12-mm glass coverslips in 24-well plates at high density (1 x 10^6 cells/ml). Media was exchanged every four days to maintain cells. Protocol was optimized and modified from previously done work (Kerrigan et al., 2006).

3.2.4 Design of peptides

Peptides were designed by the Nohe group as previously described (Bragdon et al., 2010). A prosite search including patterns with high probability of occurrence on BMPRIa yielded possible CK2 phosphorylation sites located at amino acids 213-217 (SLKD), 324-328 (SLYD), and 466-469 (SYED). The peptides were designed with the Antennapedia homeodomain signal sequence for cellular uptake and incorporated in one these binding sites: CK2.1 (SYED), CK2.2 (SLYD), or CK2.3 (SLKD). The peptides included several amino acid residues flanking each side (Bragdon et al., 2010).

3.2.5 Alcian blue staining

C3H10T1/2 cells were seeded at 1 x 10^7 cells/ml and plated as 10µl micromass culture in a 1.9 cm^2 24 well plate (Nunc, Rocskilde, Denmark). Cells were supplemented with DMEM with 10% FBS and incubated at 37°C and 5% CO_2. Cells were then stimulated with recombinant BMP2 (40 nM, or 200 nM), or the peptides CK2.1, CK2.2, and CK2.3 (100nM,) there were purchased from Genscript (Piscataway, NJ, USA). Peptide concentrations of 100nM is equivalent to the effect of BMP2 at 40nM, hence the experimental setups were stimulated accordingly(Bragdon et al., 2011b) (Denker et al., 1999).

Seven days after stimulation cultures were fixed using 10% neutral buffered formalin (pH7.4) mixed with 0.05% wt/v cetylpyridinium chloride for 20 minutes at room temperature. Cells were rinsed three times with 3% glacial acetic acid (pH 1.0), and stained using 0.5% Alcian blue 8-GX stain (Life line, Walkersville, MD) overnight. After staining cultures were rinsed with 3% glacial acetic acid (pH 1.0) and air dried. Stained cultures were viewed under an inverted light microscope (Nikon, TMS-f) using 20X magnification and the collected images were analyzed and quantified with ImageJ software (NIH, Bethesda) (Bruce et al., 2010). Samples were run in triplicates and at least 5 images per well were obtained for analysis.

3.2.6 Von Kossa staining

C3H10T1/2 cells were seeded at $1x10^4$ cell/cm^2 and were grown to 90% confluence in 1.9 cm^2 24 well plate. These cell were treated with CK2.1 (100nM or 500nM) and equivalent concentrations of BMP2 (40nM or 200nM). For comparison cells were also stained with CK2.2, CK2.3 at 100nM. Von Kossa staining was performed as described by Nohe lab previously (Bragdon et al., 2010). Samples were run in triplicates and at least 5 images per well were obtained for analysis.

3.2.7 Smad reporter assay

C3H10T1/2 cells were cultured on 60 mm dishes to 90% confluence. Prior to transfection, cells were serum starved in DMEM media without FBS overnight. Cells were transfected with 2µg of plasmids encoding pSBE-luc (Smad Binding Element)

tagged firefly luciferase and pRLuc tagged with renilla luciferase (Promega, Madison, Wisconsin) using turbofect (Fermentas, Glen Burnie, MD) transfecting reagent, according to manufacturer's protocol, in DMEM media supplemented with 10%FBS. The pSBE contains a BMP responsive Smad-Binding Elements as a readout for Smad signaling **(Jonk et al., 1998; Nohe et al., 2002).** After transfection, cells were stimulated or not stimulated for 24 hours with 40nM or 200nM of BMP2, 100nM or 500nMof peptide CK2.1, or 100nM of peptide CK2.2, or CK2.3. Cells were lysed with 1X passive lysis buffer (Biotium, Hayward, CA) and reporter gene assay was performed with a dual luciferase assay kit (30005-2) (Biotium Hayward, CA, USA).

3.2.8 Quantitative RT-PCR analysis

Total RNA was isolated after five days from cultured bovine articular chondrocytes stimulated with BMP2 (40nM), or peptide CK2.1 (100nM, 500nM). The Trizol method was used according to manufacturer's protocol (Invitrogen). 1 μg of mRNA was used to synthesize cDNA by using an iScript^{TM} cDNA synthesis kit (BioRad, Hercules, CA). Quantitative PCR reactions were run in triplicate. Primer sets specific for cartilage markers were purchased from Integrated DNA Technologies (IDT, Coralville, IA). For primers sets of *SOX9,* cAMP Responsive Element Binding protein (*CREB),* Cartilage Oligomeric Matrix Protein (*COMP),* the relative fold change in mRNA was compared to housekeeping gene *GAPDH*. Each sample was run in triplicate, cycle threshold values (C_T) values were obtained for each gene of interest. Fold change

was calculated using comparative C_T method, normalizing the target mRNA amount to *GAPDH* according to (Schmittgen and Livak, 2008; Vandesompele et al., 2002).

3.2.9 Peripheral quantitative computed tomography (pQCT)

Isolated femur lengths were measured with digital calipers (Stoelting, Wood Dale, IL), then femurs were measured for density using the SA Plus densitometer (Orthometrics, Stratec SA plus Research Unit, White Plains, NY). Calibration of the SA Plus instrument was done with hydroxyapatite standards of known density (50 - 1000 mg/mm^3) with cylindrical diameters 2.4 mm and length 24 mm that approximate mouse femurs. Assessment of defined thickness aluminum foils indicated accurate measurement of the 0.25 mm thick foil, whereas a 0.02 mm thick foil could not be measured. The bone scans were analyzed with distinct threshold settings to separate bone from soft tissue. Thresholds of 710 and 570 mg/cm^3 were used to determine cortical bone areas and surfaces. These thresholds were selected to yield area values consistent with histomorpho-metrically derived values and the defined density standards noted above. To determine mineral content, a second analysis was carried out with thresholds of 220 and 400 mg/cm^3. These lower thresholds were selected so that mineral from most partial voxels (0.07 mm) would be included in the analysis. Density values were calculated from the summed areas and associated mineral contents. Precision of the SA Plus for repeated measurement of a single femur was found to be 1.2%. Isolated femurs were scanned at 7 locations at 2 mm intervals, beginning 0.8 mm from the distal ends of the epiphyseal condyles. Due to variation in femur lengths, the femoral head

could not be scanned at the same location for each bone, and thus was not included in final data. Total vBMD values were calculated by dividing the total mineral content by the total bone volume (bone + marrow) and expressed as mg/mm^3. (Akkiraju et al., 2015; Beamer et al., 2012; Bouxsein et al., 2004)

3.2.10 Histology

After 4 weeks mice were sacrificed and extracted femurs were fixed in 10% Neutral Buffered Formalin (Sigma Aldrich, St. Louis, MO) and decalcified for 5 days in 5% formic acid in 10% sodium citrate (Sigma Aldrich, St. Louis, MO). Samples were bisected longitudinally through interchondular notch to separate medial and lateral condials for paraffin embedding. Paraffin embedded blocks were sliced to 6µm thickness and stained by Safranin O and fast green staining (Srinivasan et al., 2012). The following samples were measured for AC formation using the width in 7 different places on each samples and normalized to controls.

3.2.11 Immunostaining

Sectioned femur samples (pre-treated in xylene for 10 minutes to clear away the paraffin) and C3H10T1/2 cells and bovine chondrocytes plated on coverslips were incubated with testicular hyaluronidase for 30 minutes to expose collagen epitopes. C3H10T1/2 samples were immunofluorescently labeled for 1 hour at room temperature either with rabbit polyclonal IgG collagen type II (10µg/ml, ab34712, Abcam, UK) followed by Alexa 546 donkey anti rabbit IgG (2µg/ml. Abcam, UK) or rabbit

polyclonal collagen IX (10µg/ml, Abcam, UK) followed by Alexa 647 goat anti-rabbit IgG (2µg/ml, Invitrogen, Eugene, OR) or Goat polyclonal IgG MMP13 (10µg/ml, Santa Cruz Biotechnology, CA, USA) followed by Alexa 568 donkey anti goat (2 µg/ml, Invitrogen, Eugene, OR) or Rabbit (Rb) pAb collagen X (10µg/ml, ab58632, Abcam, UK) followed by Alexa flour 488 donkey anti-rabbit (2µg/ml. Invitrogen, Eugene, OR) or Rabbit polyclonal IgG Osteocalcin (10µg/ml, Santa Cruz Biotechnology, CA, USA) followed by Alexa flour 488 donkey anti-rabbit (2µg/ml. Invitrogen, Eugene, OR). Antibodies were diluted in 3% BSA. The nuclear stain bisbenzimide (Sigma Aldrich, St. Louis, MO, Hoechst dye No 33258, dissolved in H_2O) was administered for five minutes and coverslips were mounted on slides using Airvol as described previously (Nohe et al., 2005; Nohe and Petersen, 2007). Images were taken (n = 8 image sections/sample) on the Zeiss 780 confocal with a 20X objective (0.75NA, Beam Splitter [MBS] 458/514/561/633, 5% laser output, and [MBS] 405, 2% laser output. Images were quantified using ImageJ (NIH, Bethesda).

Chondrocytes cultured on coverslips were incubated with testicular hyaluronidase for 30 minutes to expose collagen epitopes. The samples were immunofluorescently labeled for 1 hour at room temperature either with rabbit polyclonal IgG collagen type II (10µg/ml, ab34712, Abcam, UK) followed by Alexa 488 donkey anti rabbit IgG (2µg/ml. Invitrogen, Eugene, OR) or mouse Collagen IX (Anthrogen – CIA Collagen staining kit) diluted 1:100 in 3% BSA followed by a 1:1000 dilution of Alexa 633 goat anti-mouse IgG (Invitrogen, Eugene, OR) for 1 hour or Goat polyclonal IgG (Santa Cruz Biotechnology, CA, USA) diluted 1:1000 in 3%BSA

followed by Alexa 568 donkey anti goat (1:1000; Invitrogen, Eugene, OR) or Rabbit (Rb) pAb Collagen X (Abcam) diluted with 1:100 following by Alexa flour 488 goat anti-rabbit (1:1000). The nuclear stain Hoechst (Thermoscientific, West Palm Beach, FL) was administered for two minutes and coverslips were mounted on the slides using Airvol (20g Airvol, 80ml sterile dH_2O, stirred at 60^oC-70^oC for 2 hours, 40ml glycerol, 0.2ml of 0.2M Tris pH 8.5, centrifuged at 1800 x G) (Nohe and Petersen, 2007). Samples were run in triplicates and at least 8 images per well were obtained for analysis.

3.2.12 Statistical Data Analysis

All data presented were analyzed using single factor anova, followed by Tukey Kramer post-hoc test. All experiments were repeated three or more times and normalized to control. Maximum of three outliers were removed using the Chauvenets Criterion, but minimum number of samples required for statistical significance were used for the following analysis. Error bars represent standard error of the mean (SEM), where * denotes ($p<0.05$) and ** denotes ($p<0.01$) statistical significance.

3.3 Results

3.3.1 CK2.1 but not CK2.2 or CK2.3 induced chondrogenesis in C3H10T1/2 micromasses

To evaluate the effect of CK2.1, CK2.2, and CK2.3 on chondrogenesis, C3H10T1/2 cells were cultured as micromasses and stimulated with 100nM of the corresponding peptides. Cells were stimulated with the peptides at 100nM a 2.5 times higher concentration compared to BMP2 at 40nM based on previous experiments (Bragdon et al., 2011b). After stimulating C3H10T1/2 micromasses for 3weeks proteoglycan synthesis, a marker for chondrogenesis, was evaluated by Alcian blue staining (Denker et al., 1999). Positive control cells were stimulated with BMP2 (40nM). As Figure 3.2A demonstrates only CK2.1 induced chondrogenesis in C3H10T1/2 cells similar to BMP2 stimulations. Optimal dosage of peptide CK2.1 induced chondrogenesis, was analyzed using concentration gradient stimulations on the C3H10T1/2 micromasses Figure 3.2B. This resulted in optimal dose range of the peptide at low dose 100nM to high dose at 500nM as seen in C2C12 cells for osteogenesis (Bragdon et al., 2011b). To test whether this CK2.1 induced chondrogenesis is via the activation of BMP signaling pathway I used a Smad reporter gene assay using the luciferase reporter construct pSBE-luc. C3H10T1/2 cells transfected with pSBE-luc and pRLUC (control for transfection efficiency) were stimulated with low and high doses of peptide CK2.1 and equivalent concentration of BMP2. Only cells stimulated with peptide CK2.1 and BMP2 but not CK2.2 or CK2.3 resulting in a significant increase in

SMAD activity similar between BMP2 and CK2.1 across equivalent concentrations (Fig 3.2C).

A

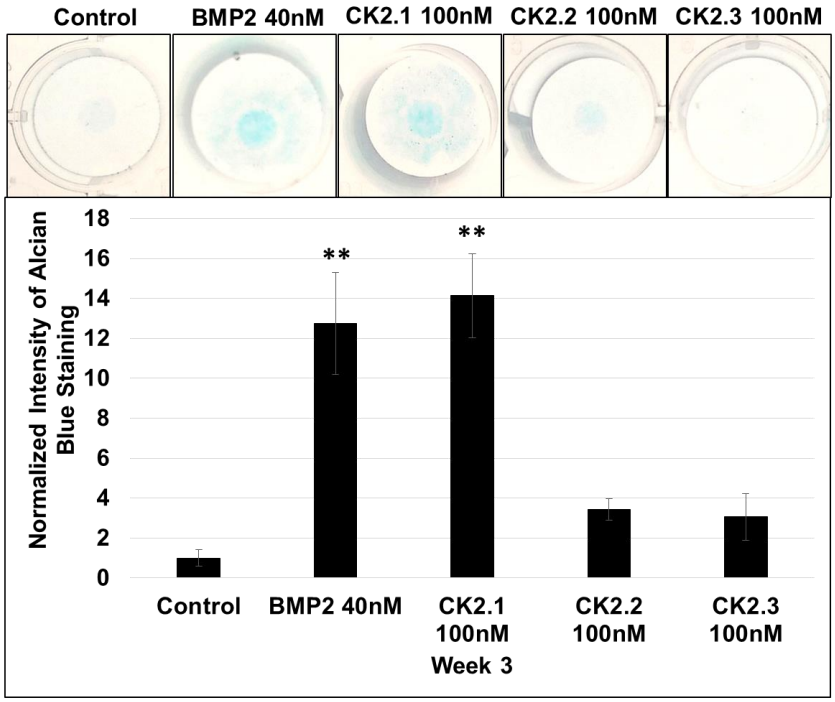
Control
BMP2 40nM
CK2.1 100nM
CK2.2 100nM
CK2.3 100nM
Normalized Intensity of Alcian Blue Staining
18
16
14
12
10
8
6
4
2
0
**
**
Control
BMP2 40nM
CK2.1 100nM Week 3
CK2.2 100nM
CK2.3 100nM

B

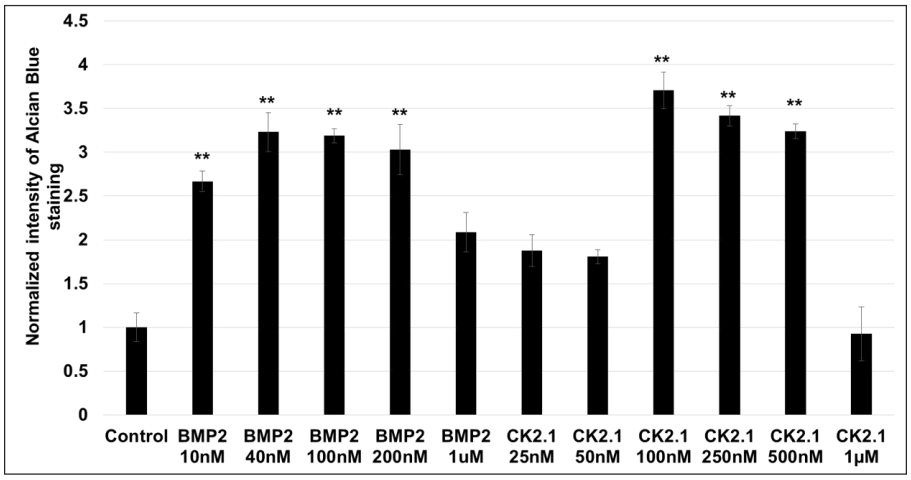
Normalized intensity of Alcian Blue staining
4.5
4
3.5
3
2.5
2
1.5
1
0.5
0
**
Control
BMP2 10nM
BMP2 40nM
BMP2 100nM
BMP2 200nM
BMP2 1uM
CK2.1 25nM
CK2.1 50nM
CK2.1 100nM
CK2.1 250nM
CK2.1 500nM
CK2.1 1µM

C

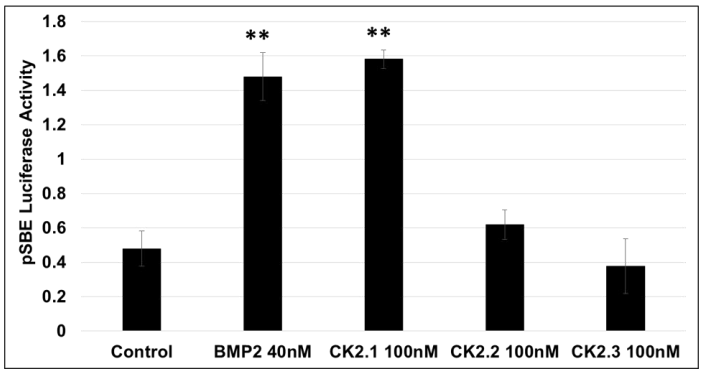
pSBE Luciferase Activity
1.8
1.6
1.4
1.2
1
0.8
0.6
0.4
0.2
0
**
Control
BMP2 40nM
CK2.1 100nM
CK2.2 100nM
CK2.3 100nM

Figure 3.2 **CK2.1 but not CK2.2 or CK2.3 induced chondrogenesis in C3H10T1/2 cells.** A) C3H10T1/2 micromass cultures were treated with either BMP2 (40nM) or peptides CK2.1 and CK2.2, CK2.3 at (100nM) and stained with Alcian blue for 3 weeks. BMP2 and CK2.1 treated cells showed a significant increase of ECM containing proteoglycans. B) Concentration curve of micromass stimulated with CK2.1 and BMP2 over 7 days. The treatments identified the concentrations of CK2.1 at 100nM to 500nM as the optimal doses for inducing chondrogenesis. C) Smad reporter gene assay performed on C3H10T1/2 cells stimulated with CK2.1 at 100nM or 500nM, CK2.2, and CK2.3 at 100nM and BMP2 at 40nM or 200nM. Only CK2.1 and BMP2 induced Smad activity and similar Smad activity was observed across the equivalent concentrations. Error bars represent SEM (* $p< 0.05$, ** $p<0.01$).

3.3.2 C3H10T1/2 and adult bovine chondrocytes cells stimulated with CK2.1 and BMP2 induced collagen type II expression

To further confirm peptide CK2.1 induced chondrogenic differentiation I examined collagen type II production in C3H10T1/2 cells. Chondrocytes actively produce collagen type II which make up the majority of collagen network in cartilage. Therefore, I stimulated C3H10T1/2 cells with the peptides CK2.1, CK2.2, and CK2.3 for 3 weeks. Similarly, primary bovine chondrocytes with CK2.1 for 3 weeks. As positive control cells were stimulated or not with BMP2. Cells were fixed and immunostained for collagen type II. Expression of collagen type II was quantified by confocal microscopy (Fig 3.3). Results demonstrate a significant increase in collagen type II production in CK2.1 stimulated cells compared to controls (Fig 3.3A, B).

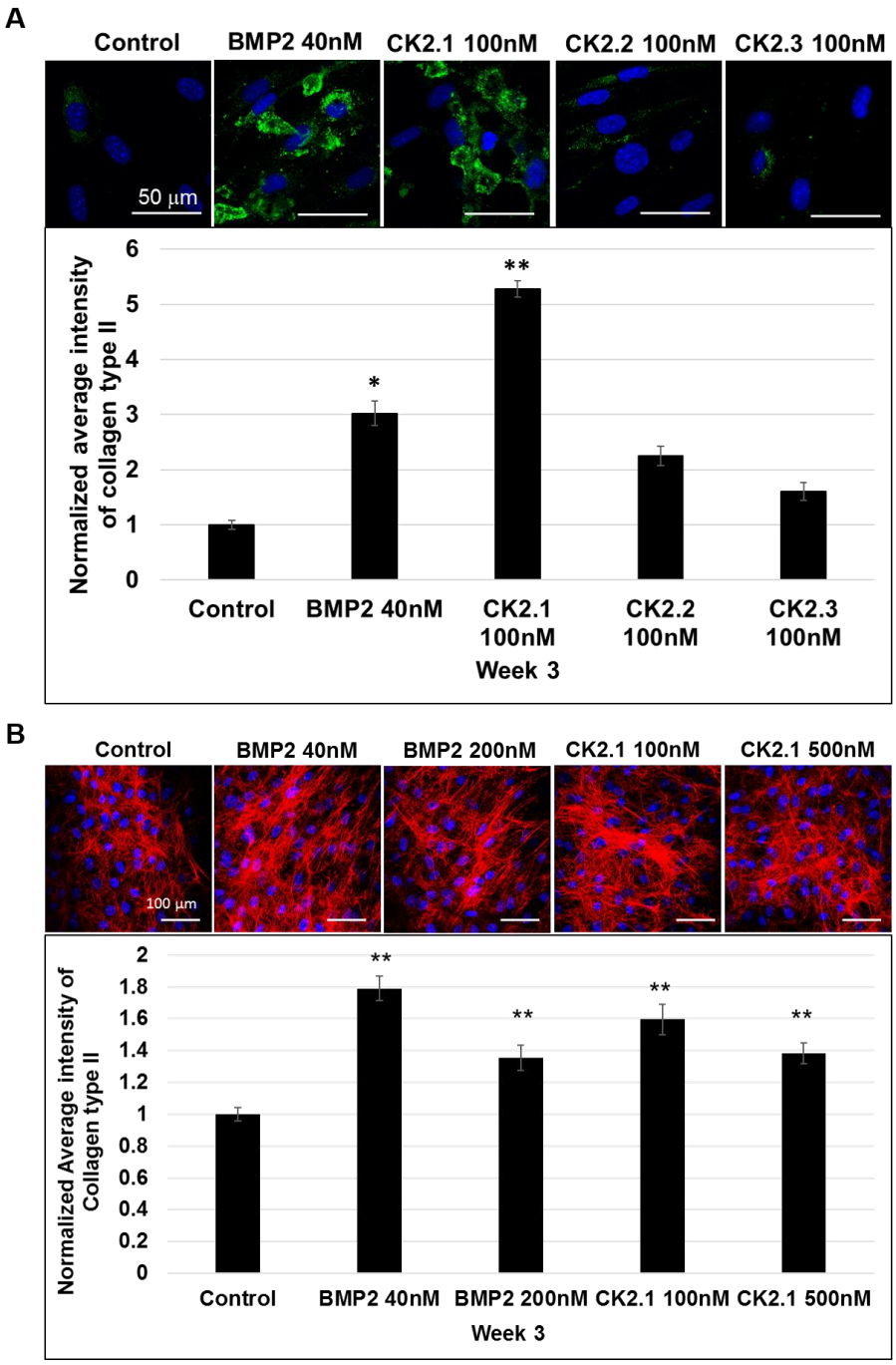
A
Control
BMP2 40nM
CK2.1 100nM
CK2.2 100nM
CK2.3 100nM
50 µm
Normalized average intensity of collagen type II
0
1
2
3
4
5
6
*
**
Control
BMP2 40nM
CK2.1 100nM
CK2.2 100nM
CK2.3 100nM
Week 3
B
Control
BMP2 40nM
BMP2 200nM
CK2.1 100nM
CK2.1 500nM
100 µm
Normalized Average intensity of Collagen type II
0
0.2
0.4
0.6
0.8
1
1.2
1.4
1.6
1.8
2
**
**
**
**
Control
BMP2 40nM
BMP2 200nM
CK2.1 100nM
CK2.1 500nM
Week 3

Figure 3.3 **CK2.1 induced collagen type II production in C3H10T1/2 cells and primary bovine chondrocytes**. A) C3H10T1/2 cells cultured for 3 weeks were stimulated with CK2.1, CK2.2 and CK2.3 at 100nM or with equivalent concentration of BMP2 40nM. B) Bovine chondrocytes cultured for 3 weeks were stimulated with CK2.1 and BMP2 that induced positive chondrogenic differentiation as a measure of collagen type II compared to control. Scale bar represent 50μm. Error bars represent SEM (* $p< 0.05$, ** $p<0.01$).

3.3.3 CK2.1 induced Collagen IX production but not Collagen X and MMP-13

C3H10T1/2 cells chondrogenic differentiation is distinguished by the synthesis of Collagen II and other early stage protein chondrogenic markers (Denker et al., 1999; Roy et al., 2010; Shea et al., 2003). However, mature cartilage marks the association of Collagen II with less abundant Collagen IX ECM protein (Poliard et al., 1999). Collagen IX along with Collagen II and XI make up two thirds of the articular cartilage (Eyre, 2002). However, Collagen IX a product of the mature chondrocyte is not found in its earlier stages of chondrocyte differentiation (Kipnes et al., 2003; Zaucke et al., 2001). Similarly, Collagen X and MMP-13 are produced by the hypertrophic chondrocytes and their upregulation marks the end stage of terminal differentiation, followed by mineralization of the tissue (Gelse et al., 2003a). Hence, mature bovine articular chondrocytes isolated and cultured were stimulated with CK2.1 (100nM or 500nM) or BMP2 (40nM) and determined protein expression levels of Collagen IX, Collagen X, and MMP-13 by immunostaining. Post 7 days of stimulation and incubation cells were fixed and stained for Collagen IX or Collagen X or MMP-13 (Fig 3.4). Protein expression was quantified by confocal microscopy. Analysis indicated an increased Collagen IX production but not Collagen X and MMP-13 with CK2.1

stimulation at concentrations of 500nM. This is in contrast to BMP2 at 40nM stimulation that resulted in a high expression of collagen type X and MMP-13 (Fig 3.4).

A

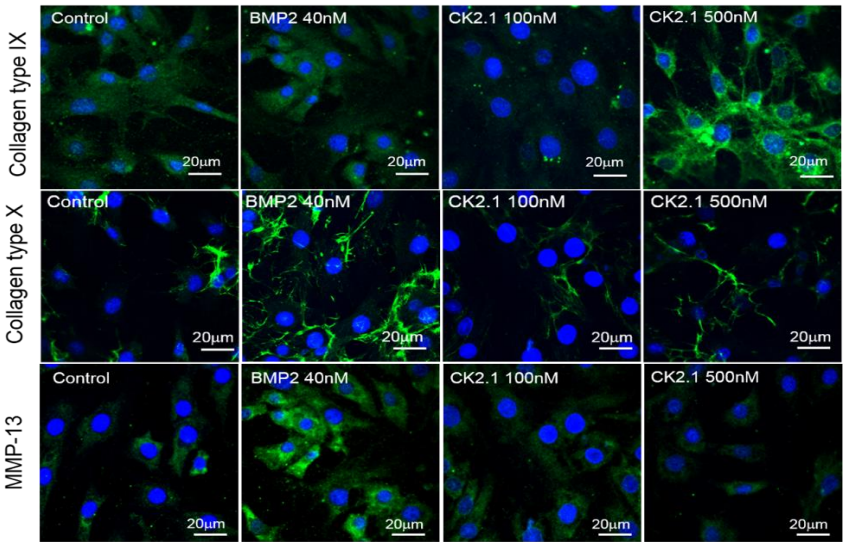
Collagen type IX
Collagen type X
MMP-13
Control
BMP2 40nM
CK2.1 100nM
CK2.1 500nM
20μm

B

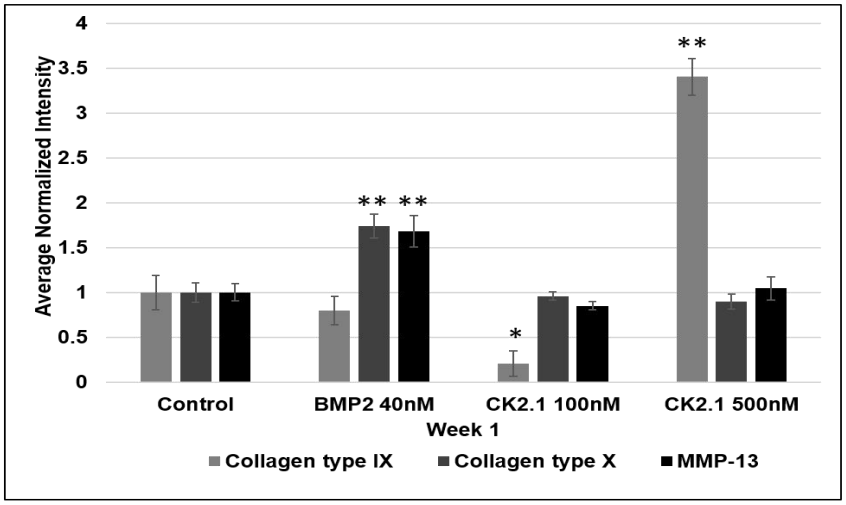
Average Normalized Intensity
4
3.5
3
2.5
2
1.5
1
0.5
0
**
**
**
*
**
Control
BMP2 40nM
CK2.1 100nM
CK2.1 500nM
Week 1
Collagen type IX
Collagen type X
MMP-13

C

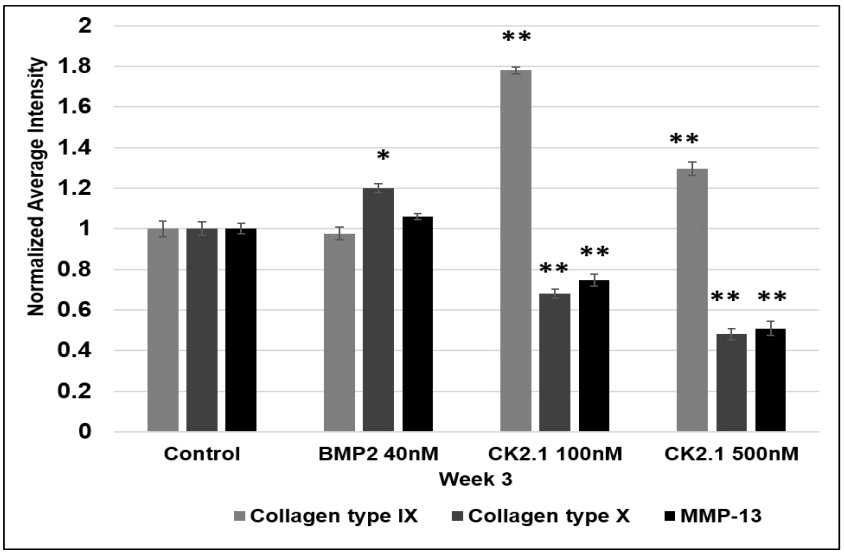
Normalized Average Intensity
2
1.8
1.6
1.4
1.2
1
0.8
0.6
0.4
0.2
0
*
**
**
**
**
**
**
Control
BMP2 40nM
CK2.1 100nM
CK2.1 500nM
Week 3
Collagen type IX
Collagen type X
MMP-13

Figure 3.4 **Collagen type IX production induced by peptide CK2.1 but not BMP2.** Primary bovine chondrocytes isolated from six-month old calf knee were cultured and stimulated with BMP2 40nM or peptide CK2.1 (100nM, 500nM) for 7 days and 21 days then fixed and immunostained for A) collagen type IX or collagen type X or MMP-13. In these representative figures collagen type IX, X, and MMP-13 staining was represented using green and the nuclear stain in blue. B) Images from week 1 C) Images from week 3 were analyzed and the data were normalized to controls. There was a significant difference in collagen type IX production in cells stimulated with peptide CK2.1 500nM compared to control, BMP2 40nM, or peptide CK2.1 100nM (B). But by week 3 CK2.1 at 100nM and 500nM had a significantly high collagen type IX and significantly low collagen type X. However, collagen type X production was significantly higher in cells stimulated with BMP2 40nM in comparison to control or cells treated with peptide CK2.1 100nM or 500nM. Experiments were averaged and normalized to controls and graphed with SEM as error bars (*, $p<0.05$), (**, $p<0.001$). Scale bars represent 20μm. Error bars represent SEM (* $p< 0.05$, **$p<0.01$).

3.3.4 Upregulation of chondrogenic specific markers upon CK2.1stimulation

Immunostaining confirmed protein expressions of the chondrogenic markers in MSCs and mature bovine articular chondrocytes. However, chondrocyte lineage dictates the synthesis of specific collagens that differ during chondrocyte life cycle. I selectively chosen markers that are present through the various stages of chondrogenic proliferation and maturation, before chondrocyte hypertrophy takes place. These markers *SOX9, CREB, COMP* (Cartilage Oligomeric Matrix Protein), *NKX3.2, RUNX2, MEF2C, ACAN*, regulators of chondrogenesis and collagen production, are essential for the chondrocyte function. Cultured mature bovine chondrocytes were treated with CK2.1(100nM and 500nM) and compared against BMP2(40nM) for chondrogenic mRNA expression levels of *SOX9*, *COMP*, and *CREB* that are present throughout chondrocyte differentiation and maturation (Ionescu et al., 2001; Kipnes et al., 2003; Pan et al., 2008) (Fig 3.5). Transcript levels were measured using qRT-PCR method

(Fig 3.5). CK2.1 stimulation promoted cartilage specific gene expression in primary chondrocytes comparable to BMP2 stimulated cells. Expression of these genes correlated well with the concentration of CK2.1 used. Expression levels were higher at both concentrations of CK2.1 in comparison to BMP2. Interesting note made was, *SOX9* was significantly lower and *MEF2C* higher in BMP2 treated cells compared to CK2.1 treated. The lowered *SOX9* activity in BMP2 treated correlated to the lowered chondrogenic activity and increased *MEF2C* change in expression correlates to collagen type X production shown (Fig 3.5).

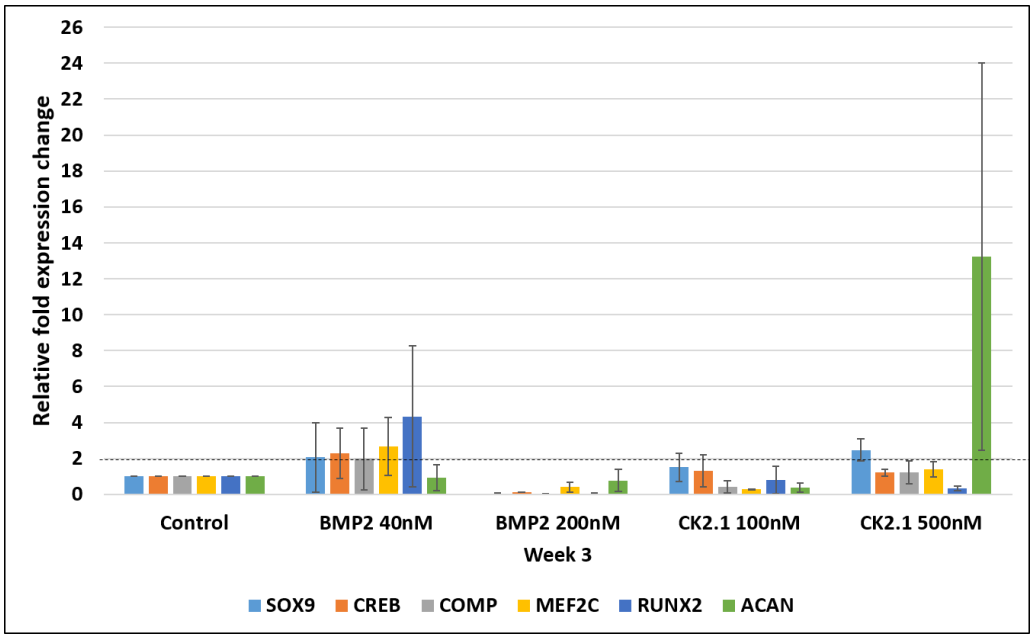

Figure 3.5 **Expression of genes associated with chondrogenesis.** Primary bovine chondrocytes were cultured for 3 weeks and were stimulated with BMP2 (40nM or 200nM), or peptide CK2.1 (100nM or 500nM). Expression of SOX9, CREB, and COMP, MEF2C, RUNX2, aggrecan (ACAN) were evaluated. Cells treated with CK2.1 at 500nM had a significant increase in SOX9, and ACAN. BMP2 treated cells demonstrated increase in RUNX2, MEF2C but CK2.1 treated did not. Fold change in mRNA levels shown are normalized to the house keeping gene GAPDH. Error bars represent SEM.

3.3.5 BMP2, CK2.2, CK2.3, but not CK2.1 induced mineralization in C3H10T1/2 cells

BMP2 known to induce chondrogenic as well as osteogenic differentiation in MPCs (Kwon et al., 2013; Shea et al., 2003). BMP2 influence on chondrocytes is also known to induce chondrocyte hypertrophy and the regulation of collagen type X (Hanada et al., 2001). Nohe lab previously demonstrated strong osteogenic capability of BMP2 and the peptides in C2C12 cells (Bragdon et al., 2011b). Therefore,

C3H10T1/2 cells were stimulated with CK2.1, CK2.2, and CK2.3 were measured for collagen type X (marker for chondrocyte hypertrophy) and osteocalcin (marker for Osteoblast activity) (Christenson, 1997). Furthermore, von Kossa staining for the deposition of mineral phosphates was used as an endpoint. Collagen type X expression in cells stimulated with CK2.1 was not significantly higher compared to controls, but cells stimulated with BMP2 showed a higher expression level. (Fig 3.6A). Moreover, there was no significant elevation in osteocalcin levels or mineral content in cells stimulated with CK2.1 even at the end of 3 weeks of stimulations as compared to controls (Fig 3.6). However, BMP2, CK2.3, and CK2.2 induced osteocalcin expression and mineralization.

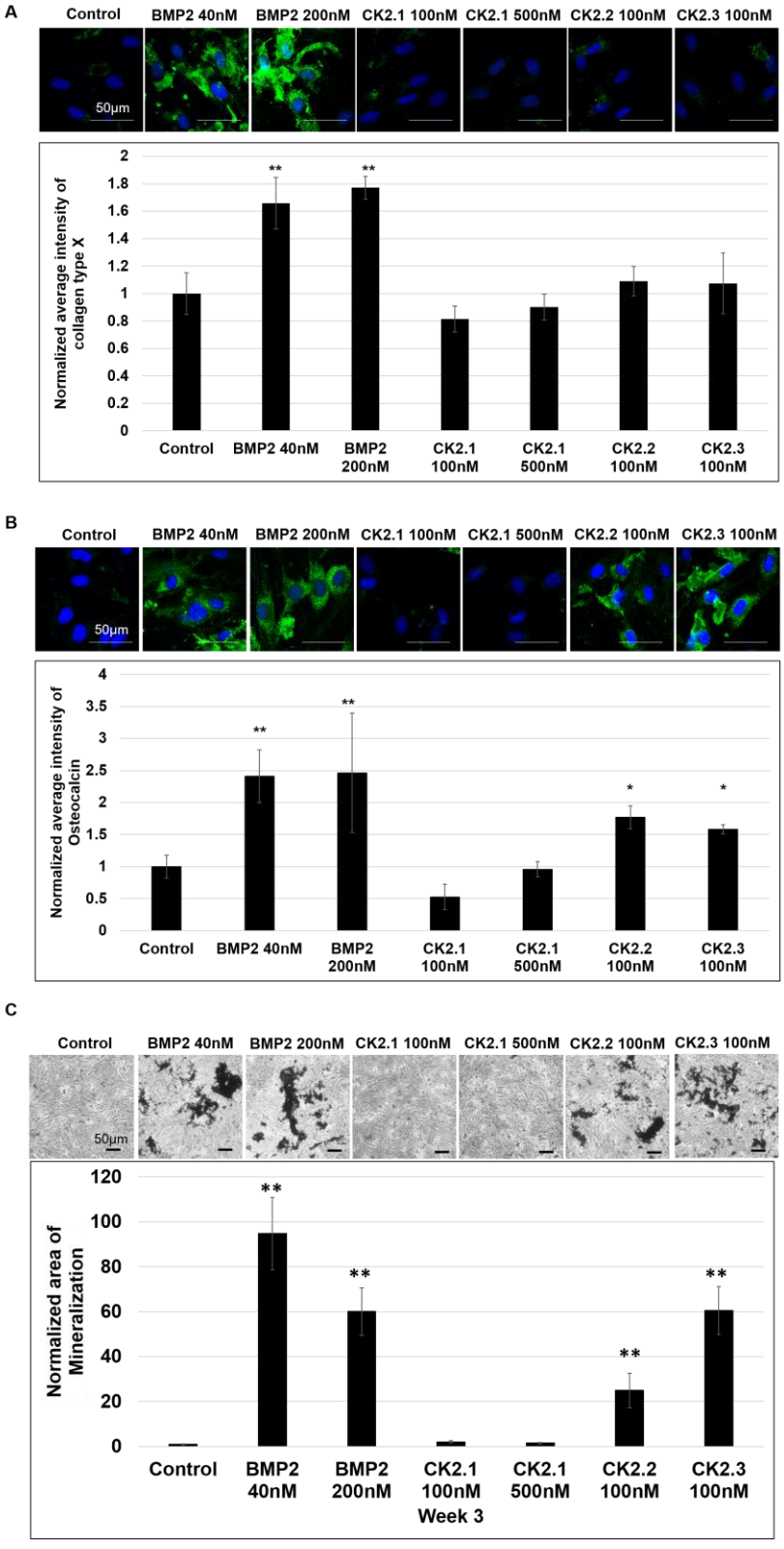
A
Control
BMP2 40nM
BMP2 200nM
CK2.1 100nM
CK2.1 500nM
CK2.2 100nM
CK2.3 100nM
50μm
Normalized average intensity of collagen type X
2
1.8
1.6
1.4
1.2
1
0.8
0.6
0.4
0.2
0
**
**
Control
BMP2 40nM
BMP2 200nM
CK2.1 100nM
CK2.1 500nM
CK2.2 100nM
CK2.3 100nM
B
Control
BMP2 40nM
BMP2 200nM
CK2.1 100nM
CK2.1 500nM
CK2.2 100nM
CK2.3 100nM
50μm
Normalized average intensity of Osteocalcin
4
3.5
3
2.5
2
1.5
1
0.5
0
**
**
*
*
Control
BMP2 40nM
BMP2 200nM
CK2.1 100nM
CK2.1 500nM
CK2.2 100nM
CK2.3 100nM
C
Control
BMP2 40nM
BMP2 200nM
CK2.1 100nM
CK2.1 500nM
CK2.2 100nM
CK2.3 100nM
50μm
Normalized area of Mineralization
120
100
80
60
40
20
0
**
**
**
**
Control
BMP2 40nM
BMP2 200nM
CK2.1 100nM
CK2.1 500nM
CK2.2 100nM
CK2.3 100nM
Week 3

Figure 3.6 **BMP2, CK2.2 and CK2.3 but not CK2.1 induced chondrocyte hypertrophy and mineralization of C3H120T1/2 cells.** C3H10T1/2 cells cultured for 3 weeks and stimulated with CK2.1 (100nM or 500nM), or 100nM of CK2.2 or CK2.3 and stimulated or not with the equivalent concentration of BMP2 (40nM or 200nM) as controls. Cells were fixed and then nuclei stained with Hoechst (blue) A) collagen type X (green), B) Osteocalcin (green) C) and von Kossa and analyzed for results using ImageJ. Experiments were averaged and normalized to controls and graphed with SEM as error bars (*, $p<0.05$), (**, $p<0.001$). Scale bar represents 50µm. Error bars represent SEM (* $p< 0.05$, **$p<0.01$).

3.3.6 CK2.1 injection into the tail vein of mice resulted in increased AC formation

In vitro analysis of CK2.1 demonstrated positive chondrogenic activity without the induction of chondrocyte hypertrophy. Therefore, I investigated the effect of CK2.1 on cartilage formation *in vivo*. To understand the systemic effects of the peptide CK2.1, C57BL/6J mice were injected via the tail vein over 5 consecutive days. C57BL/6J mice are the most widely used in bred model for biological and biomedical research (Mouse Genome Sequencing et al., 2002; Navarro et al., 2012), and were implemented for this study. As a positive control mice were injected with BMP2. Cartilage degenerative diseases like OA affect the AC of diarthrodial joints, but the AC of the long bones like the femurs are mostly affected by this condition (Blagojevic et al., 2010). Therefore, cartilage turnover is evaluated by studying the articular cartilage that surrounds the femurs in these mice. Four weeks after the last injection, mice were sacrificed, femurs were fixed, decalcified, and paraffin embedded. Paraffin blocks were sectioned at 6µm thickness and stained with Safranin O and Fast Green (Srinivasan et al., 2012). Figure

3.7 shows enhanced AC formation in mice injected with CK2.1 similar to BMP2 and compared to PBS.

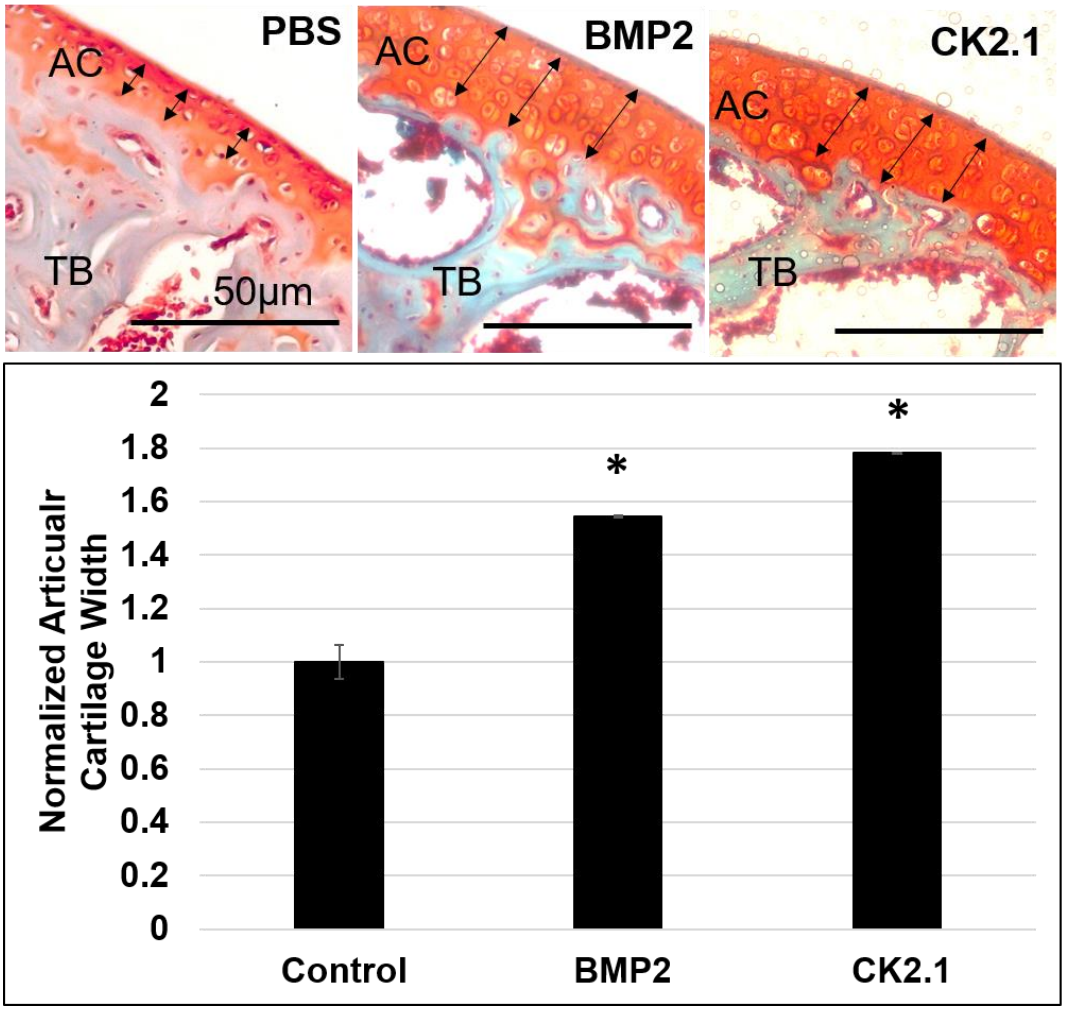

Figure 3.7 **Increased articular cartilage in mice injected with CK2.1 and BMP2.** C57BL/6J mice (n=7/group) were injected with PBS, BMP2 and CK2.1. AC formation was measured from the subchondral base to the tip of AC in at least in 7 regions of each mouse femur and were calculated for width. Experiments were averaged and normalized to controls and graphed with SEM as error bars (*, $p<0.05$). Scale bar representing 50µm.

3.3.7 Increased expression of collagen type II and type IX synthesis in the AC of mice injected with CK2.1

Collagen type II and type IX are two markers that are upregulated during AC formation by chondrocytes. Since CK2.1 and BMP2 injection into the tail vein of mice led to increased AC growth, I next analyzed the cartilage sections for collagen type II and collagen type IX expression. Collagen type II expression was higher in mice injected with CK2.1 and BMP2 as compared to mice injected with PBS (Fig 3.8A). Interestingly, collagen type IX level was higher only in mice injected with CK2.1 but not PBS or BMP2 (Fig 3.8B).

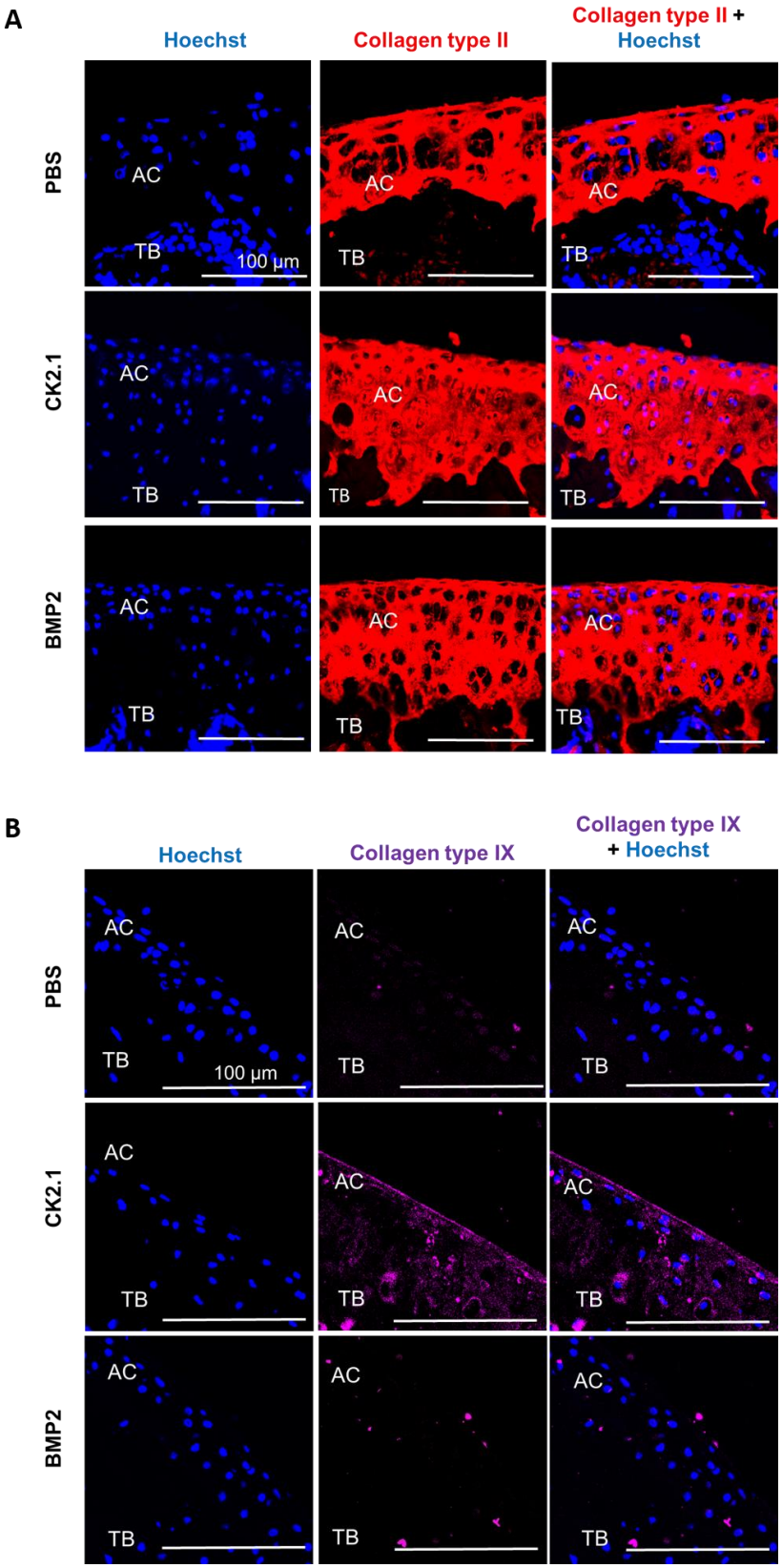
A
Hoechst
Collagen type II
Collagen type II + Hoechst
PBS
CK2.1
BMP2
AC
TB
100 µm
B
Hoechst
Collagen type IX
Collagen type IX + Hoechst
PBS
CK2.1
BMP2
AC
TB
100 µm

Figure 3.8 **CK2.1 but not BMP2 or PBS induced collagen type II and IX expression in articular cartilage.** C57BL/6J mice injected with PBS, CK2.1, and BMP2 were immunostained for collagen type II (red) and collagen type IX (magenta). Hoechst (blue) was used to determine the nucleus of the residing cell and location (AC-Articular Cartilage, TB-Trabecular Bone). A) CK2.1 and BMP2 injected mice expressed relatively equivalent collagen type II levels. B) CK2.1 injected mice demonstrated an increased expression of collagen type IX in AC but not BMP2 or PBS injected mice. Images of the AC were imaged (n=7/group). Scale bar representing 100μm.

3.3.8 Increased expression of collagen type X in mice inejected with BMP2 but not CK2.1

One of the major drawbacks for using BMP2 as a therapeutic for cartilage repair is that BMP2 induces chondrocyte hypertrophy. Therefore, I next immunofluoresecently stained the cartilage sections for collagen type X and MMP13, both markers for chondrocyte hypertrophy (D'Angelo et al., 2000; Zheng et al., 2003). As Figure 3.9 demonstrates collagen type X is upregulated in mice injected with BMP2.

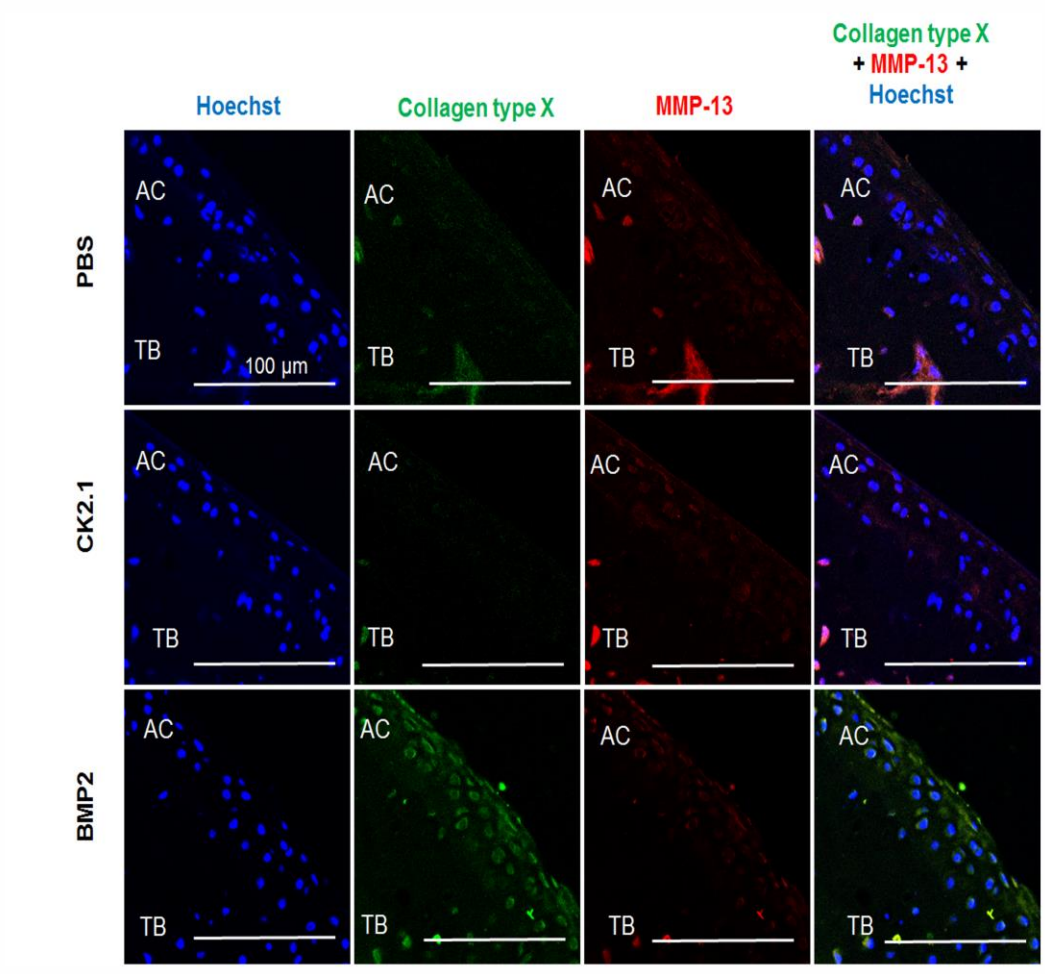

Figure 3.9 **BMP2 but not CK2.1 or PBS induced collagen type X expression in articular cartilage.** C57BL/6J mice injected with PBS, CK2.1, and BMP2 were immunostained for collagen type X (green) and MMP-13 (red). Hoechst stain (blue) was used to determine the nucleus of the residing cell and location (AC-Articular Cartilage, TB-Trabecular Bone). Images of the AC were imaged (n=7/group). Immunostaining demonstrates increased collagen type X expression in AC of BMP2 injected mice but not CK2.1 or PBS injected mice. Scale bar representing 100µm.

3.3.9 BMD was unchanged in mice injected with CK2.1

To determine the changes in trabecular Bone Mineral Density (BMD) and cortical BMD of mice injected with BMP2 and CK2.1 femurs were processed and

assessed by pQCT (Schmidt et al., 2003). pQCT analysis of femurs from mice injected with CK2.1 showed no changes in trabecular or cortical BMD as compared to PBS injected mice. However, BMP2 injected mice had a significant increase in trabecular BMD but not cortical BMD (Fig 3.10).

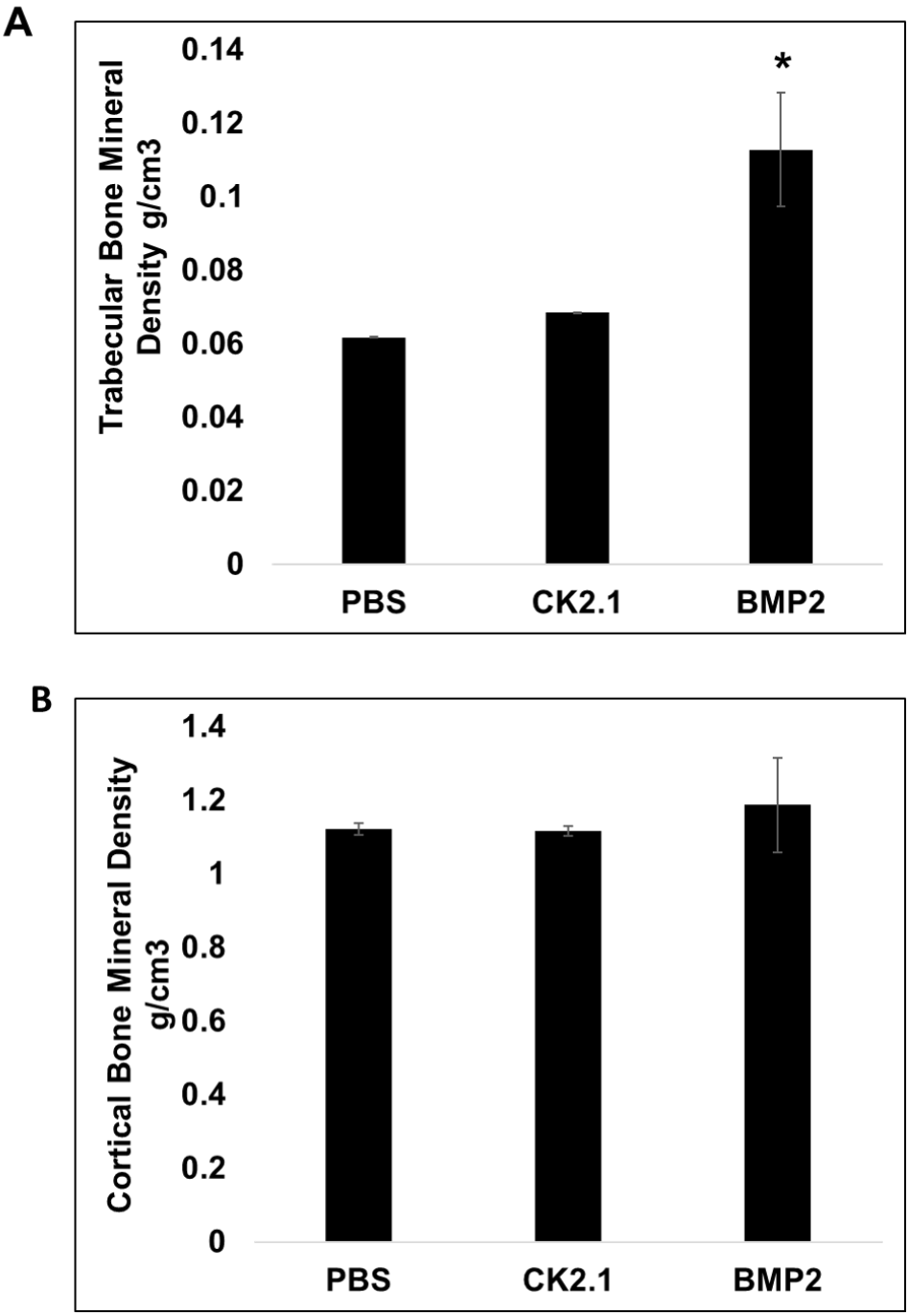

Figure 3.10 **Trabecular BMD is increased in mice injected with BMP2 but not CK2.1.** Femurs of mice injected with PBS, CK2.1, and BMP2 (n=7/group) were analyzed by pQCT. A) Trabecular Bone Mineral Density, B) Cortical Bone Mineral Density. Error bars represent SEM (* $p < 0.05$).

3.4 Discussion

I previously demonstrated the activation of the BMP signaling pathway using peptides CK2.1 (Fig 1B), CK2.2, and CK2.3 in the absence of the ligand leading to osteogenesis (Akkiraju et al., 2015; Bragdon et al., 2011b; Bragdon et al., 2010). In this study I investigated the ability of the novel peptide CK2.1 to induce chondrogenesis *in vitro* and *in vivo*. C3H10T1/2 micromasses stimulated with CK2.1 but not CK2.2 and CK2.3 exhibited increased proteoglycan secretion and collagen type II expression similar to that of cells stimulated with BMP2. BMP signaling is also known to induce chondrocyte hypertrophy and osteogenic response in C3H10T1/2 cells (Roy et al., 2010; Shea et al., 2003). This was evident in C3H10T1/2 cell stimulations using peptides CK2.2, and CK2.3 that induced osteocalcin expression and mineral deposition as a consequence of osteoblast differentiation similar to BMP2 stimuations, while CK2.1 alone did not. I further confirmed this CK2.1 induced chondrogenic activity in primary bovine chondrocytes that can produce the chondrogenic ECM. Collagen type II, type IX, and collagen type X (hypertrophic marker) were analyzed using primary chondrocytes treated with CK2.1 or BMP2. Similar to C3H10T1/2 cells, CK2.1 treatments induced collagen type II, and also collagen type IX. However, BMP2 stimulations, while inducing collagen type II, also induced collagen type X production but not collagen type IX. Aditionally in 3 week study of primary chodnrocyte study using mRNA profiling, BMP2 enhanced MEF2C (hypertorphic marker), but CK2.1 did not. Furthermore, I demonstrated this CK2.1 mediated chondrogenesis is through BMPRIa downstream Smad signaling.

In vivo systemic tail vein injection of CK2.1 and BMP2 in mice resulted in increased AC formation. This study demonstrated the CK2.1 potential in inducing chondrogenesis in similar capacity to BMP2. Previously reported systemic injection of BMP2 in mice at a concentration 0.5µg/kg to 5µg/kg for 20 consecutive days resulted in increased AC formation (Turgeman et al., 2002). In this current study I saw an increase in TBMD with BMP2 injections along with AC growth. However, mice injected with CK2.1 exhibited no significant growth in other areas of the body except AC. The major differences between CK2.1 injected versus BMP2 injected mice was observed in the collagen composition of the AC ECM. While collagen type II expression is similar in CK2.1 and BMP2 injected mice, differences were observed in collagen type IX expression. Collagen type IX was higher in mice injected with CK2.1 compared to BMP2 or PBS. In sharp contrast BMP2 injected mice expressed a higher level of collagen type X compared to CK2.1 or PBS injected mice. The expression of collagen type X in BMP2 injected mice indicates the terminal differentiation of chondrocytes. This effect of BMP2 is well described in the literature (Shu et al., 2011). Interestingly mice injected with CK2.1 did not show this effect. This may be due to the time frame of the study or the concentration of CK2.1 used in this study. *In vitro* analysis as well of collagen type X expression in C3H10T1/2 cells or in primary chondrocytes did not demonstrate a significant increase in CK2.1 stimulations compared to BMP2. Furthermore, at the end of 3 weeks CK2.1 treatment in primary chondrocytes positively regulated collagen type IX production that is necessary for forming proper collagen framework, and induced SOX9 and ACAN mRNA regulation that are positive

chondrogenic markers. Whereas BMP2 induced MEF2C mRNA regulation in accordance to collagen type X production demonstrates terminal differentiation of the chondrocytes. Moreover, CK2.2 or CK2.3 exhibited no significant collagen type X production in these cells, as they failed in inducing chondrogenic differentiation in these cells. As demonstrated in the dose response curve, the optimal dose of the peptide CK2.1 in *in vitro* analysis is at doses between 100nM and 500nM. These results are similar to the results found in previous study using C2C12 cells, where 100nM was found be the ideal concentration to induce osteogenesis for CK2.1 (Bragdon et al., 2011b). Furthermore, the SMAD activity readout between 100nM and 500nM of CK2.1 compared to 40nM and 200nM of BMP2 was similar. However, it is not known what effects the peptide CK2.1 may yield at doses beyond the optimized values. As C3H10T1/2 cells are multipotent MSCs they may illicit different phenotypic effects. Although, the doses used demonstrate chondrogenic activity without the induction of osteogenesis or chondrocyte hypertrophy within these cells compared to BMP2, this maybe different at higher concentrations. An alternative explanation may be that CK2.1 affects only the differentiation of mesenchymal cells to chondrocytes and maintains their chondrogenic potential. Additionally, injections of BMP2 alone but not CK2.1 led to increased trabecular BMD in mice. Moreover, BMP2, CK2.3, and CK2.2, but not CK2.1 induced mineralization in C3H10T1/2 cells (Bragdon et al., 2011c). I previously showed that injection of CK2.3 into the tail vein of mice increased trabecular BMD (Akkiraju et al., 2015). Therefore, the mechanism is still unclear on how CK2.1 induces chondrogenic activity differently than BMP2 ligand, utilizing similar signaling

pathways without inducing chondrocyte hypertrophy or osteogenesis. However, there are still questions to be answered for future studies, as it is still unclear how CK2.1 actuates this specific response towards the articular capsule, as AC being avascular and can only be explained by the blood supply through the synovial capsule (Davies and Edwards, 1948), along with the diffusion rates of the peptide into the cells. Similarly, the rate of tissue growth due to either proteoglycan osmotic swelling or due to the appositional growth and also the ability of CK2.1 to induce cartilage repair in a disease model. My data presented here and previously, further indicate that CK2.1 as well as CK2.3 may signal through more specific signaling pathways compared to BMP2 (Akkiraju et al., 2015; Bragdon et al., 2011c). As included in the hypothetical signaling schematic that illustrates a possible mode of peptide induced BMPRIa activation in Figure 3.1. However, more experiments are needed to answer these questions. Based on my data, CK2.1 induces chondrogenesis without inducing chondrocyte hypertrophy and may be one of the few peptides developed or proteins discovered with this capability and may be used for cartilage repair in OA related cartilage loss.

Chapter 4

BONE MORPHOGENETIC PROTEIN RECEPTOR TYPE IA MIMETIC PEPTIDE CK2.1 REPAIRS DAMAGED CARTILAGE

4.1 Background

Osteoarthritis (OA) is a cartilage metabolic disease 21.7 million people each year and is the 11th contributor of disability and costs over $28.5 billion dollars a year (Allen and Golightly, 2015; Murphy and Helmick, 2012; Sacks et al., 2010). In OA, the articular cartilage (AC) undergoes progressive loss of normal cartilaginous extracellular matrix (ECM), losing its overall function (Buckwalter et al., 2005). AC is viscoelastic connective tissue that covers the articular ends of the femoral bone and is essential for the free movement of the joints. It consists of chondrocytes that are responsible for the production of ECM within this tissue. This ECM network maintains the load bearing properties for mechanical compression across the joint (Poole, 1997). Chondrogenic ECM is composed of proteoglycans, such as aggrecans, and collagens, including type II, type IX and type XI, that form a cross-linked network to regulate its biological properties (Eyre et al., 2006). More importantly, AC is an avascular tissue that displays poor tissue regenerative capacity. This loss in regeneration results in poor cartilage tissue regeneration and enhances the loss of AC. In addition OA is accompanied by

remodeling and sclerosis of the subchondral bone and formation of osteophytes (Poole et al., 1993).

Among many growth factors that influence the progression of OA, bone morphogenetic proteins (BMPs), such as BMP2, greatly accelerate the overall loss of AC (Blaney Davidson et al., 2007a). However, the same BMP2 is a potent growth factor consisting of many pleiotropic functions plays a crucial role in the formation of the AC (Bragdon et al., 2012a; van der Kraan et al.). BMP2 is also known to induces chondrocyte hypertrophy followed by cartilage calcification (van der Kraan et al.). Therefore, BMP2 may not be valuable as a therapeutic for cartilage restoration in degenerative diseases such as osteoarthritis (OA).

BMP2 signals through binding to type I and type II serine/threonine kinase receptors. Upon ligand binding, type I receptor is phosphorylated by the constitutively active type II receptor at the GS box (glycine/Serine rich region) to initiate downstream signaling (Bragdon et al.). Nohe lab has previously reported that the protein Casein Kinase 2 (CK2) interacts with the bone morphogenetic protein receptor type Ia (BMPRIa) (Bragdon et al., 2011a) and that loss of this interaction leads to the activation of BMP signaling in the absence of the ligand (Bragdon et al., 2012b; Bragdon et al., 2009; Bragdon et al., 2011c). Furthermore, Nohe lab has identified a peptide, CK2.1, that induces the release of CK2 from BMPRIa (Bragdon et al., 2010). I previously demonstrated the potency of one of the peptides CK2.1 induced chondrogenesis *in vitro* and *in vivo* (Akkiraju et al., 2016). Here I evaluate the potential of the peptides to induce cartilage repair *in vivo*. To develop a more feasible approach of delivery of the peptide

as a treatment for OA, we conjugated the peptide CK2.1 to hyaluronic acid (HA)-based hydrogels particles (HGPs) through hydrolytically degradable ester linkages for its slow release. This injectable formulation is referred to as HGP-CK2.1. I used destabilization of the medial meniscus (DMM) surgery to create an OA like condition in mice. After 6 weeks post-secondary injury to AC, I injected HGP-CK2.1 intra-articularly twice once every 2 weeks for sustained release. HA HGP drug depots have proven to be advantages for carrying various proteins and peptides for controlled release (Xiao et al., 2013; Xu et al., 2012). Six weeks after the injection, mice were sacrificed and the femurs were analyzed for the AC restoration. I performed immunohistochemical analysis to identify the proteoglycan synthesis. Furthermore, using immunofluorescence we analyzed the femur samples for collagen type II, type IX, type X and osteocalcin. I discovered that collagen type II and type IX were significantly increased in mice treated with HGP-CK2.1, but not those treated with PBS. However, while PBS injected mice demonstrated a significant increase in collagen type X and osteocalcin production, HGP-CK2.1 injected mice did not. My data show that localized intra-articular injections of HGP-CK2.1 restored the AC and reconstructed the cartilaginous ECM.

4.2 Materials and Methods

4.2.1 Mice

All 10 week old male C57BL/6J mice were obtained from The Jackson Laboratory (Bar Harbor, ME) and maintained under conventional conditions. The animal protocol was approved by IUCAC at the University of Delaware.

4.2.2 Design of peptides

Peptides were designed by Nohe group as previously described (Bragdon et al.). A prosite search including patterns with high probability of occurrence on BMPRIa yielded possible CK2 phosphorylation sites located at amino acids 466-469 (SYED). The peptides were designed with the Antennapedia homeodomain signal sequence for cellular uptake and incorporated in one these binding sites: CK2.1 (SYED). The peptides included several amino acid residues flanking each side (Bragdon et al., 2010).

4.2.3 Preparation of CK2.1-conjugated HGPs

HA-based HGPs with a mean diameter of 10 μm were formulated by an inverse emulsion cross-linking technique, following previously reported procedures (Ge et al., 2007). Separately, a heterobifunctional linker, containing a thiol-reactive acrylate group and an amine-reactive N-hydroxysuccinimide ester (NHS) with 3 lactic acid (LA) repeats, was synthesized according to reported methods (Sahoo et al., 2008). Next, HA HGPs (10 mg) and the bifunctional linker (4.5 mg) were mixed in 2 ml DMSO and the

reaction was allowed to proceed for 24 h at 40 ºC under constant stirring. The modified particles were then washed thoroughly with water, ethanol and acetone before being dried at 37 °C in the incubator overnight. Subsequently, the modified HGPs (10 mg) was added to 10 ml PBS containing 10mg cysteine-tagged CK2.1 peptide (QIKIWFQNRRKWKKMVPSDPSYEDMGGC, GenScript). The reaction was allowed to proceed at room temperature for 24 hr. The product, HGP-CK2.1, was washed thoroughly with PBS, isolated by centrifugation at 3,000 rpm for 5 min and finally reconstituted in PBS at the desired concentration. The peptide content in HGP-CK2.1 was determined by subtracting the unreacted peptide in the washing supernatant from that in feed, as quantified by UV-Vis spectrophotometer at 280 nm based on a standard curve of CK2.1 in PBS (62.5-1000 μg/ml). To prepare sterile particle formulations, HGPs were first suspended and sterilized in 70% ethanol overnight before reacting with sterile-filtered (0.22 μm) CK2.1 peptide in PBS.

4.2.4 *In vitro* release of CK2.1

HGP-CK2.1 (2mg) was dispersed in PBS (0.5 ml) under constant rotation at 37 ºC. At predetermined time points, the supernatant was collected by centrifugation (3,000 rpm for 5 min), and the release medium was replenished with an equal amount of fresh PBS. The released peptide in PBS was quantified by UV-Vis spectrophotometer at 280 nm. The cumulative release was calculated as the total amount of CK2.1 peptide released into the medium at a particular time relative to the initial loading.

4.2.5 Surgical Destabilization of the Medial Meniscus

Mice were anesthetized using isoflurane prior to surgery. All mice had their right knees shaved using an electric trimmer and wiped using alcohol swabs to sanitize the area of surgery. A 3-mm longitudinal incision over the distal patella to tibial plateau was created. The joint capsule medial to the patellar tendon was incised with a #11 blade and the capsule was opened with micro-iris scissors. Dissection of the fat pad over intercondylar area exposed the intercondylar region, providing visualization of the medial meniscus. An incision is made at the tibial plateau to destabilize the medial meniscus (Glasson et al., 2007). Gauze dabbed with alcohol was used to stop any bleeding. Joint capsule was closed with a continuous 8-0 vicryl® suture and skin was closed by the application of tissue adhesive. Mice were checked for regular movement and antibiotics and pain killer were applied every 12 hr during the first day, and monitored every day until the time of intra-articular injections. Mice were allowed to sustain secondary insult leading OA-like damage to the cartilage 6 weeks post-surgery. HGP-CK2.1, HGP alone diluted in PBS, or PBS alone were injected once every two weeks post 6 weeks of DMM surgery.

4.2.6 Cell Culture

C3H10T1/2 cells were purchased from American Type Culture Collection (CCL-26) (Manassas, VA) and monolayer cultures were maintained in T-75 flasks grown in Dulbecco's Modified Eagle's Medium (DMEM) (Mediatech, Manassas, VA) supplemented with 10% (v/v) fetal bovine serum (FBS) (Gemini Bioproducts, West

Sacramento, CA), 0.5% (v/v) L-glutamine (Mediatech, Manassas, VA), and 1% (v/v) penicillin/streptomycin (100IU/ml penicillin, 100 µg/ml streptomycin, Fisher Scientific, Pittsburg, PA). Cultures were incubated at 37°C and 5% CO_2, and cells were passaged at 90% confluency with 0.05% Trypsin-EDTA (Gemini Bioproducts, West Sacramento, CA).

4.2.7 Alcian blue staining

C3H10T1/2 cells were seeded at 1 x 10^7 cells/ml and plated as 10 µl micromass culture in a 1.9 cm^2 24 well plate (Nunc, Rocskilde, Denmark). Cells were supplemented with DMEM with 10% FBS and incubated at 37°C and 5% CO_2. Cells were then stimulated with recombinant BMP2 (40 nM) or HAHGPCK2.1 (5nM or 10nM or 30nM or 50nM/day release concentration).

Seven days after stimulation cultures were fixed using 10% neutral buffered formalin (pH7.4) mixed with 0.05% wt/v cetylpyridinium chloride for 20 minutes at room temperature. Cells were rinsed three times with 3% glacial acetic acid (pH 1.0), and stained using 0.5% Alcian blue 8-GX stain (Life line, Walkersville, MD) overnight. After staining cultures were rinsed with 3% glacial acetic acid (pH 1.0) and air dried. Stained cultures were viewed under an inverted light microscope (Nikon, TMS-f) using 20X magnification and the collected images were analyzed and quantified with ImageJ software (NIH, Bethesda) (Bruce et al., 2010).

4.2.8 Histological Scoring

After 2 weeks of the last intra-articular injections mice were sacrificed and extracted femurs were fixed in 10% Neutral Buffered Formalin (Sigma Aldrich, St. Louis, MO) and decalcified for 5 days in 5% formic acid in 10% sodium citrate (Sigma Aldrich, St. Louis, MO). Samples were paraffin embedded and sectioned at 6µm thickness. Sectioned slide samples were stained by Safranin O and fast green staining (Kang Q K, 2003; Padma P Srinivasan et al., 2012). Scoring was done in four compartments of the knee using a modified semi-quantitative scoring scale as described (Glasson et al., 2007). The scoring analysis used in this study are: score 0= normal cartilage, score 0.5 = loss of safranin O staining with a normal articular surface, score 1 = small fibrillations or roughened articular surface, and score 2 = fibrillations extending into the superficial lamina. For each knee analyzed, 12 slides around the entire joint were blinded and scored by two independent observers.

4.2.9 Immunostaining

Sectioned femur samples (pre-treated in xylene for 10 minutes to clear away the paraffin) were incubated with testicular hyaluronidase for 30 minutes to expose collagen epitopes. The samples were immunofluorescently labeled for 1 hr at room temperature either with rabbit polyclonal IgG collagen type II (10µg/ml, ab34712, Abcam, UK) followed by Alexa 488 donkey anti rabbit IgG (2µg/ml. Invitrogen, Eugene, OR) or rabbit polyclonal collagen IX (10µg/ml, Abcam, UK) followed by Alexa 647 goat anti-rabbit IgG (2µg/ml, Invitrogen, Eugene, OR) or Goat polyclonal IgG MMP13 (10µg/ml,

Santa Cruz Biotechnology, CA, USA) followed by Alexa 568 donkey anti goat (2 µg/ml, Invitrogen, Eugene, OR) or Rabbit (Rb) pAb collagen X (10µg/ml, ab58632, Abcam, UK) followed by Alexa flour 488 donkey anti-rabbit (2µg/ml. Invitrogen, Eugene, OR) or Rabbit polyclonal IgG Osteocalcin (10µg/ml, Santa Cruz Biotechnology, CA, USA) followed by Alexa flour 488 donkey anti-rabbit (2µg/ml. Invitrogen, Eugene, OR). Antibodies were diluted in 3% BSA. The nuclear stain bisbenzimide (Sigma Aldrich, St. Louis, MO, Hoechst dye No 33258, dissolved in H_2O) was administered for five minutes and coverslips were mounted on slides using Airvol as described previously (Nohe et al., 2005; Nohe and Petersen, 2007). Images were taken (n = 8 image sections/sample) on the Zeiss 780 confocal with a 20X objective (0.75NA, Beam Splitter [MBS] 458/514/561/633, 5% laser output, and [MBS] 405, 2% laser output. Images were quantified using ImageJ (NIH, Bethesda).

4.2.10 Statistical Data Analysis

All data presented were analyzed using single factor Anova, followed by Tukey Kramer post-hoc test. All experiments were repeated three or more times and normalized to control. Maximum of three outliers were removed using the Chauvenets Criterion, but minimum number of samples required for statistical significance were used for the following analysis. Error bars represent standard error of the mean (SEM), where * denotes ($p<0.05$) and ** denotes ($p<0.01$) statistical significance.

4.3 Results

4.3.1 CK2.1 was released from HGPs in controlled manner

CK2.1 peptide was covalently conjugated to the hydrogel particles via Michael addition using cysteine-tagged peptide and acrylated HGPs (Fig 4.1A). Approximately 48 µg CK2.1 was conjugated to 1 mg of HGPs. The peptide was released (Fig 4.1B) from the HGPs at a rate of + 9.4 wt%/day from day 0 to day 4 and + 5.3 wt% day from day 4 to day 7. By day 7 when the experiment was terminated, a total of 54.6 wt% of the initially loaded peptide was released from the particles.

Next I used C3H10T1/2 cells in micromass cultures to test chondrogenic potency of the slow release HGP-CK2.1. My previous study demonstrated positive chondrogenic activity in C3H10T1/2 cells in micromass cultures stimulated with peptide CK2.1 with concentrations ranging from CK2.1 at 100nM (lowest) to 500nM (highest) (Akkiraju et al., 2016). Therefore, an overall concentration of 50nM, 100nM, 300nM, and 500nM were adjusted according to HGP-CK2.1 per day release profile. Where the adjusted HGP-CK2.1 (+9.4%/day) release value of the following concentrations as (50nM) 5nM/day, (100nM) 10nM/day, (300nM) 30nM/day, and (500nM) 50nM/day (Fig 4.1C). Single treatment of HGP-CK2.1 for 7 days at the given concentration on C3H10T1/2 micromass cultures demonstrated best chondrogenic activity at 5nM/day concentration analyzed using alcian blue staining.

A

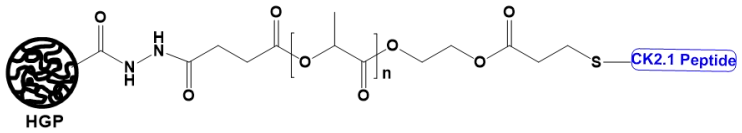
HGP
CK2.1 Peptide

B

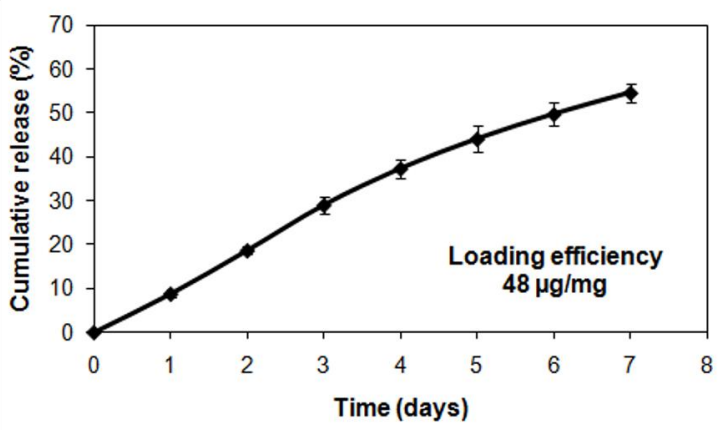
Cumulative release (%)
Time (days)
Loading efficiency
48 µg/mg

C

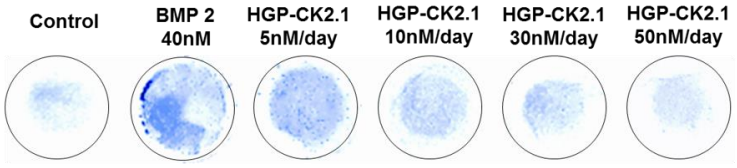
Control
BMP 2 40nM
HGP-CK2.1 5nM/day
HGP-CK2.1 10nM/day
HGP-CK2.1 30nM/day
HGP-CK2.1 50nM/day

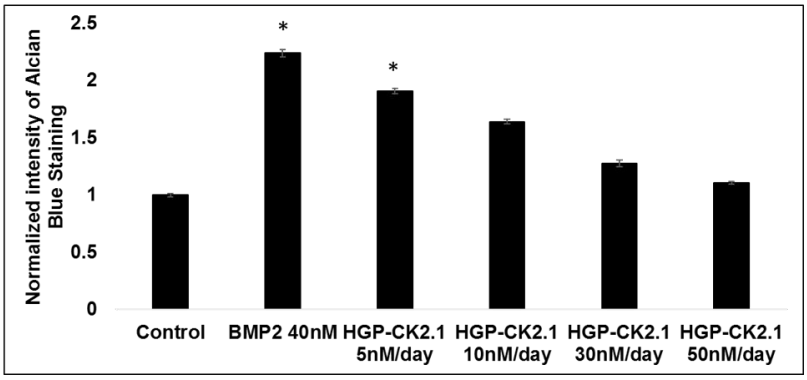
Normalized intensity of Alcian Blue Staining
Control
BMP2 40nM
HGP-CK2.1 5nM/day
HGP-CK2.1 10nM/day
HGP-CK2.1 30nM/day
HGP-CK2.1 50nM/day

Figure 4.1 **Synthesis of HGP-CK2.1 drug depots for sustained release.** A) Schematic illustration of CK2.1 peptide immobilized to HA HGPs via a hydrolytically degradable linker. **B)** Cumulative release of CK2.1 from HA HGPs; Peptide release was monitored by UV-Vis at 280 nm. Sustained release achieved with +9.4 wt% release over days 0-4, and +5.3 wt% release days 5-7. **C)** C3H10T1/2 micromass cultures were treated with either BMP2 (40nM) or HAHGPCK2.1 (5nM/day, or 10nM/day, or 30nM/day, or 50nM/day release concentration) stained with Alcian blue after 7 days. BMP2 and HGP-CK2.1 treated cells showed a significant increase of ECM containing proteoglycans. Samples were averaged and normalized to controls. Error bars represent SEM (* $p<0.05$).

4.3.2 Intra-articular injections of HGP-CK2.1 restored cartilage homeostasis in DMM mice

Destabilization of medial meniscus was performed on male C57BL/6J mice of age 10 weeks. After 6 weeks, allowing for the secondary injury to be taken place these mice were injected with PBS, or 6µM of HGP-CK2.1, or HGP alone via intra-articularly once every two weeks. Concentration of HGP-CK2.1 at 6 µM was chosen based on peptide loading that release CK2.1 at 500nM per day basis. Two weeks upon the second injection mice were sacrificed and femurs were processed, decalcified and embedded in paraffin. These samples were sliced and stained for Safranin O and Fast Green. These samples were scored for cartilage damage levels using mankins modified semi quantitative analysis (Padma P Srinivasan et al., 2012). Analysis compared to SHAM operated mice demonstrated a greater repair in mice injected with HGP-CK2.1 versus that to HGP alone or PBS (Fig 4.2). Where PBS injected mice had the greatest damage sustained with deep fissures and loss of proteoglycan contents.

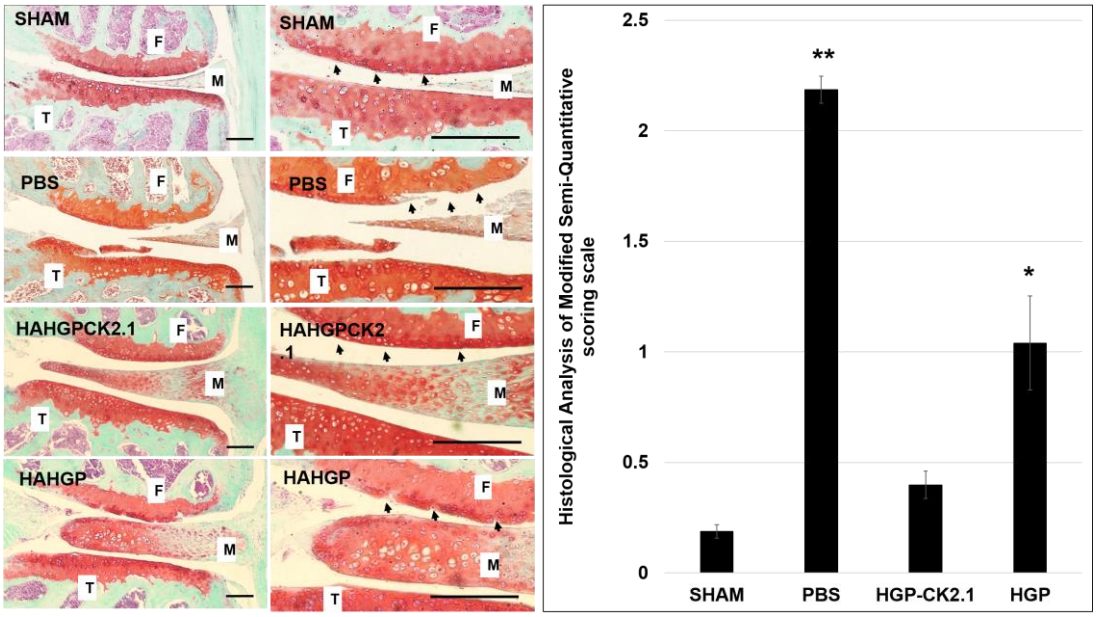

Figure 4.2 **Intra-articular injections of HGP-CK2.1 induces articular cartilage repair in DMM mice**. DMM mice post 6 weeks of surgery (n=6/group) were injected intra-articularly with PBS or HGPCK2.1 (6µM) or HGP (6µM) compared to SHAM mice. Sample sections were stained using safranin O (red) and fast green (turquoise) and scoring was done in four compartments of the knee using a modified semi-quantitative scoring scale. Mice injected with HGP-CK2.1 showed the greatest cartilage repair compared to SHAM. T, tibia; F, femur; M, meniscus. Scale bar represents 50 µm.

4.3.3 Increased expression of collagen type II and type IX in HGP-CK2.1 injected DMM mice

The previous experiment demonstrated HAHGPCK2.1 injected DMM mice showed the best restoration of cartilage in comparison to HGP or PBS injected mice. AC ECM is intricately packed to include a collagenous and proteoglycan framework. Chondrocytes of the AC secret collagen type II that making up the majority of collagen. Only 10% is reserved for collagen type IX and XI that is necessary to form covalent cross fibrillation for the tensile strength (Eyre, 2002; Itoh et al., 2001). Therefore, to

understand the ECM composition of the newly regenerated cartilage, I immunostained these DMM cartilage samples for collagen type II and type IX. Analysis of DMM mice injected with HAHGPCK2.1 showed collagen type II production was consistent when compared to HGP or PBS injected mice but demonstrated elevated levels of collagen type IX (Fig 4.3). Increased collagen type IX production, along with collagen type II in mice injected with HGP-CK2.1 marks the clear restoration of AC tissue ECM components.

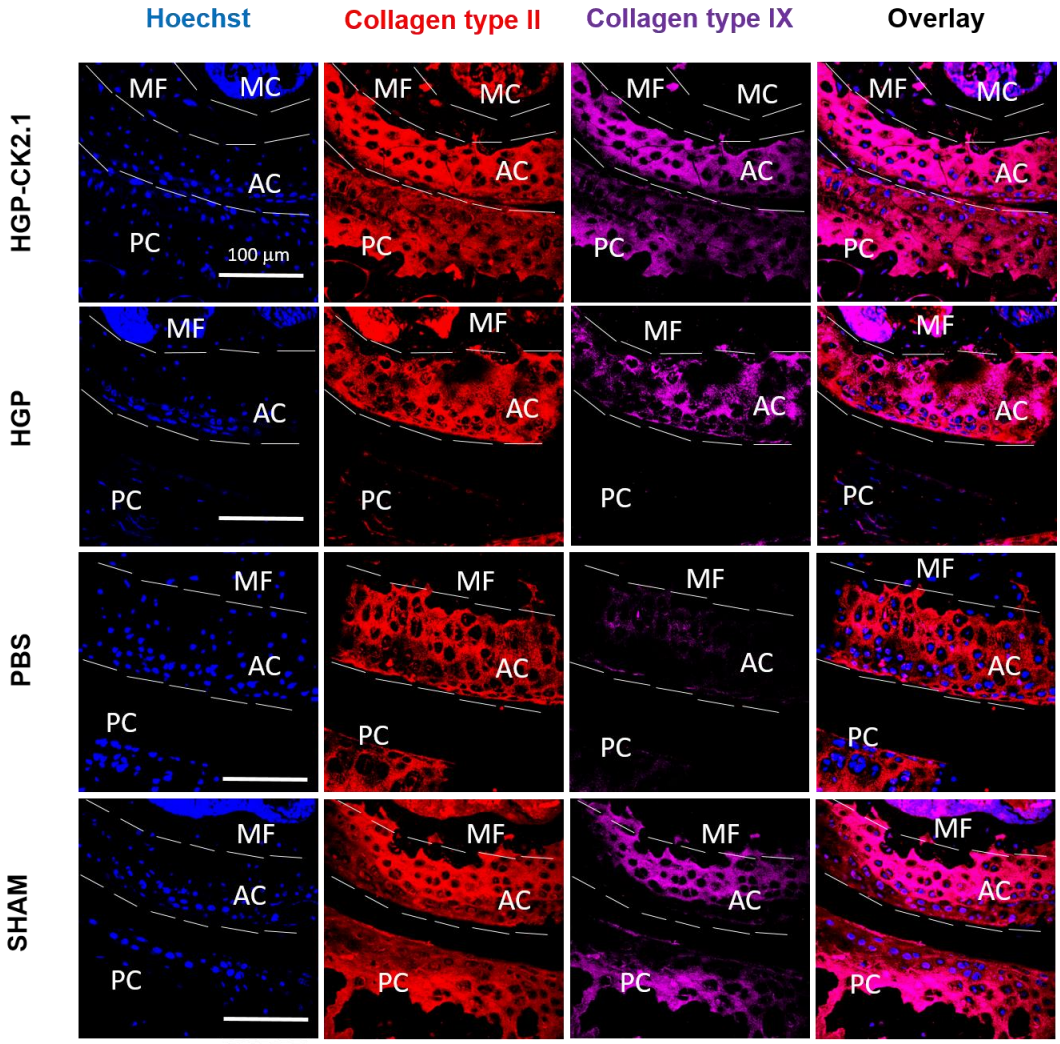

Figure 4.3 **HGP-CK2.1 induced cartilage restoration as a result of collagen type II and collagen type IX expression.** DMM mice injected with PBS or HGP-CK2.1 or HGP and SHAM mice were immunostained for collagen type II (red) and type IX (magenta) and Hoechst (blue) was used to determine the nucleus of the residing cell and location MF, Medial Femur; AC, Articular Cartilage; MC, Marrow Cavity; PC, Patellar Cavity. HAHGPCK2.1 injected mice demonstrated higher levels of collagen type IX levels compared to SHAM but in HGP or PBS injected mice. Scale bar representing 100 µm.

4.3.4 Increased expression of collagen type X in HGP and PBS injected mice but not HGP-CK2.1 injected

In OA, chondrocyte hypertrophy is a hallmark event. This terminal differentiation of chondrocytes is marked by the production of collagen type X. A transition from the production of collagen profile from collagen type II, IX to collagen type X necessitates chondrocyte hypertrophy and cartilage degradation. Mechanical forces may further aid in this process of cartilage tissue remodeling by enhancing collagen type X. Therefore, I immunostained samples for collagen type X. HAHGP alone injected mice exhibited a moderate cartilage regeneration in these mice compared to PBS, there was still a significant increase in collagen type X in these samples similar to PBS injected mice. However, HAHGPCK2.1 injected mice resulted in a low expression of collagen type X in the regions of restoration (Fig 4.4).

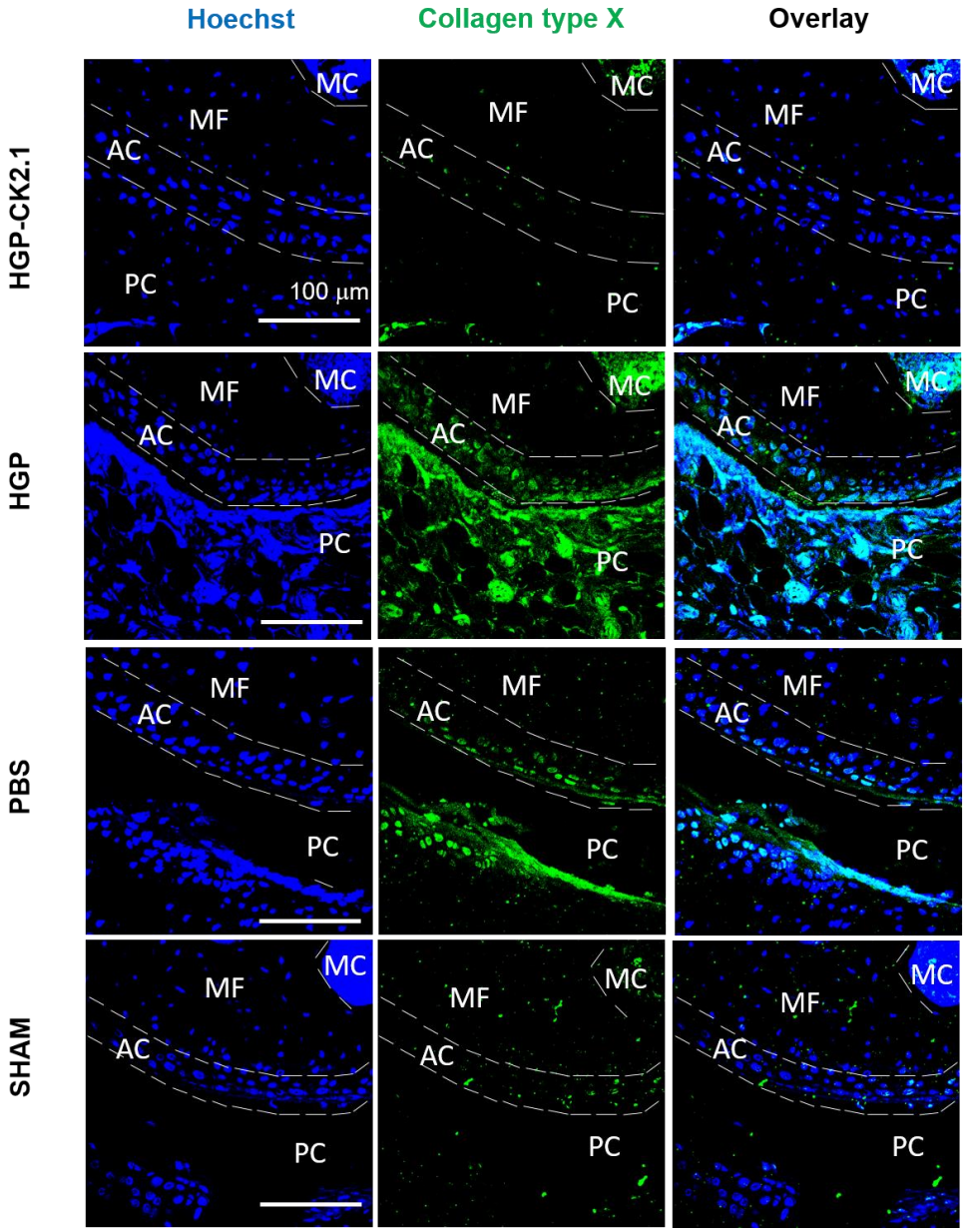

Figure 4.4 **DMM mice injected with PBS and HGP induced collagen type X expression in articular cartilage but not HGP-CK2.1.** DMM mice injected PBS or HGP-CK2.1 (6µM) or HGP (6µM) and SHAM mice were immunostained for collagen type X (green) and Hoechst (blue) was used to determine the nucleus of the residing cell and location MF, Medial Femur; AC, Articular Cartilage; MC, Marrow Cavity; PC, Patellar Cavity. Immunostaining demonstrates increased collagen type X expression in AC of PBS and HGP injected mice but not HGP-CK2.1. Scale bar representing 100 µm.

4.3.5 No changes in subchondral bone or osteophyte formation in HGP-CK2.1 injected mice

Osteophyte formation following cartilage degradation is commonly seen in OA like conditions. This phenomenon is shown to be aggravated with excess mechanical forces and influence of surrounding growth factor signaling factors on AC. Growth factors signaling like that of BMP2 in OA AC is known to enhance cartilage degradation and osteophyte formation. Osteocalcin secretion are marked by osteoblast activity (Christenson, 1997). HAHGPCK2.1 DMM mice samples were immunostained for osteocalcin. The samples did not show osteocalcin expression. Only PBS injected mice showed some significant expression of osteocalcin (Fig 4.5).

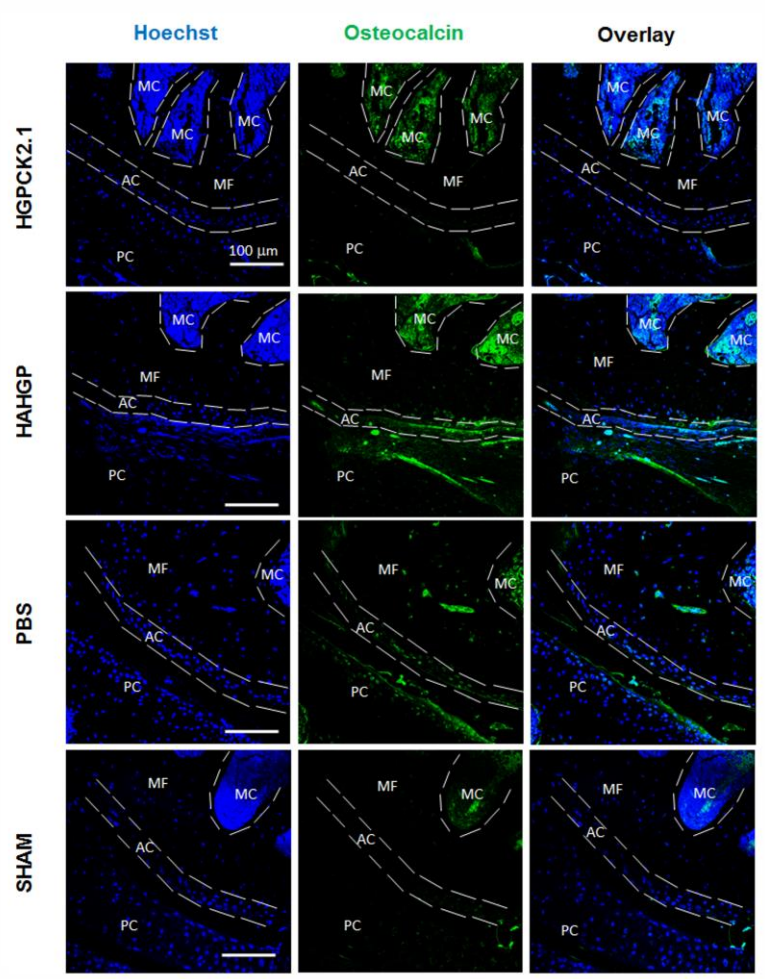

Figure 4.5 **DMM mice injected with PBS results in osteocalcin expression but not HGP-CK2.1.** DMM mice injected PBS or HGP-CK2.1 (6µM) or HGP (6µM) and SHAM mice were immunostained for osteocalcin (green) and Hoechst (blue) was used to determine the nucleus of the residing cell and location MF, Medial Femur; AC, Articular Cartilage; MC, Marrow Cavity; PC, Patellar Cavity. Immunostaining demonstrates increased osteocalcin expression in AC of PBS injected mice but not HAHGPCK2.1. Scale bar representing 100 µm.

4.4 Discussion

My previous work demonstrated the potency of CK2.1 induced chondrogenesis *in vitro* and cartilage formation in *in vivo* (Akkiraju et al., 2016). Here I demonstrated the ability of this novel peptide CK2.1 in cartilage repair and cartilage tissue regeneration. In this study, a hydrogel particle-based delivery system for the sustained release of CK2.1 peptide was developed to effectively stimulate cartilage regeneration. The CK2.1 peptide was covalently conjugated to HGPs through the reaction between the acrylate groups on modified HGPs and the cysteine thiol on the peptide by Michael-type addition reaction. CK2.1 was attached to particles via a thiol-ether linkage with neighboring ester groups and thus the obtained slow release profile of CK2.1 was attributed to the hydrolysis of esters groups. Mice were subjected to DMM surgery (OA model) and were allowed to sustain secondary insult over 6 weeks post-surgery to create OA like conditions (Glasson et al., 2007). Upon 6 weeks post-surgery these mice were injected using slow release HGP-CK2.1, or HGP or PBS alone intra-articularly compared to SHAM. Injected twice over 4 weeks once every 2 weeks these mice injected with HGP-CK2.1 demonstrated the greatest cartilage repair in compared to SHAM. Analysis of collagen type II, exhibited a correlation toward cartilage repair and ECM formation. However, the greatest difference seen among these groups was in analysis of collagen type IX and type X. HGP-CK2.1 alone demonstrated a greater collagen type IX expression in these samples but not collagen type X, whereas HGP and PBS injected had high levels of collagen type X but not type IX. This data confirms with the

previously reported data of CK2.1 induced collagen type IX expression in the AC of systemic injected mice (Akkiraju et al., 2016).

Osteoarthritis is characterized by a slow progressive degeneration of the cartilaginous tissue. This involves the disruption of structural and mechanical integrity organized around proteoglycans and the collagen framework of collagen type II, type IX, and type XI fibrillar structures (Poole et al., 1993). Surgical destabilization of the medial meniscus instability in animal served as OA models (Glasson et al., 2007). Therefore, I used DMM surgery to induce secondary insult to damage the AC. However, while instability models like the DMM demonstrate significant damage to the AC, it is to be noted that the internal cellular OA like mechanisms may be not be replicated. These OA animal models tend to develop susceptibility towards biomechanical loading, or regenerative changes like subchondral bone remodeling or osteophyte formation (Glasson et al., 2007). However, the DMM model provided the best reproducibility and progressive degradation of AC emulating the OA conditions (Glasson et al., 2007). For this reason, DMM models were used for this study. Moreover, to minimize the number to intra-articular injections of the peptide CK2.1. I employed a slow release system using HGP-CK2.1 at the localized site.

HA is among the most commonly found proteoglycan macromolecule that is considered for clinical usage as viscosupplements for joint mobility enhancement (Kirchner and Marshall, 2006; Xu et al., 2012). However, HA alone cannot induce cartilage repair, it does provide temporary alleviation of pain at the knee (Jazrawi and Rosen, 2011). Recently, HA-based hydrogels containing covalently integrated soft and

deformable drug depots were developed to release therapeutic molecules in response to mechanical forces (Xiao et al., 2013). Intra-articular injection of HGP-CK2.1 is a non-invasive procedure for the delivery of the therapeutic peptide. Such a particle-based formulation allowed for a sustained release for proper tissue regeneration. This cartilage tissue regeneration demonstrated a higher level of collagen type II and type IX in HGP-CK2.1 injected mice that is crucial for the overall development of collagen framework. It is well documented that OA chondrocytes actively enhance the levels of collagen type II expression in a self-reparative process while simultaneously secreting proteolytic enzymes like MMPs (Grimmer et al., 2006). Moreover, an increased expression of collagen type IX in HGP-CK2.1 injected mice was observed. AC collagen framework depends on the covalent crosslinking of the collagen type II making up majority of the collagen network, to collagen type IX and type XI to provide the structural integrity and tensile strength (Eyre, 2002). This data confirms with my previous study, where an increased expression of collagen type IX in AC was observed in mice injected with peptide CK2.1 systemically via the tail vein (Akkiraju et al., 2016). However, hypertrophic chondrocytes along with enhanced production of collagen type X, (marker of the terminally differentiated chondrocytes) also produces collagen type II. These hypertrophic chondrocytes marked by the expression of collagen type X actively produce matrix metalloproteinases (MMPs) further accelerating the overall destruction of the AC collagen framework (van der Kraan and van den Berg, 2012). In this study I observed that only HGP and PBS injected mice demonstrated higher levels of collagen type X expression but not HGP-CK2.1 injected mice. Moreover, along with AC

degradation, OA cartilage also commonly exhibits expression of osteocalcin and osteophyte formation (van der Kraan and van den Berg, 2012). My evaluation of mice injected with HGP-CK2.1 did not demonstrate an increase in collagen type X or osteocalcin levels. Suggesting an inhibitory mechanism for chondrocyte hypertrophy, but this needs to be evaluated in the future studies confirming its effects. However, there are many questions yet to be answered for future work. For instance, the mechanism in which peptide actuates this particular process. Similarly, specific CK2.1 induced signaling factors that differ from BMP signaling that contribute to this reparative process. Taken together my data suggests this novel peptide CK2.1 regenerates damaged cartilage without the induction of chondrocyte hypertrophy and may be a promising therapeutic candidate for the treatment OA like conditions.

Chapter 5

DISCUSSION AND CONCLUSIONS

Osteoarthritis and osteoporosis, the two most common skeletal disorders are idiopathic in nature. These degenerative diseases are commonly observed in aging population. Limited number of treatment options are available today, however with many side effects and unsuccessful long term outcomes as studies demonstrate (Doggrell, 2003; Gates et al., 2009; Mobasheri, 2013). There is no treatment today available that can reverse the loss of bone or cartilage. Therapeutic development of antibodies, growth factors and peptides treatments are under investigation to slow the progression or reverse the loss of bone or cartilage. Among the growth factors, BMPs are a potent class of proteins that induce bone and cartilage tissue regeneration (Scarfi, 2016; van der Kraan et al., 2010). Therefore, BMP signaling pathways are an excellent target for the treatment for musculoskeletal diseases like osteoporosis and OA. As BMPs are necessary for the development and maintenance of tissue homeostasis. Moreover, BMP2 and BMP7 have already been approved for the clinical application in nonunion bone fractures and spinal fusions and may therefore be considered for osteoporosis related facture treatment. Several studies have also been carried out with BMP2 and BMP7 as a treatment for cartilage repair (Badlani et al., 2009; Padma P Srinivasan et al., 2012). Therefore, exploiting their signaling pathways to develop

therapeutic targets is an ideal goal for this study. Nohe lab previously demonstrated the novel interaction between BMPRIa and CK2 (Bragdon et al., 2010). Nohe lab has designed peptides (CK2.1, CK2.2, and CK2.3) that block the interaction of CK2 with BMPRIa, resulting in the activation of downstream signaling in ligand independent manner (Bragdon et al., 2011b; Bragdon et al., 2010). This following study allowed me to explore peptide mediated activation of osteogenesis and chondrogenesis *in vitro* and *in vivo* utilizing BMPRIa downstream signaling pathways (Akkiraju et al., 2015; Bragdon et al., 2011b; Moseychuk et al., 2013). This study aims to understand the role of BMPRIa mimetic peptides CK2.3 and CK2.1 in bone and cartilage formation respectively. Previous study successfully demonstrated CK2.3 mediated osteoblastogenesis *in vitro* via the activation of the BMPRIa downstream signaling pathway in absence of the ligand (Bragdon et al., 2011c). Additionally, CK2.3 localized administrations to calvaria induced bone growth in mice (Bragdon et al., 2011b). In this study I have demonstrated that systemic administration of CK2.3 induces trabecular bone growth by enhancing osteoblastogenesis and osteoblast activity while simultaneously reducing osteoclastogenesis and osteoclast activity (Akkiraju et al., 2015). Similarly, I have demonstrated CK2.1 induced BMPRIa downstream signaling, that resulted in chondrogenesis *in vitro* and cartilage formation and repair *in vivo*.

5.1 BMP2 induced osteoblast and osteoclast activity, potential osteoporosis therapeutic?

Research has demonstrated the activity of BMPs in their ability to induce bone and cartilage formation by influencing the MSC commitment to bone and cartilage cells (Tsumaki et al., 2002). However, recent studies have also demonstrated the effects of BMP2 induced osteoclastogenesis (Itoh et al., 2001). This synergistic function of osteoblasts and osteoclasts form the mineralized matrix provide the skeletal frame work. BMP2 induced Smad and MAPK signaling in osteoblastogenesis is well documented (Yamaguchi et al., 1996). Moreover, it has been demonstrated that BMP2 induces osteoclast differentiation indirectly by activating osteoblast induced RANKL secretion and cross talk with NF-κβ signaling pathway allows for osteoclast survival (Itoh et al., 2001). An imbalance between the osteoclast and osteoblast activity where bone resorption exceeds bone formation leads to progressive degenerative disorders like osteoporosis. Therefore, BMP2 treatments may not be a considerable option, as its action in inducing osteoclastogenesis and activity may lead to accelerated bone loss in aging population. This is consistent with previously published data demonstrating increased osteoclast activity induced by BMP2 (Akkiraju et al., 2015; Bragdon et al., 2011b). However, instead of higher osteoclast number, higher osteoclast activity was observed in mice injected with BMP2 (Akkiraju et al., 2015). While this peptide CK2.3 mediated osteogenesis downstream of BMPRIa led increased bone formation similar to BMP2 treatments. However, CK2.3 injected group demonstrated neither osteoclast number nor their activity (Akkiraju et al., 2015).

5.2 CK2.3, BMPRIa mimetic peptide an alternative to BMP2

BMP2 may not be a suitable standalone therapeutic for osteoporosis due to its potential side effects. In my study BMPRIa mimetic peptide CK2.3 induced mineralization and bone formation without the effects of osteoclast activity. Serum levels of mice injected with CK2.3 consisted of higher Osteocalcin and ALP levels (markers of osteoblast activity), but no effect was seen in TRAC5B levels (marker of osteoclast activity). Although, BMP2 injected mice demonstrated significant bone formation their serum levels of TRAC5B were also elevated indicative of the osteoclast activity (Akkiraju et al., 2015). CK2.3 induced bone formation demonstrated an increase in overall trabecular density greater than that of BMP2 injected group. However, since these mice were administered BMP2 and CK2.3 doses for a short period of time may result in limited potency. Furthermore, Nohe lab has previously report CK2.3 in the inhibition of osteoclastogenesis and osteoclast activity (Bragdon et al., 2011b). This was confirmed in current study of mice systemically injected with CK2.3 resulting in the inhibition of osteoclast differentiation and activity (Akkiraju et al., 2015). These data confer the specificity of CK2.3 induced osteoblast activation and bone formation without osteoclast activation. Thus proving CK2.3 as a potential alternative to BMP2 for inducing bone formation.

5.3 CK2.3 induced specific BMPRIa downstream signaling for bone growth

Previous work also demonstrated that CK2.3 stimulations of C2C12 cells induced mineralization alone but not adipogenesis, while peptide CK2.1 induced both (Bragdon

et al., 2011b; Moseychuk et al., 2013). Moreover, studies using site directed mutations of the CK2.3 site (MCK2.3) on BMPRIa yielded similar results as that of peptide CK2.3 stimulations. Similar to peptide CK2.3 treatments, MCK2.3 transfections exhibited the potential to mineralize by inducing osteoblast differentiation but not adipocyte differentiation in C2C12 cells (Moseychuk et al., 2013). In this study I have demonstrated CK2.3 induced bone formation is possible through the activation of pERK1/2 *in vivo* (Akkiraju et al., 2015), this is confirmative from previous MCK2.3 *in vitro* study (Moseychuk et al., 2013). Furthermore, previously reported treatments of CK2.3 and MCK2.3 induced osteogenesis utilizing Smad and ERK1/2 pathways *in vitro* (Bragdon et al., 2011b; Moseychuk et al., 2013). It is shown that ERK1/2 activation is necessary for osteoblast differentiation (Matsushita et al., 2009). However, the ERK1/2 pathway that initiates osteoblastogenesis also regulates osteoclastogenesis as a secondary effect (Matsushita et al., 2009). This effect was not observed in CK2.3 induced ERK1/2 activation *in vivo*. Therefore, CK2.3 seems to be more specific in its activity of bone formation without inducing osteoclast activity.

With aging of the bone, there is a shift in bone marrow composition. In adult BMSCs from bone marrow commonly favor adipogenesis over osteoblastogenesis. In osteoporosis, this is a major concern. Osteoporotic bone is composed of increasing adipocytes and elevated levels of active osteoclast (Boyle et al., 2003; Yeung et al., 2005). Skeletal ageing studies reported that anabolic activity of BMP2 induced osteoblastogenesis is decreased, suggesting that impairment of BMP2 function may be

characterized as a molecular pathogenic response in osteoporosis (Bessho and Iizuka, 1993; Fleet et al., 1996; Matsumoto et al., 2001). BMP2 being pleiotropic also functions in inducing adipogenic differentiation of BMSCs (Takada et al., 2012; Zappitelli et al., 2015). This may explain BMP signaling shift from bone formation to fat formation of the marrow, resulting in adipocyte development in areas where bone is lost. Moreover, long term studies have not been conducted from research confirming BMP2 as a potential therapeutic. For that reason, we need to consider these possibilities when choosing BMP2 as a long term therapeutic especially in osteoporotic conditions.

Unlike BMP2 treatments, BMPRIa mimetic peptide CK2.3 treatments demonstrated no signs of adipogenic response or the activation of osteoclasts *in vivo* as demonstrated previously (Akkiraju et al., 2015; Bragdon et al., 2011b; Moseychuk et al., 2013). Moreover, I detected peptide CK2.3 in the trabecular marrow cavities, suggesting a higher half-life compared to BMP2 (Akkiraju et al., 2015; Friess et al., 1999). Therefore, CK2.3 not only inhibits osteoclasts, and activates osteoblasts, but also does not demonstrate divergent functions as BMPs do. Using peptide CK2.3 I have a unique opportunity to understand BMP induced signaling events that control bone formation. This could allow us to identify the molecular targets for future therapeutic development.

5.4 BMP2 in cartilage and OA

Another well-known function of BMP2 is formation and maintenance of articular cartilage. BMPs are present in all phases of chondrogenesis, they have shown to regulate

this by activating several chondrocyte specific gene expression (Chimal-Monroy et al., 2003; Pan et al., 2008). BMPs control all phases of chondrocyte development from MSC to chondrogenic differentiation to terminal differentiation of the chondrocyte till apoptosis. Their activity is indispensable for the proper articular cartilage formation. BMPs not only stimulate MSC condensation, but also have a strong effect on chondrocyte proliferation and matrix synthesis (Goldring et al., 2006; van der Kraan et al., 2010). Overexpression of BMP2 resulted in up-regulation of Sox9 gene expression in murine fracture models indicating enhancement of chondrogenesis mediated by BMP2 (Uusitalo et al., 2001). BMP2 is not limited to cartilage formation alone, but also for cartilage repair and cartilage homeostasis.

BMP activity boosts all phases of chondrocyte differentiation, via the Smad 1/5 and MAPK signaling pathways, including chondrocyte terminal differentiation (Kobayashi et al., 2005; Pizette and Niswander, 2000; Retting et al., 2009). Although, BMP2 is chondro protective, BMP2 also induces terminal differentiation of chondrocytes. Once terminally differentiated, chondrocytes switch protein production profiles of collagen type II, type IX, type XI, and proteoglycan production to collagen type X that in turns increases the expression levels of MMPs (Goldring, 2012; van der Kraan et al., 2010). In OA cartilage, BMP2 levels increase beyond their physiological levels (Liu et al., 2015), as a consequence elevation of MMPs like MMP13 are commonly observed (Caron et al., 2013; Zheng et al., 2003). However, elevated levels of BMP2 in OA not only increase the levels of MMP13 but also collagen type II. This

simultaneous secretion of collagen type II and MMP13 may be an attempt for repairing the lost cartilage ECM to balance tissue homeostasis (Aigner et al., 2006; Aigner et al., 2001; Hermansson et al., 2004). However, the imbalance between ECM production and excessive ECM degradation leads to OA. Furthermore, osteophyte formation is also a secondary consequence of OA. BMP2 along with TGFβ and Wnt signaling have shown to induce osteophyte formation (Nakase et al., 2003) Therefore, therapeutic approaches should consider not only restoring cartilage structures but also slow the progression of OA and lowering chondrocyte terminal differentiation. My study with the peptide CK2.1 demonstrated promising results by inducing chondrogenesis *in vitro* and cartilage formation and cartilage repair *in vivo* without inducing chondrocyte hypertrophy.

5.5 CK2.1 induced chondrogenesis; a possible inhibitor of chondrocyte hypertrophy

In this study I demonstrated the potential of the peptide CK2.1 mediated chondrogenic properties, via the activation of BMPRIa downstream signaling pathways. Previous studies in C2C12 cells have demonstrated CK2.1 mediated Smad activity, in the absence of BMP2 ligand (Bragdon et al., 2011b). CK2.1 mediated signaling initiated mineralization in C2C12 cells, this is due to C2C12 commitment is limited to adipocyte, osteoblast, myoblast but not chondrocytic development. Therefore, choosing a cell line that is known for multiple differentiation pathways I implemented the use of C3H10T1/2 cells, a commonly used model to test osteogenesis and chondrogenesis. I

have also used primary bovine chondrocyte cultures for their potential to secrete chondrogenic ECM. It has been shown that BMP2 induces osteogenesis in monolayers and in micromass cultures chondrogenic differentiation in C3H10T1/2 (Denker et al., 1999). My initial testing of the CK2.1 treatment in monolayer and micromasses yield interesting results. *In vitro* stimulations of CK2.1 in C3H10T1/2 micromasses induced chondrogenic differentiation equivalent to BMP2 stimulations (fig 3.2). Although, monolayer C2C12 cells treated with CK2.1 at 100nM induced osteogenesis in C3H10T1/2 cells it did not. However, BMP2 stimulations and peptides CK2.2, and CK2.3 were consistent in inducing osteogenesis (fig 3.6). Therefore, peptide CK2.1 alone demonstrated positive chondrogenic potential without the induction of osteogenesis while CK2.2 and CK2.3 induced osteogenic potential but not chondrogenic. *In vitro* treatments of CK2.1 induced chondrogenesis in C3H10T1/2 cells also enhanced protein production of collagen type II, but not collagen type X (marker of hypertrophic chondrocytes). This was also similar in bovine chondrocytes stimulated with CK2.1 that produced a positive collagen type IX along with collagen type II. This is in sharp contrast to BMP2 stimulations, while enhancing collagen type II production, also induced collagen type X production in C3H10T1/2 and bovine chondrocytes but not collagen type IX that is observed in CK2.1 treatments of bovine chondrocytes. This demonstrated BMP2 activity in influencing chondrocyte hypertrophic differentiation. These results were confirmed by analyzing the following mRNA profiles of adult chondrocytes that are known to actuate the following chondrogenic protein production. By the end of third week CK2.1 stimulated cells greatly expressed SOX9 and ACAN

but not MEF2C or RUNX2 (markers of hypertrophy). These genes are responsible for inducing chondrogenic potential that would correlate to the protein production observed from my analysis (Blumbach et al., 2009; Juhasz et al., 2014; Pan et al., 2008; Rainbow et al., 2014). However, BMP2 stimulations resulted in the expression of MEF2C and RUNX2 that are known to be chondrocyte hypertrophic markers (Arnold et al., 2007; Yoshida et al., 2004). *In vitro* analysis of CK2.1 has provided us the insight into its chondrogenic potential without the induction of chondrocyte hypertrophy. Furthermore, *in vivo* testing also resulted in similar results.

In vivo systemic administration of CK2.1 in mice induced cartilage growth similar to that of BMP2 administered groups. To investigate the development of OA in the knee I analyzed femurs for cartilage formation. Both BMP2 and CK2.1 injected mice femurs demonstrated collagen type II production, but major discrepancies were observed in the profiles of collagen type IX and type X. In my *in vitro* data I demonstrated that mice injected with CK2.1 induced collagen type IX along with collagen type II but not collagen type X. In contrast, BMP2 injected mice demonstrated higher levels of collagen type X but not collagen type IX. In chapter 2 I discussed systemic injections of BMP2 induced bone growth, and in chapter 3 I demonstrated that CK2.1 injected mice did not induce bone growth as BMP2 injected group. This may be an indication of subchondral changes that may have manifested if the study had gone longer and more dosages were administered to these mice. BMP2 systemic injections led to bone growth and AC formation. Furthermore, I observed the activity of BMP2

induced chondrocyte hypertrophy while CK2.1 treatment do not. This is particularly interesting as BMP2 is reported to be catabolic to cartilage only in OA conditions (Liu et al., 2015). Therefore, highlights the relationship between BMP2 and hypertrophic phenotype that would indicate subchondral bone turnover. As reports indicate that progression of OA leads to changes in subchondral changes (Buckland-Wright, 2004). Also to be noticed is that in CK2.1 injected mice there were no abnormal changes in organs weights or shapes. However, a complete comprehensive study to understand clearance rates, and toxicity across a range of CK2.1 doses should be performed in the future to identify changes associated with CK2.1 administration.

The potential of CK2.1 as truly chondrogenic and chondro protective nature was observed in the OA model. Previously it has been shown that slow release BMP2 as a potential therapeutic model in enzyme induced damage to the articular tissue in mice (Srinivasan et al., 2012). However, the severity of this model is not robust to emulate OA conditions. Therefore, I adopted DMM model for my studies as it is robust in emulating progression of OA (Glasson SS, 2007). Using hyaluronic acid based gels as drug depots CK2.1 was covalently conjugated to the gels that will release based on ester bond hydrolysis (Xiao et al., 2013). Mice with post-secondary damage to the AC of the knee were intra-articularly injected with slow release HAHGPCK2.1 that were injected intra-articularly twice over 4 weeks, once every two weeks resulted in a proficient cartilage repair. Main differences observed were in the collagen profiles as previously seen from the systemic CK2.1 injected mice. While this collagen type II was normal

across the groups, collagen type IX was highly expressed in HAHGPCK2.1 injected group alone and the least collagen type X secretion indicating a complete recovery of AC. Collagen molecules usually take a long time to produce in comparison to proteoglycans(Eyre, 2002). To form the collagenous framework, it is necessary to have larger collagen type II, and the smaller collagen type IX. This is interesting due to the fact till now there is no protein or pharmacological agent that had shown complete recovery of the damaged AC tissue and restoring collagen framework. Peptide CK2.1 consistently demonstrated chondrogenic potential without inducing chondrocyte hypertrophy *in vitro* and *in vivo*. This is a unique peptide that actuates complete cartilage repair in mice without the side effects that is reported with BMP2 usage.

5.6 Specific CK2.1 activated BMPRIa signaling for chondrogenesis

I demonstrated the CK2.1 mediated BMPRIa downstream activation of Smad pathway using reporter assays in C3H10T1/2 cells. This reporter assay for Smad activity was consistent with the previously reported work, in C2C12 cells (Bragdon et al., 2011b). Here ERK1/2, and AKT may be involved in the chondrogenic activity and may thus maintain a chondro protective role by inhibiting chondrocyte hypertrophy. It is reported that Smad 1 and Smad 5 are necessary for development and maturation of chondrocytes for the formation of AC (Retting et al., 2009). Also BMP induced TAB1/TAK1 and MAPK pathways can induce chondrogenesis (Retting et al., 2009). There are many studies that report the differences in ERK1/2 and p38 activation induced by BMP2. However, a conclusive stand point has not been reached that demonstrates a

possible MAPK mechanism that induces chondrogenesis and that inhibiting chondrocyte hypertrophy. Recent studies demonstrated that ERK1/2 is necessary for the maturation of chondrocytes, while p38 necessary maintaining chondrogenic potential without inducing chondrocyte hypertrophy (Braem et al., 2012; Jin et al., 2006; Kim and Im, 2010; Nakamura et al., 1999). Another downstream signal activated by BMP2 is PI3K/AKT that has also shown to induce chondrocyte maturation but inhibiting chondrocyte hypertrophy (Kakoi et al., 2014).

In this study I observed that BMPRIa mimetic peptide CK2.1 as a potent inducer of chondrogenesis *in vitro* and *in vivo* without inducing chondrocyte hypertrophy. Data analysis using CK2.1 mediated chondrogenesis was consistent in *in vitro* and *in vivo*. The protein profiles analyzed demonstrates chondrogenic activity enhancing the production of collagen type II and collagen type IX without collagen type X production. This is important as research demonstrates the generation of collagenous framework requires the larger collagen type II, and the smaller collagens type IX and type XI (Eyre, 2002). I demonstrated equivalent levels of Smad activity between CK2.1 and BMP2 treatments. However, the phenotypical results vary where BMP2 treatments induced chondrocyte hypertrophy but CK2.1 did not. This is expected as BMP2 is pleiotropic in nature and may initiate multiple pathways, while peptide CK2.1 may activate specific BMPRIa signaling pathways to steadily enhance the chondrogenesis and inhibit terminal differentiation. However, it is not sure if peptides can elicit similar level of potency as that of TGFβ or BMP2, but it could be used synergistically to exploit its

chondrocyte hypertrophy inhibitory attributes to develop a more sustained drug therapeutic. For future studies it is important to identify the proper signaling cascades stimulated by CK2.1 mediated BMPRIa activation, to understand the process of chondrogenesis and identify those signaling factors that inhibit terminal differentiation pathways. There are no current pharmacotherapies that can restore the lost cartilage nor slow the progression of OA. Current treatments for the late stage OA, are either arthroplasty or the more recent MSC therapies. Both are expensive and invasive procedures, non-invasive and economical approaches are necessary for long term treatment option. Understanding the peptide mediated signaling cascades allows for the development of a more suitable target that can treat OA.

5.7 BMPRIa mimetic peptides CK2.3 and CK2.1, potential therapeutic for osteoporosis and osteoarthritis?

This novel mimetic peptides CK2.3 and CK2.1 provides an interesting approach for understanding the BMPRIa mediated signaling pathways that can be exploited as targets for osteoporosis and OA therapeutic development. There are still many things to be considered before these peptides themselves can be used as therapeutics. Understanding peptide mediated BMPRIa activation is crucial to understand to mediate signaling events that can be controlled. Following things have to be addressed still; 1) rate of uptake of these peptides into the cells, 2) confirm peptide interaction with CK2 at BMPRIa site and identify potential crosstalk, 3) delineate the signaling pathways initiated by the peptide downstream of BMPRIa, and 4) look for dose responses in

animals to identify EC50, IC50 and also to rule out LD50 values for safety of administration. All these aspects must be addressed for the development of these peptides as therapeutics. Nevertheless, these peptides CK2.3 and CK2.1 are unique, and I can use them as tools to identify the molecular targets that can be used to treat bone loss in osteoporosis and cartilage repair in OA.

Chapter 6

FUTURE DIRECTIONS

6.1 Assess peptide induced BMPRIa activation

Previous work from Nohe lab and this study demonstrated the peptide mediated Smad activity downstream of BMPRIa (Akkiraju et al., 2016; Bragdon et al., 2011b). In the absence of the ligand, I was able to demonstrate the peptide mediated osteogenesis, and chondrogenesis equivalent to that of BMP2 treatment *in vitro* and their activity of bone and cartilage formation *in vivo*. However, peptide activity at the receptor level is yet to be identified. These peptides are sequenced with the CK2 binding motifs of the BMPRIa receptor and antennapedia homeodomain (amphiphilic in nature) for cellular uptake. I observed the various affects peptides elicit *in vitro* and *in vivo*, but there are many questions to be answered for understanding the peptide mediated activity. Therefore, it is vital to delineate the mechanism behind peptide mediated BMPRIa activation.

Peptides were designed to interact with CK2 sparing the receptor. This interaction can be hypothesized as a competitive inhibition. This possible Competitive inhibition of CK2 by the peptides may allow for the phosphorylation sites to be available on BMPRIa for downstream signaling. Moreover, by identifying the kinetics of peptide

binding to CK2 and CK2 binding to BMPRIa, we could determine the receptor phosphorylation levels that modulate receptor activation sequences for downstream signaling. Nohe lab has demonstrated that BMP2 ligand binding to the receptor complex leads to the release of CK2 from the type I receptor (Bragdon et al., 2009; Bragdon et al., 2010). However, it is not yet known if the CK2 binding leads to phosphorylation of a certain serine kinase that inhibits the downstream signaling. It is therefore important to identify the role of CK2 interaction to BMPRIa. Furthermore, identifying peptide cellular uptake ratios for receptor activation times specific to each peptide may shed light on the specificity of the peptide mediated BMPRIa activation and the level of CK2 interaction with the receptor. This will allow proper identification of the downstream signal pattern pertaining to the individual peptides. Additionally, it is necessary to identify the route of peptides induced receptor activation either by endocytosis through caveolae or CCP. It is reported earlier that receptor activation through specific lipid domains cause specific signaling cascades to be initiated (Bragdon et al., 2009; Hartung et al., 2006). To prove that peptides activation is through blocking CK2 interaction I have used site directed mutagenesis studies of the receptor. I have tested site directed mutations of CK2.3 (MCK2.3) and CK2.2 (MCK2.2) that proved to elicit similar activity as peptide induced signaling activity and affects (Moseychuk et al., 2013), mutations of CK2.1 site (MCK2.1) is yet to be tested *in vitro*. Identifying the differences of MCK2.1 versus CK2.1 would ascertain the differences in receptor signaling that controls the cellular phenotype.

Interestingly, BMP ligands are a class of potent proteins that interact with multiple receptors unlike the peptide which are specific to single receptor. However, it is also important to truly confirm the peptide specificity towards a single receptor. As I demonstrated in this study that peptide CK2.3 and CK2.1 demonstrated equivalent potency as BMP2 mediated bone and cartilage growth respectively. While BMP2 treatments *in vivo* induced both cartilage and bone, peptides were specific in their activity. It is interesting to note that BMP2 affinity to bind to multiple receptors in different tissues led to off target effects while peptide treatments maintained their potency to one particular tissue compartment. This being said, peptides may not be as truly potent as the ligand itself, but by consistently modulating single receptor activity could override other possible off target effects leading to the overall bone and cartilage formation. However, this needs to be answered in more detail to completely understand how the peptides may mediate this specificity. Addressing these questions will lead us closer to understanding receptor activation mechanisms and also allow us to control the target areas of the receptor to activate specific downstream signals.

6.2 Identify specific signaling cascades activated downstream of BMPRIa by the peptides

My work demonstrated the peptides CK2.3 and CK2.1 activity *in vitro* and *in vivo* by activating the BMPRIa downstream signaling for initiating osteogenesis, and chondrogenesis as demonstrated in chapters 2, 3, and 4 (Akkiraju et al., 2016; Akkiraju et al., 2015; Bragdon et al., 2011b; Moseychuk et al., 2013). However, peptide mediated

osteogenesis, and chondrogenesis utilizing different signaling pathways downstream of the same receptor system. Furthermore, peptide CK2.3 initiated osteoblastogenesis and bone formation, but not osteoclastogenesis and bone resorption as a secondary consequence commonly observed in BMP2 mediated bone formation (Itoh et al., 2001). Similarly, CK2.1 induced chondrogenesis, cartilage formation and cartilage restoration is not followed by chondrocyte hypertrophy, that is commonly the path influenced by BMPs especially BMP2 that is known to induce chondrocyte hypertrophy (van der Kraan et al., 2010). Interestingly, by identifying the peptide affinity towards the CK2 at the receptor level could provide us the information necessary to understand the dynamics of receptor phosphorylation. This may answer the specific modality of downstream signal activation specific to the particular peptide and those signaling pathways that contribute to the affects observed in this study. Studying these peptide mediated signaling pathways is ideal for identifying therapeutic targets beneficial for bone and cartilage formation. Identifying the canonical and non-canonical signaling cascades not only allow for development of therapeutic targets but also provide us the insight into understanding the signaling events specific to bone and cartilage formation.

6.3 Identify the differentially regulated genes activated by peptide mediated BMPRIa downstream signals

I demonstrated the potential of these peptides activity in bone and cartilage formation (Bragdon et al., 2011b). Along with the identification of the downstream signals, it is also important to identify the differentially regulated genes that are

responsible for the phenotypical outcome initiated by the peptides. Many studies using growth factors report the genes that regulate protein productions. Since these peptides exhibit linearly controlled activity, identifying their genes that control these signaling cascades will be beneficial at the transcriptional stages. This allows for greater understanding of transcriptional regulators for tissue formation.

6.4 Study peptide CK2.3 mediated bone formation in disease models

Previous studies and this current study used healthy mice as animal models for bone formation (Bragdon et al., 2011b). Using osteoporotic disease animal models better helps us determine the peptide efficacy in initiating the overall bone regeneration in animals with low bone density (Bonucci and Ballanti, 2014). Osteoporosis is caused by many factors in the aging population. Most commonly affecting post-menopausal women due to the varied levels of estrogenic activity. Therefore, using ovariectomized (OVX) animals that better represents the osteoporotic conditions can serve to test the peptides activity (Lelovas et al., 2008). Similarly, glucocorticoid induced activity could also lead to osteoporosis and inducing such conditions in animal models is another method to test if the peptide could reinvigorate bone formation (Fraser and Adachi, 2009). It is also beneficial to do strain tests on the peptide CK2.3 treated OVX animals to determine the condition of the bone regenerated.

In aged population the major drawback of instigating repair of musculoskeletal tissue is the variations of MSCs populations surrounding the tissue (Veronesi et al., 2011). It would be worth noting the mechanism in which the peptides actuate their

response in tissue growth or repair. Interestingly, it could be through either the utilization of MSC cell progenitors from the marrow cavities or through the re-differentiation of the cellular populations or activating the existing population of differentiated cells around the tissue. It is important to answer this as in aged population MSC levels vary greatly and depletion of MSC leads to the lack of proper repair, and by trans-differentiating the cellular population may lead to unexpected or unwanted results.

6.5 Test peptide CK2.1 induced cartilage formation in higher species and using biophysical analysis to validate tissue construction

Peptide CK2.1 treatments exhibited cartilage formation in similar capacity to BMP2 treatments and complete cartilage recovery. It is necessary to test the collagen fibril formation and complex interwoven structures using biophysical analysis like Second Harmonic Generation (SHG) imaging that can determine the proper crosslinking of newly formed collagenous tissue and overall nanomechanics of the ECM (Han et al., 2011). This will help us understand if restored cartilage from DMM mice induced by peptide CK2.1 has properly formed collagen network that is necessary to withstand the tensile forces placed on the joint. It would be beneficial to test the peptides activity in animal systems other than rodents, namely canine models that naturally suffer from joint issues. *In vitro* peptide CK2.1 activity was tested in mouse and bovine cells. It would be interesting to determine the peptides activity on chondrocytes of species like that of human or canine, that generally suffer from the cartilage related diseases allows

for studying the peptide CK2.1 action on receptor activation in disease proned conditions and not only in induced damage models like DMM (Gregory et al., 2012).

6.6 Design nanoparticle conjugate systems to deliver and monitor peptide trafficking *in vivo*

Nanoparticle conjugate systems would allow us to track the peptide movement *in vivo*. Utilizing this we could track and systematically deliver the peptide to the compartment of choice using new age nanoparticle delivery systems as described by Altai et al (Altai et al., 2016).

6.7 Study Osteo-Chondro crosstalk

I have observed the peptides CK2.3 Specificity for bone formation and CK2.1 specificity for cartilage formation. By studying the synergistic effects of these peptides *in vitro* in multipotent stem cells and differentiated osteoblasts and chondrocytes would provide a prospect in delineating the underlying signals that are responsible for subchondral bone crosstalk with chondrocytes of AC that initiates chondrocyte hypertrophy, and also determine the differences within the common signaling factors that are necessary for MSC differentiation to chondrocyte and osteoblasts.

REFERENCES

Aigner, T., Fundel, K., Saas, J., Gebhard, P. M., Haag, J., Weiss, T., Zien, A., Obermayr, F., Zimmer, R. and Bartnik, E. (2006). Large-scale gene expression profiling reveals major pathogenetic pathways of cartilage degeneration in osteoarthritis. *Arthritis Rheum* **54**, 3533-44.

Aigner, T., Zien, A., Gehrsitz, A., Gebhard, P. M. and McKenna, L. (2001). Anabolic and catabolic gene expression pattern analysis in normal versus osteoarthritic cartilage using complementary DNA-array technology. *Arthritis Rheum* **44**, 2777-89.

Akkiraju, H., Bonor, J. and Nohe, A. (2016). CK2.1, a novel peptide, induces articular cartilage formation in vivo. *J Orthop Res*.

Akkiraju, H., Bonor, J., Olli, K., Bowen, C., Bragdon, B., Coombs, H., Donahue, L. R., Duncan, R. and Nohe, A. (2015). Systemic injection of CK2.3, a novel peptide acting downstream of bone morphogenetic protein receptor BMPRIa, leads to increased trabecular bone mass. *J Orthop Res* **33**, 208-15.

Allen, K. D. and Golightly, Y. M. (2015). State of the evidence. *Curr Opin Rheumatol* **27**, 276-83.

Allende, J. E. and Allende, C. C. (1995). Protein kinases. 4. Protein kinase CK2: an enzyme with multiple substrates and a puzzling regulation. *FASEB J* **9**, 313-23.

Altai, M., Perols, A., Tsourma, M., Mitran, B., Honarvar, H., Robillard, M., Rossin, R., Ten Hoeve, W., Lubberink, M., Orlova, A. et al. (2016). Feasibility of Affibody-Based Bioorthogonal Chemistry-Mediated Radionuclide Pretargeting. *J Nucl Med* **57**, 431-6.

Archer, C. W. and Francis-West, P. (2003). The chondrocyte. *Int J Biochem Cell Biol* **35**, 401-4.

Arnold, M. A., Kim, Y., Czubryt, M. P., Phan, D., McAnally, J., Qi, X., Shelton, J. M., Richardson, J. A., Bassel-Duby, R. and Olson, E. N. (2007). MEF2C transcription factor controls chondrocyte hypertrophy and bone development. *Dev Cell* **12**, 377-89.

Badlani, N., Oshima, Y., Healey, R., Coutts, R. and Amiel, D. (2009). Use of bone morphogenic protein-7 as a treatment for osteoarthritis. *Clin Orthop Relat Res* **467**, 3221-9.

Bancroft, J. D. and Stevens, A. (1982). Theory and Practice of Histological Techniques: Churchill Livingstone.

Beamer, W. G., Shultz, K. L., Coombs, H. F., Horton, L. G., Donahue, L. R. and Rosen, C. J. (2012). Multiple quantitative trait loci for cortical and trabecular

bone regulation map to mid-distal mouse chromosome 4 that shares linkage homology to human chromosome 1p36. *J Bone Miner Res* **27**, 47-57.

Bekker, P. J., Holloway, D. L., Rasmussen, A. S., Murphy, R., Martin, S. W., Leese, P. T., Holmes, G. B., Dunstan, C. R. and DePaoli, A. M. (2004). A single-dose placebo-controlled study of AMG 162, a fully human monoclonal antibody to RANKL, in postmenopausal women. *J Bone Miner Res* **19**, 1059-66.

Bengtsson, L., Schwappacher, R., Roth, M., Boergermann, J. H., Hassel, S. and Knaus, P. (2009). PP2A regulates BMP signalling by interacting with BMP receptor complexes and by dephosphorylating both the C-terminus and the linker region of Smad1. *J Cell Sci* **122**, 1248-57.

Bessho, K. and Iizuka, T. (1993). Changes in bone inducing activity of bone morphogenetic protein with aging. *Ann Chir Gynaecol Suppl* **207**, 49-53.

Bhardwaj, N., Nguyen, Q. T., Chen, A. C., Kaplan, D. L., Sah, R. L. and Kundu, S. C. (2011). Potential of 3-D tissue constructs engineered from bovine chondrocytes/silk fibroin-chitosan for in vitro cartilage tissue engineering. *Biomaterials* **32**, 5773-81.

Bhosale, A. M. and Richardson, J. B. (2008). Articular cartilage: structure, injuries and review of management. *Br Med Bull* **87**, 77-95.

Bilezikian, J. P. (2006). Osteonecrosis of the jaw--do bisphosphonates pose a risk? *N Engl J Med* **355**, 2278-81.

Blagojevic, M., Jinks, C., Jeffery, A. and Jordan, K. P. (2010). Risk factors for onset of osteoarthritis of the knee in older adults: a systematic review and meta-analysis. *Osteoarthritis Cartilage* **18**, 24-33.

Blain, E. J. (2007). Mechanical regulation of matrix metalloproteinases. *Front Biosci* **12**, 507-27.

Blaney Davidson, E., Vitters, E., van Lent, P., van de Loo, F., van den Berg, W. and van der Kraan, P. (2007a). Elevated extracellular matrix production and degradation upon bone morphogenetic protein-2 (BMP-2) stimulation point toward a role for BMP-2 in cartilage repair and remodeling. *Arthritis Research & Therapy* **9**, R102.

Blaney Davidson, E. N., Vitters, E. L., van Lent, P. L., van de Loo, F. A., van den Berg, W. B. and van der Kraan, P. M. (2007b). Elevated extracellular matrix production and degradation upon bone morphogenetic protein-2 (BMP-2) stimulation point toward a role for BMP-2 in cartilage repair and remodeling. *Arthritis Res Ther* **9**, R102.

Blom, A. B., van Lent, P. L., Holthuysen, A. E., van der Kraan, P. M., Roth, J., van Rooijen, N. and van den Berg, W. B. (2004). Synovial lining macrophages mediate osteophyte formation during experimental osteoarthritis. *Osteoarthritis Cartilage* **12**, 627-35.

Blumbach, K., Bastiaansen-Jenniskens, Y. M., DeGroot, J., Paulsson, M., van Osch, G. J. and Zaucke, F. (2009). Combined role of type IX collagen and cartilage oligomeric matrix protein in cartilage matrix assembly: cartilage oligomeric

matrix protein counteracts type IX collagen-induced limitation of cartilage collagen fibril growth in mouse chondrocyte cultures. *Arthritis Rheum* **60**, 3676-85.

Blythe, D., Hand, N. M., Jackson, P., Barrans, S. L., Bradbury, R. D. and Jack, A. S. (1997). Use of methyl methacrylate resin for embedding bone marrow trephine biopsy specimens. *J Clin Pathol* **50**, 45-9.

Boehm, O., Zur, B., Koch, A., Tran, N., Freyenhagen, R., Hartmann, M. and Zacharowski, K. (2007). Clinical chemistry reference database for Wistar rats and C57/BL6 mice. *Biol Chem* **388**, 547-54.

Bonewald, L. F. (2007a). Osteocyte messages from a bony tomb. *Cell Metab* **5**, 410-1.

Bonewald, L. F. (2007b). Osteocytes as dynamic multifunctional cells. *Ann N Y Acad Sci* **1116**, 281-90.

Bonucci, E. and Ballanti, P. (2014). Osteoporosis-bone remodeling and animal models. *Toxicol Pathol* **42**, 957-69.

Bouxsein, M., Uchiyama, T., Rosen, C., Shultz, K., Donahue, L., Turner, C., Sen, S., Churchill, G., Muller, R. and Beamer, W. (2004). Mapping quantitative trait loci for vertebral trabecular bone volume fraction and microarchitecture in mice. *J Bone Miner Res* **19**, 587-599.

Bouxsein, M. L., Boyd, S. K., Christiansen, B. A., Guldberg, R. E., Jepsen, K. J. and Müller, R. (2010). Guidelines for assessment of bone microstructure in rodents using micro-computed tomography. *J Bone Miner Res* **25**, 1468-86.

Boyle, W. J., Simonet, W. S. and Lacey, D. L. (2003). Osteoclast differentiation and activation. *Nature* **423**, 337-42.

Braem, K., Luyten, F. P. and Lories, R. J. (2012). Blocking p38 signalling inhibits chondrogenesis in vitro but not ankylosis in a model of ankylosing spondylitis in vivo. *Ann Rheum Dis* **71**, 722-8.

Bragdon, B., Bonor, J., Shultz, K. L., Beamer, W. G., Rosen, C. J. and Nohe, A. (2012a). Bone morphogenetic protein receptor type Ia localization causes increased BMP2 signaling in mice exhibiting increased peak bone mass phenotype. *J Cell Physiol* **227**, 2870-9.

Bragdon, B., D'Angelo, A., Gurski, L., Bonor, J., Schultz, K. L., Beamer, W. G., Rosen, C. J. and Nohe, A. (2012b). Altered plasma membrane dynamics of bone morphogenetic protein receptor type Ia in a low bone mass mouse model. *Bone* **50**, 189-99.

Bragdon, B., Moseychuk, O., Saldanha, S., King, D., Julian, J. and Nohe, A. Bone morphogenetic proteins: a critical review. *Cell Signal* **23**, 609-20.

Bragdon, B., Moseychuk, O., Saldanha, S., King, D., Julian, J. and Nohe, A. (2011a). Bone morphogenetic proteins: a critical review. *Cell Signal* **23**, 609-20.

Bragdon, B., Thinakaran, S., Bonor, J., Underhill, T. M., Petersen, N. O. and Nohe, A. (2009). FRET reveals novel protein-receptor interaction of bone morphogenetic proteins receptors and adaptor protein 2 at the cell surface. *Biophys J* **97**, 1428-35.

Bragdon, B., Thinakaran, S., Moseychuk, O., Gurski, L., Bonor, J., Price, C., Wang, L., Beamer, W. G. and Nohe, A. (2011b). Casein kinase 2 regulates in vivo bone formation through its interaction with bone morphogenetic protein receptor type Ia. *Bone* **49**, 944-54.

Bragdon, B., Thinakaran, S., Moseychuk, O., Gurski, L., Bonor, J., Price, C., Wang, L., Beamer, W. G. and Nohe, A. (2011c). Casein kinase 2 regulates in vivo bone formation through its interaction with bone morphogenetic protein receptor type Ia. *Bone*.

Bragdon, B., Thinakaran, S., Moseychuk, O., King, D., Young, K., Litchfield, D. W., Petersen, N. O. and Nohe, A. (2010). Casein kinase 2 beta-subunit is a regulator of bone morphogenetic protein 2 signaling. *Biophys J* **99**, 897-904.

Brandi, M. L. (2009). Microarchitecture, the key to bone quality. *Rheumatology (Oxford)* **48 Suppl 4**, iv3-8.

Broadhead, M. L., Clark, J. C., Myers, D. E., Dass, C. R. and Choong, P. F. (2011). The molecular pathogenesis of osteosarcoma: a review. *Sarcoma* **2011**, 959248.

Bruce, S. J., Butterfield, N. C., Metzis, V., Town, L., McGlinn, E. and Wicking, C. (2010). Inactivation of Patched1 in the mouse limb has novel inhibitory effects on the chondrogenic program. *J Biol Chem* **285**, 27967-81.

Bruder, S. P. and Caplan, A. I. (1989). Cellular and molecular events during embryonic bone development. *Connect Tissue Res* **20**, 65-71.

Bucay, N., Sarosi, I., Dunstan, C. R., Morony, S., Tarpley, J., Capparelli, C., Scully, S., Tan, H. L., Xu, W., Lacey, D. L. et al. (1998). osteoprotegerin-deficient mice develop early onset osteoporosis and arterial calcification. *Genes Dev* **12**, 1260-8.

Buckland-Wright, C. (2004). Subchondral bone changes in hand and knee osteoarthritis detected by radiography. *Osteoarthritis Cartilage* **12 Suppl A**, S10-9.

Buckwalter, J. A., Anderson, D. D., Brown, T. D., Tochigi, Y. and Martin, J. A. (2013). The Roles of Mechanical Stresses in the Pathogenesis of Osteoarthritis: Implications for Treatment of Joint Injuries. *Cartilage* **4**, 286-294.

Buckwalter, J. A., Mankin, H. J. and Grodzinsky, A. J. (2005). Articular cartilage and osteoarthritis. *Instr Course Lect* **54**, 465-80.

Buckwalter, J. A., Saltzman, C. and Brown, T. (2004). The impact of osteoarthritis: implications for research. *Clin Orthop Relat Res*, S6-15.

Canalis, E. (2013). Wnt signalling in osteoporosis: mechanisms and novel therapeutic approaches. *Nat Rev Endocrinol* **9**, 575-83.

Canalis, E., Brunet, L. J., Parker, K. and Zanotti, S. (2012). Conditional inactivation of noggin in the postnatal skeleton causes osteopenia. *Endocrinology* **153**, 1616-26.

Caron, J. P., Fernandes, J. C., Martel-Pelletier, J., Tardif, G., Mineau, F., Geng, C. and Pelletier, J. P. (1996). Chondroprotective effect of intraarticular injections of interleukin-1 receptor antagonist in experimental osteoarthritis. Suppression of collagenase-1 expression. *Arthritis Rheum* **39**, 1535-44.

Caron, M. M., Emans, P. J., Cremers, A., Surtel, D. A., Coolsen, M. M., van Rhijn, L. W. and Welting, T. J. (2013). Hypertrophic differentiation during chondrogenic differentiation of progenitor cells is stimulated by BMP-2 but suppressed by BMP-7. *Osteoarthritis Cartilage* **21**, 604-13.

Champagne, C. M., Takebe, J., Offenbacher, S. and Cooper, L. F. (2002). Macrophage cell lines produce osteoinductive signals that include bone morphogenetic protein-2. *Bone* **30**, 26-31.

Chan, B. Y. and Little, C. B. (2012). The interaction of canonical bone morphogenetic protein- and Wnt-signaling pathways may play an important role in regulating cartilage degradation in osteoarthritis. *Arthritis Res Ther* **14**, 119.

CharlesRiver. (2012). Biochemistry and Hematology for C57BL/6NCrl Mouse Colonies in North American for January 2008 – December 2011, vol. 2012, pp. Technical Reference: Charles River.

Chen, G., Deng, C. and Li, Y. P. (2012). TGF-β and BMP signaling in osteoblast differentiation and bone formation. *Int J Biol Sci* **8**, 272-88.

Chevalier, X. (2010). Intraarticular treatments for osteoarthritis: new perspectives. *Curr Drug Targets* **11**, 546-60.

Chimal-Monroy, J., Rodriguez-Leon, J., Montero, J. A., Gañan, Y., Macias, D., Merino, R. and Hurle, J. M. (2003). Analysis of the molecular cascade responsible for mesodermal limb chondrogenesis: Sox genes and BMP signaling. *Dev Biol* **257**, 292-301.

Choy, E. H., Isenberg, D. A., Garrood, T., Farrow, S., Ioannou, Y., Bird, H., Cheung, N., Williams, B., Hazleman, B., Price, R. et al. (2002). Therapeutic benefit of blocking interleukin-6 activity with an anti-interleukin-6 receptor monoclonal antibody in rheumatoid arthritis: a randomized, double-blind, placebo-controlled, dose-escalation trial. *Arthritis Rheum* **46**, 3143-50.

Christenson, R. H. (1997). Biochemical markers of bone metabolism: an overview. *Clin Biochem* **30**, 573-93.

Chung, H. W., Seo, J. S., Hur, S. E., Kim, H. L., Kim, J. Y., Jung, J. H., Kim, L. H., Park, B. L. and Shin, H. D. (2003). Association of interleukin-6 promoter variant with bone mineral density in pre-menopausal women. *J Hum Genet* **48**, 243-8.

Clarke, B. (2008). Normal bone anatomy and physiology. *Clin J Am Soc Nephrol* **3 Suppl 3**, S131-9.

Clutterbuck, A. L., Asplin, K. E., Harris, P., Allaway, D. and Mobasheri, A. (2009). Targeting matrix metalloproteinases in inflammatory conditions. *Curr Drug Targets* **10**, 1245-54.

Compston, J. (2004). Bone histomorphometry [mdash] the renaissance? *IBMS BoneKEy* **1**, 9-12.

Cutolo, M., Sulli, A., Barone, A., Seriolo, B. and Accardo, S. (1993). Macrophages, synovial tissue and rheumatoid arthritis. *Clin Exp Rheumatol* **11**, 331-9.

D'Angelo, M., Yan, Z., Nooreyazdan, M., Pacifici, M., Sarment, D. S., Billings, P. C. and Leboy, P. S. (2000). MMP-13 is induced during chondrocyte hypertrophy. *J Cell Biochem* **77**, 678-93.

Datta, H. K., Ng, W. F., Walker, J. A., Tuck, S. P. and Varanasi, S. S. (2008). The cell biology of bone metabolism. *J Clin Pathol* **61**, 577-87.

Davies, D. V. and Edwards, D. A. (1948). The blood supply of the synovial membrane and intra-articular structures. *Ann R Coll Surg Engl* **2**, 142-46.

Denker, A. E., Haas, A. R., Nicoll, S. B. and Tuan, R. S. (1999). Chondrogenic differentiation of murine C3H10T1/2 multipotential mesenchymal cells: I. Stimulation by bone morphogenetic protein-2 in high-density micromass cultures. *Differentiation* **64**, 67-76.

Dimai, H. P., Linkhart, T. A., Linkhart, S. G., Donahue, L. R., Beamer, W. G., Rosen, C. J., Farley, J. R. and Baylink, D. J. (1998). Alkaline phosphatase levels and osteoprogenitor cell numbers suggest bone formation may contribute to peak bone density differences between two inbred strains of mice. *Bone* **22**, 211-6.

Doggrell, S. A. (2003). Present and future pharmacotherapy for osteoporosis. *Drugs Today (Barc)* **39**, 633-57.

Donoso, O., Pino, A. M., Seitz, G., Osses, N. and Rodriguez, J. P. (2015). Osteoporosis-associated alteration in the signalling status of BMP-2 in human MSCs under adipogenic conditions. *J Cell Biochem* **116**, 1267-77.

Duncan, J. S. and Litchfield, D. W. (2008). Too much of a good thing: the role of protein kinase CK2 in tumorigenesis and prospects for therapeutic inhibition of CK2. *Biochim Biophys Acta* **1784**, 33-47.

Erben, R. G. (1997). Embedding of bone samples in methylmethacrylate: an improved method suitable for bone histomorphometry, histochemistry, and immunohistochemistry. *J Histochem Cytochem* **45**, 307-13.

Eyre, D. (2002). Collagen of articular cartilage. *Arthritis Res* **4**, 30-5.

Eyre, D. R., Weis, M. A. and Wu, J. J. (2006). Articular cartilage collagen: an irreplaceable framework? *Eur Cell Mater* **12**, 57-63.

Falah, M., Nierenberg, G., Soudry, M., Hayden, M. and Volpin, G. (2010). Treatment of articular cartilage lesions of the knee. *Int Orthop* **34**, 621-30.

Falahati-Nini, A., Riggs, B. L., Atkinson, E. J., O'Fallon, W. M., Eastell, R. and Khosla, S. (2000). Relative contributions of testosterone and estrogen in regulating bone resorption and formation in normal elderly men. *J Clin Invest* **106**, 1553-60.

Ferguson, V. L., Ayers, R. A., Bateman, T. A. and Simske, S. J. (2003). Bone development and age-related bone loss in male C57BL/6J mice. *Bone* **33**, 387-98.

Findlay, D. M. and Atkins, G. J. (2014). Osteoblast-chondrocyte interactions in osteoarthritis. *Curr Osteoporos Rep* **12**, 127-34.

Fleet, J. C., Cashman, K., Cox, K. and Rosen, V. (1996). The effects of aging on the bone inductive activity of recombinant human bone morphogenetic protein-2. *Endocrinology* **137**, 4605-10.

Fortier, L. A., Barker, J. U., Strauss, E. J., McCarrel, T. M. and Cole, B. J. (2011). The role of growth factors in cartilage repair. *Clin Orthop Relat Res* **469**, 2706-15.

Fraser, L. A. and Adachi, J. D. (2009). Glucocorticoid-induced osteoporosis: treatment update and review. *Ther Adv Musculoskelet Dis* **1**, 71-85.

Friess, W., Uludag, H., Foskett, S., Biron, R. and Sargeant, C. (1999). Characterization of absorbable collagen sponges as rhBMP-2 carriers. *Int J Pharm* **187**, 91-9.

Fromigue, O., Modrowski, D. and Marie, P. J. (2004). Growth factors and bone formation in osteoporosis: roles for fibroblast growth factor and transforming growth factor beta. *Curr Pharm Des* **10**, 2593-603.

Fujimoto, T., Kogo, H., Nomura, R. and Une, T. (2000). Isoforms of caveolin-1 and caveolar structure. *J Cell Sci* **113 Pt 19**, 3509-17.

Gates, B. J., Sonnett, T. E., Duvall, C. A. and Dobbins, E. K. (2009). Review of osteoporosis pharmacotherapy for geriatric patients. *Am J Geriatr Pharmacother* **7**, 293-323.

Ge, C., Xiao, G., Jiang, D. and Franceschi, R. T. (2007). Critical role of the extracellular signal-regulated kinase-MAPK pathway in osteoblast differentiation and skeletal development. *J Cell Biol* **176**, 709-18.

Gelse, K., Pöschl, E. and Aigner, T. (2003a). Collagens--structure, function, and biosynthesis. *Adv Drug Deliv Rev* **55**, 1531-46.

Gelse, K., Söder, S., Eger, W., Diemtar, T. and Aigner, T. (2003b). Osteophyte development--molecular characterization of differentiation stages. *Osteoarthritis Cartilage* **11**, 141-8.

Gerritsen, H. C. and De Grauw, C. J. (1999). Imaging of optically thick specimen using two-photon excitation microscopy. *Microsc Res Tech* **47**, 206-9.

Gilboa, L., Nohe, A., Geissendorfer, T., Sebald, W., Henis, Y. I. and Knaus, P. (2000). Bone morphogenetic protein receptor complexes on the surface of live cells: a new oligomerization mode for serine/threonine kinase receptors. *Mol Biol Cell* **11**, 1023-35.

Glantschnig, H., Fisher, J. E., Wesolowski, G., Rodan, G. A. and Reszka, A. A. (2003). M-CSF, TNFalpha and RANK ligand promote osteoclast survival by signaling through mTOR/S6 kinase. *Cell Death Differ* **10**, 1165-77.

Glasson, S. S., Blanchet, T. J. and Morris, E. A. (2007). The surgical destabilization of the medial meniscus (DMM) model of osteoarthritis in the 129/SvEv mouse. *Osteoarthritis Cartilage* **15**, 1061-9.

Glasson SS, B. T., Morris EA. (2007). The surgical destabilization of the medial meniscus (DMM) model of osteoarthritis in the 129/SvEv mouse. *Osteoarthritis Cartilage* **9**, 1061-9.

Goldring, M. B. (2012). Chondrogenesis, chondrocyte differentiation, and articular cartilage metabolism in health and osteoarthritis. *Ther Adv Musculoskelet Dis* **4**, 269-85.

Goldring, M. B. and Goldring, S. R. (2007). Osteoarthritis. *J Cell Physiol* **213**, 626-34.

Goldring, M. B., Otero, M., Tsuchimochi, K., Ijiri, K. and Li, Y. (2008). Defining the roles of inflammatory and anabolic cytokines in cartilage metabolism. *Ann Rheum Dis* **67 Suppl 3**, iii75-82.

Goldring, M. B., Tsuchimochi, K. and Ijiri, K. (2006). The control of chondrogenesis. *J Cell Biochem* **97**, 33-44.

Gregory, M. H., Capito, N., Kuroki, K., Stoker, A. M., Cook, J. L. and Sherman, S. L. (2012). A review of translational animal models for knee osteoarthritis. *Arthritis* **2012**, 764621.

Grimmer, C., Balbus, N., Lang, U., Aigner, T., Cramer, T., Muller, L., Swoboda, B. and Pfander, D. (2006). Regulation of type II collagen synthesis during osteoarthritis by prolyl-4-hydroxylases: possible influence of low oxygen levels. *Am J Pathol* **169**, 491-502.

Guicheux, J., Lemonnier, J., Ghayor, C., Suzuki, A., Palmer, G. and Caverzasio, J. (2003). Activation of p38 mitogen-activated protein kinase and c-Jun-NH2-terminal kinase by BMP-2 and their implication in the stimulation of osteoblastic cell differentiation. *J Bone Miner Res* **18**, 2060-8.

Gupta, P. K., Das, A. K., Chullikana, A. and Majumdar, A. S. (2012). Mesenchymal stem cells for cartilage repair in osteoarthritis. *Stem Cell Res Ther* **3**, 25.

Hadjidakis, D. J. and Androulakis, II. (2006). Bone remodeling. *Ann N Y Acad Sci* **1092**, 385-96.

Hall, B. K. and Miyake, T. (1995). Divide, accumulate, differentiate: cell condensation in skeletal development revisited. *Int J Dev Biol* **39**, 881-93.

Han, L., Grodzinsky, A. J. and Ortiz, C. (2011). Nanomechanics of the Cartilage Extracellular Matrix. *Annu Rev Mater Res* **41**, 133-168.

Hanada, K., Solchaga, L. A., Caplan, A. I., Hering, T. M., Goldberg, V. M., Yoo, J. U. and Johnstone, B. (2001). BMP-2 induction and TGF-beta 1 modulation of rat periosteal cell chondrogenesis. *J Cell Biochem* **81**, 284-94.

Hanna, W., Barnes, P., Berendt, R., Chang, M., Magliocco, A., Mulligan, A. M., Rees, H., Miller, N., Elavathil, L., Gilks, B. et al. (2012). Testing for her2 in breast cancer: current pathology challenges faced in Canada. *Curr Oncol* **19**, 315-23.

Hardingham, T. and Bayliss, M. (1990). Proteoglycans of articular cartilage: changes in aging and in joint disease. *Semin Arthritis Rheum* **20**, 12-33.

Hartung, A., Bitton-Worms, K., Rechtman, M. M., Wenzel, V., Boergermann, J. H., Hassel, S., Henis, Y. I. and Knaus, P. (2006). Different routes of bone morphogenic protein (BMP) receptor endocytosis influence BMP signaling. *Mol Cell Biol* **26**, 7791-805.

Hashimoto, S., Creighton-Achermann, L., Takahashi, K., Amiel, D., Coutts, R. D. and Lotz, M. (2002). Development and regulation of osteophyte formation during experimental osteoarthritis. *Osteoarthritis Cartilage* **10**, 180-7.

Hassel, S., Schmitt, S., Hartung, A., Roth, M., Nohe, A., Petersen, N., Ehrlich, M., Henis, Y. I., Sebald, W. and Knaus, P. (2003). Initiation of Smad-

dependent and Smad-independent signaling via distinct BMP-receptor complexes. *J Bone Joint Surg Am* **85-A Suppl 3**, 44-51.

Hata, K., Nishimura, R., Ikeda, F., Yamashita, K., Matsubara, T., Nokubi, T. and Yoneda, T. (2003). Differential roles of Smad1 and p38 kinase in regulation of peroxisome proliferator-activating receptor gamma during bone morphogenetic protein 2-induced adipogenesis. *Mol Biol Cell* **14**, 545-55.

Hatori, M., Klatte, K. J., Teixeira, C. C. and Shapiro, I. M. (1995). End labeling studies of fragmented DNA in the avian growth plate: evidence of apoptosis in terminally differentiated chondrocytes. *J Bone Miner Res* **10**, 1960-8.

Hattner, R. and Frost, H. M. (1963). An Equation for the Mesenchymal Cell Activation Function in the Lamellar Bone Remodelling Equations. *Henry Ford Hosp Med Bull* **11**, 455-73.

Hermansson, M., Sawaji, Y., Bolton, M., Alexander, S., Wallace, A., Begum, S., Wait, R. and Saklatvala, J. (2004). Proteomic analysis of articular cartilage shows increased type II collagen synthesis in osteoarthritis and expression of inhibin betaA (activin A), a regulatory molecule for chondrocytes. *J Biol Chem* **279**, 43514-21.

Hill, P. A. (1998). Bone remodelling. *Br J Orthod* **25**, 101-7.

Hwang, J., Bae, W. C., Shieu, W., Lewis, C. W., Bugbee, W. D. and Sah, R. L. (2008). Increased hydraulic conductance of human articular cartilage and subchondral bone plate with progression of osteoarthritis. *Arthritis Rheum* **58**, 3831-42.

Ionescu, A. M., Schwarz, E. M., Vinson, C., Puzas, J. E., Rosier, R., Reynolds, P. R. and O'Keefe, R. J. (2001). PTHrP modulates chondrocyte differentiation through AP-1 and CREB signaling. *J Biol Chem* **276**, 11639-47.

Israel, D. I., Nove, J., Kerns, K. M., Kaufman, R. J., Rosen, V., Cox, K. A. and Wozney, J. M. (1996). Heterodimeric bone morphogenetic proteins show enhanced activity in vitro and in vivo. *Growth Factors* **13**, 291-300.

Itoh, K., Udagawa, N., Katagiri, T., Iemura, S., Ueno, N., Yasuda, H., Higashio, K., Quinn, J. M., Gillespie, M. T., Martin, T. J. et al. (2001). Bone morphogenetic protein 2 stimulates osteoclast differentiation and survival supported by receptor activator of nuclear factor-kappaB ligand. *Endocrinology* **142**, 3656-62.

Itoh, S., Itoh, F., Goumans, M. J. and Ten Dijke, P. (2000). Signaling of transforming growth factor-beta family members through Smad proteins. *Eur J Biochem* **267**, 6954-67.

Jazrawi, L. M. and Rosen, J. (2011). Intra-articular hyaluronic acid: potential treatment of younger patients with knee injury and/or post-traumatic arthritis. *Phys Sportsmed* **39**, 107-13.

Jensen, E. D., Pham, L., Billington, C. J., Espe, K., Carlson, A. E., Westendorf, J. J., Petryk, A., Gopalakrishnan, R. and Mansky, K. (2010). Bone morphogenic protein 2 directly enhances differentiation of murine osteoclast precursors. *J Cell Biochem* **109**, 672-82.

Jiao, Y., Sun, Z., Lee, T., Fusco, F. R., Kimble, T. D., Meade, C. A., Cuthbertson, S. and Reiner, A. (1999). A simple and sensitive antigen retrieval method for free-floating and slide-mounted tissue sections. *J Neurosci Methods* **93**, 149-62.

Jin, E. J., Lee, S. Y., Choi, Y. A., Jung, J. C., Bang, O. S. and Kang, S. S. (2006). BMP-2-enhanced chondrogenesis involves p38 MAPK-mediated down-regulation of Wnt-7a pathway. *Mol Cells* **22**, 353-9.

Jonk, L. J., Itoh, S., Heldin, C. H., ten Dijke, P. and Kruijer, W. (1998). Identification and functional characterization of a Smad binding element (SBE) in the JunB promoter that acts as a transforming growth factor-beta, activin, and bone morphogenetic protein-inducible enhancer. *J Biol Chem* **273**, 21145-52.

Juhasz, T., Matta, C., Somogyi, C., Katona, E., Takacs, R., Soha, R. F., Szabo, I. A., Cserhati, C., Szody, R., Karacsonyi, Z. et al. (2014). Mechanical loading stimulates chondrogenesis via the PKA/CREB-Sox9 and PP2A pathways in chicken micromass cultures. *Cell Signal* **26**, 468-82.

Jun, J. H., Yoon, W. J., Seo, S. B., Woo, K. M., Kim, G. S., Ryoo, H. M. and Baek, J. H. (2010). BMP2-activated Erk/MAP kinase stabilizes Runx2 by increasing p300 levels and histone acetyltransferase activity. *J Biol Chem* **285**, 36410-9.

Jurukovski, V., Dabovic, B., Todorovic, V., Chen, Y. and Rifkin, D. B. (2005). Methods for measuring TGF-b using antibodies, cells, and mice. *Methods Mol Med* **117**, 161-75.

Kakoi, H., Maeda, S., Shinohara, N., Matsuyama, K., Imamura, K., Kawamura, I., Nagano, S., Setoguchi, T., Yokouchi, M., Ishidou, Y. et al. (2014). Bone morphogenic protein (BMP) signaling up-regulates neutral sphingomyelinase 2 to suppress chondrocyte maturation via the Akt protein signaling pathway as a negative feedback mechanism. *J Biol Chem* **289**, 8135-50.

Kanakaris, N. K., Petsatodis, G., Tagil, M. and Giannoudis, P. V. (2009). Is there a role for bone morphogenetic proteins in osteoporotic fractures? *Injury* **40 Suppl 3**, S21-6.

Kang Q K, L. J. C., Gruber H E and An Y H. (2003). Histological techniques for decalcified bone and cartilageHandbook of Histology Methods for Bone and Cartilage: Totowa: Humana Press Inc.

Kapoor, M., Martel-Pelletier, J., Lajeunesse, D., Pelletier, J. P. and Fahmi, H. (2011). Role of proinflammatory cytokines in the pathophysiology of osteoarthritis. *Nat Rev Rheumatol* **7**, 33-42.

Katagiri, T. and Takahashi, N. (2002). Regulatory mechanisms of osteoblast and osteoclast differentiation. *Oral Dis* **8**, 147-59.

Katagiri, T., Yamaguchi, A., Komaki, M., Abe, E., Takahashi, N., Ikeda, T., Rosen, V., Wozney, J. M., Fujisawa-Sehara, A. and Suda, T. (1994). Bone morphogenetic protein-2 converts the differentiation pathway of C2C12 myoblasts into the osteoblast lineage. *J Cell Biol* **127**, 1755-66.

Kerrigan, M. J., Hook, C. S., Qusous, A. and Hall, A. C. (2006). Regulatory volume increase (RVI) by in situ and isolated bovine articular chondrocytes. *J Cell Physiol* **209**, 481-92.

Khosla, S., Westendorf, J. J. and Oursler, M. J. (2008). Building bone to reverse osteoporosis and repair fractures. *J Clin Invest* **118**, 421-8.

Kim, H. J. and Im, G. I. (2010). The effects of ERK1/2 inhibitor on the chondrogenesis of bone marrow- and adipose tissue-derived multipotent mesenchymal stromal cells. *Tissue Eng Part A* **16**, 851-60.

Kipnes, J., Carlberg, A. L., Loredo, G. A., Lawler, J., Tuan, R. S. and Hall, D. J. (2003). Effect of cartilage oligomeric matrix protein on mesenchymal chondrogenesis in vitro. *Osteoarthritis Cartilage* **11**, 442-54.

Kirchner, M. and Marshall, D. (2006). A double-blind randomized controlled trial comparing alternate forms of high molecular weight hyaluronan for the treatment of osteoarthritis of the knee. *Osteoarthritis Cartilage* **14**, 154-62.

Kobayashi, T. and Kronenberg, H. M. (2014). Overview of skeletal development. *Methods Mol Biol* **1130**, 3-12.

Kobayashi, T., Lyons, K. M., McMahon, A. P. and Kronenberg, H. M. (2005). BMP signaling stimulates cellular differentiation at multiple steps during cartilage development. *Proc Natl Acad Sci U S A* **102**, 18023-7.

Kostenuik, P. J. (2005). Osteoprotegerin and RANKL regulate bone resorption, density, geometry and strength. *Curr Opin Pharmacol* **5**, 618-25.

Kostoulas, G., Lang, A., Nagase, H. and Baici, A. (1999). Stimulation of angiogenesis through cathepsin B inactivation of the tissue inhibitors of matrix metalloproteinases. *FEBS Lett* **455**, 286-90.

Kuettner, K. E., Memoli, V. A., Pauli, B. U., Wrobel, N. C., Thonar, E. J. and Daniel, J. C. (1982). Synthesis of cartilage matrix by mammalian chondrocytes in vitro. II. Maintenance of collagen and proteoglycan phenotype. *J Cell Biol* **93**, 751-7.

Kurihara, N., Suda, T., Miura, Y., Nakauchi, H., Kodama, H., Hiura, K., Hakeda, Y. and Kumegawa, M. (1989). Generation of osteoclasts from isolated hematopoietic progenitor cells. *Blood* **74**, 1295-302.

Kurozumi, K., Nishita, M., Yamaguchi, K., Fujita, T., Ueno, N. and Shibuya, H. (1998). BRAM1, a BMP receptor-associated molecule involved in BMP signalling. *Genes Cells* **3**, 257-64.

Kwon, S. H., Lee, T. J., Park, J., Hwang, J. E., Jin, M., Jang, H. K., Hwang, N. S. and Kim, B. S. (2013). Modulation of BMP-2-induced chondrogenic versus osteogenic differentiation of human mesenchymal stem cells by cell-specific extracellular matrices. *Tissue Eng Part A* **19**, 49-58.

Leask, A. and Abraham, D. J. (2004). TGF-beta signaling and the fibrotic response. *FASEB J* **18**, 816-27.

Leask, A., Denton, C. P. and Abraham, D. J. (2004). Insights into the molecular mechanism of chronic fibrosis: the role of connective tissue growth factor in scleroderma. *J Invest Dermatol* **122**, 1-6.

Lee, K., Jessop, H., Suswillo, R., Zaman, G. and Lanyon, L. (2003). Endocrinology: bone adaptation requires oestrogen receptor-alpha. *Nature* **424**, 389.

Lelovas, P. P., Xanthos, T. T., Thoma, S. E., Lyritis, G. P. and Dontas, I. A. (2008). The laboratory rat as an animal model for osteoporosis research. *Comp Med* **58**, 424-30.

Lerner, U. H. (2006). Bone remodeling in post-menopausal osteoporosis. *J Dent Res* **85**, 584-95.

Li, B. (2008). Bone morphogenetic protein-Smad pathway as drug targets for osteoporosis and cancer therapy. *Endocr Metab Immune Disord Drug Targets* **8**, 208-19.

Liao, Q. C., Li, Y. L., Qin, Y. F., Quarles, L. D., Xu, K. K., Li, R., Zhou, H. H. and Xiao, Z. S. (2008). Inhibition of adipocyte differentiation by phytoestrogen genistein through a potential downregulation of extracellular signal-regulated kinases 1/2 activity. *J Cell Biochem* **104**, 1853-64.

Lin, P. M., Chen, C. T. and Torzilli, P. A. (2004). Increased stromelysin-1 (MMP-3), proteoglycan degradation (3B3- and 7D4) and collagen damage in cyclically load-injured articular cartilage. *Osteoarthritis Cartilage* **12**, 485-96.

Litchfield, D. W. (2003). Protein kinase CK2: structure, regulation and role in cellular decisions of life and death. *Biochem J* **369**, 1-15.

Litchfield, D. W., Lozeman, F. J., Piening, C., Sommercorn, J., Takio, K., Walsh, K. A. and Krebs, E. G. (1990). Subunit structure of casein kinase II from bovine testis. Demonstration that the alpha and alpha' subunits are distinct polypeptides. *J Biol Chem* **265**, 7638-44.

Litchfield, D. W., Slominski, E., Lewenza, S., Narvey, M., Bosc, D. G. and Gietz, R. D. (1996). Analysis of interactions between the subunits of protein kinase CK2. *Biochem Cell Biol* **74**, 541-7.

Little, S. C. and Mullins, M. C. (2009). Bone morphogenetic protein heterodimers assemble heteromeric type I receptor complexes to pattern the dorsoventral axis. *Nat Cell Biol* **11**, 637-43.

Liu, F., Ventura, F., Doody, J. and Massague, J. (1995). Human type II receptor for bone morphogenic proteins (BMPs): extension of the two-kinase receptor model to the BMPs. *Mol Cell Biol* **15**, 3479-86.

Liu, Y., Hou, R., Yin, R. and Yin, W. (2015). Correlation of bone morphogenetic protein-2 levels in serum and synovial fluid with disease severity of knee osteoarthritis. *Med Sci Monit* **21**, 363-70.

Liu, Z., Shen, J., Pu, K., Katus, H. A., Ploger, F., Tiefenbacher, C. P., Chen, X. and Braun, T. (2009). GDF5 and BMP2 inhibit apoptosis via activation of BMPR2 and subsequent stabilization of XIAP. *Biochim Biophys Acta* **1793**, 1819-27.

Lodewyckx, L. and Lories, R. J. (2009). WNT Signaling in osteoarthritis and osteoporosis: what is the biological significance for the clinician? *Curr Rheumatol Rep* **11**, 23-30.

Lou, J., Tu, Y., Li, S. and Manske, P. R. (2000). Involvement of ERK in BMP-2 induced osteoblastic differentiation of mesenchymal progenitor cell line C3H10T1/2. *Biochem Biophys Res Commun* **268**, 757-62.

Lu, M., Lin, S. C., Huang, Y., Kang, Y. J., Rich, R., Lo, Y. C., Myszka, D., Han, J. and Wu, H. (2007). XIAP induces NF-kappaB activation via the BIR1/TAB1 interaction and BIR1 dimerization. *Mol Cell* **26**, 689-702.

Luna, L. G. (1968). Manual of Histologic Staining Methods of the Armed Forces Institute of Pathology. NY: Blackiston Division, McGraw-Hill.

Mackie, E. J., Ahmed, Y. A., Tatarczuch, L., Chen, K. S. and Mirams, M. (2008). Endochondral ossification: how cartilage is converted into bone in the developing skeleton. *Int J Biochem Cell Biol* **40**, 46-62.

Marcus R, F. D., Nelson DA, Rosen CJ. (2008). Osteoporosis: Elsevier Academic Press.

Mariani, E., Pulsatelli, L. and Facchini, A. (2014). Signaling pathways in cartilage repair. *Int J Mol Sci* **15**, 8667-98.

Marie, P. J. and Kassem, M. (2011). Osteoblasts in osteoporosis: past, emerging, and future anabolic targets. *Eur J Endocrinol* **165**, 1-10.

Martin, J. A. and Buckwalter, J. A. (2001a). Roles of articular cartilage aging and chondrocyte senescence in the pathogenesis of osteoarthritis. *Iowa Orthop J* **21**, 1-7.

Martin, J. A. and Buckwalter, J. A. (2001b). Telomere erosion and senescence in human articular cartilage chondrocytes. *J Gerontol A Biol Sci Med Sci* **56**, B172-9.

Martin, J. A., Ellerbroek, S. M. and Buckwalter, J. A. (1997). Age-related decline in chondrocyte response to insulin-like growth factor-I: the role of growth factor binding proteins. *J Orthop Res* **15**, 491-8.

Massague, J. (1998). TGF-beta signal transduction. *Annu Rev Biochem* **67**, 753-91.

Matos, L. L., Trufelli, D. C., de Matos, M. G. and da Silva Pinhal, M. A. (2010). Immunohistochemistry as an important tool in biomarkers detection and clinical practice. *Biomark Insights* **5**, 9-20.

Matsumoto, A., Yamaji, K., Kawanami, M. and Kato, H. (2001). Effect of aging on bone formation induced by recombinant human bone morphogenetic protein-2 combined with fibrous collagen membranes at subperiosteal sites. *J Periodontal Res* **36**, 175-82.

Matsuo, K. and Irie, N. (2008). Osteoclast-osteoblast communication. *Arch Biochem Biophys* **473**, 201-9.

Matsushita, T., Chan, Y. Y., Kawanami, A., Balmes, G., Landreth, G. E. and Murakami, S. (2009). Extracellular signal-regulated kinase 1 (ERK1) and ERK2 play essential roles in osteoblast differentiation and in supporting osteoclastogenesis. *Mol Cell Biol* **29**, 5843-57.

Matyas, J. R., Sandell, L. J. and Adams, M. E. (1997). Gene expression of type II collagens in chondro-osteophytes in experimental osteoarthritis. *Osteoarthritis Cartilage* **5**, 99-105.

Mazerbourg, S. and Hsueh, A. J. (2006). Genomic analyses facilitate identification of receptors and signalling pathways for growth differentiation factor 9 and related orphan bone morphogenetic protein/growth differentiation factor ligands. *Hum Reprod Update* **12**, 373-83.

Mazzaccara, C., Labruna, G., Cito, G., ScarfÃ², M., De Felice, M., Pastore, L. and Sacchetti, L. (2008). Age-Related Reference Intervals of the Main Biochemical and Hematological Parameters in C57BL/6J, 129SV/EV and C3H/HeJ Mouse Strains. *PLoS One* **3**, e3772.

Merchant, S. N., Burgess, B., O'Malley, J., Jones, D. and Adams, J. C. (2006). Polyester wax: a new embedding medium for the histopathologic study of human temporal bones. *Laryngoscope* **116**, 245-9.

Miyazono, K., Kusanagi, K. and Inoue, H. (2001). Divergence and convergence of TGF-beta/BMP signaling. *J Cell Physiol* **187**, 265-76.

Mobasheri, A. (2013). The future of osteoarthritis therapeutics: emerging biological therapy. *Curr Rheumatol Rep* **15**, 385.

Moerman, E. J., Teng, K., Lipschitz, D. A. and Lecka-Czernik, B. (2004). Aging activates adipogenic and suppresses osteogenic programs in mesenchymal marrow stroma/stem cells: the role of PPAR-gamma2 transcription factor and TGF-beta/BMP signaling pathways. *Aging Cell* **3**, 379-89.

Moseychuk, O., Akkiraju, H., Dutta, J., D'Angelo, A., Bragdon, B., Duncan, R. L. and Nohe, A. (2013). Inhibition of CK2 binding to BMPRIa induces C2C12 differentiation into osteoblasts and adipocytes. *J Cell Commun Signal*.

Mouse Genome Sequencing, C. Waterston, R. H. Lindblad-Toh, K. Birney, E. Rogers, J. Abril, J. F. Agarwal, P. Agarwala, R. Ainscough, R. Alexandersson, M. et al. (2002). Initial sequencing and comparative analysis of the mouse genome. *Nature* **420**, 520-62.

Mueller, M., Wacker, K., Hickey, W. F., Ringelstein, E. B. and Kiefer, R. (2000). Co-localization of multiple antigens and specific DNA. A novel method using methyl methacrylate-embedded semithin serial sections and catalyzed reporter deposition. *Am J Pathol* **157**, 1829-38.

Murphy, L. and Helmick, C. G. (2012). The impact of osteoarthritis in the United States: a population-health perspective: A population-based review of the fourth most common cause of hospitalization in U.S. adults. *Orthop Nurs* **31**, 85-91.

Nakamura, K., Shirai, T., Morishita, S., Uchida, S., Saeki-Miura, K. and Makishima, F. (1999). p38 mitogen-activated protein kinase functionally contributes to chondrogenesis induced by growth/differentiation factor-5 in ATDC5 cells. *Exp Cell Res* **250**, 351-63.

Nakase, T., Miyaji, T., Tomita, T., Kaneko, M., Kuriyama, K., Myoui, A., Sugamoto, K., Ochi, T. and Yoshikawa, H. (2003). Localization of bone

morphogenetic protein-2 in human osteoarthritic cartilage and osteophyte. *Osteoarthritis Cartilage* **11**, 278-84.

Navarro, S. J., Trinh, T., Lucas, C. A., Ross, A. J., Waymire, K. G. and Macgregor, G. R. (2012). The C57BL/6J Mouse Strain Background Modifies the Effect of a Mutation in Bcl2l2. *G3 (Bethesda)* **2**, 99-102.

Nohe, A., Hassel, S., Ehrlich, M., Neubauer, F., Sebald, W., Henis, Y. I. and Knaus, P. (2002). The mode of bone morphogenetic protein (BMP) receptor oligomerization determines different BMP-2 signaling pathways. *J Biol Chem* **277**, 5330-8.

Nohe, A., Keating, E., Knaus, P. and Petersen, N. O. (2004a). Signal transduction of bone morphogenetic protein receptors. *Cell Signal* **16**, 291-9.

Nohe, A., Keating, E., Loh, C., Underhill, M. T. and Petersen, N. O. (2004b). Caveolin-1 isoform reorganization studied by image correlation spectroscopy. *Faraday Discuss* **126**, 185-95; discussion 245-54.

Nohe, A., Keating, E., Underhill, T. M., Knaus, P. and Petersen, N. O. (2005). Dynamics and interaction of caveolin-1 isoforms with BMP-receptors. *J Cell Sci* **118**, 643-50.

Nohe, A. and Petersen, N. O. (2007). Image correlation spectroscopy. *Sci STKE* **2007**, pl7.

O'Brien, F. J., Taylor, D., Dickson, G. R. and Lee, T. C. (2000). Visualisation of three-dimensional microcracks in compact bone. *J Anat* **197 Pt 3**, 413-20.

Oberlender, S. A. and Tuan, R. S. (1994). Expression and functional involvement of N-cadherin in embryonic limb chondrogenesis. *Development* **120**, 177-87.

Olivotto, E., Otero, M., Marcu, K. B. and Goldring, M. B. (2015). Pathophysiology of osteoarthritis: canonical NF-kappaB/IKKbeta-dependent and kinase-independent effects of IKKalpha in cartilage degradation and chondrocyte differentiation. *RMD Open* **1**, e000061.

Olsten, M. E., Canton, D. A., Zhang, C., Walton, P. A. and Litchfield, D. W. (2004). The Pleckstrin homology domain of CK2 interacting protein-1 is required for interactions and recruitment of protein kinase CK2 to the plasma membrane. *J Biol Chem* **279**, 42114-27.

Padma P Srinivasan, S. Y. M., Amit K Jha,, and, W. Y. X. J. M. C. F.-C. and Kirn-Safran, C. B. (2012). Injectable perlecan domain 1-hyaluronan microgels potentiate the cartilage repair
effect of BMP2 in a murine model of early
osteoarthritis. *Biomed. Mater.* **6**.

Pan, Q., Yu, Y., Chen, Q., Li, C., Wu, H., Wan, Y., Ma, J. and Sun, F. (2008). Sox9, a key transcription factor of bone morphogenetic protein-2-induced chondrogenesis, is activated through BMP pathway and a CCAAT box in the proximal promoter. *J Cell Physiol* **217**, 228-41.

Papathanasiou, I., Malizos, K. N. and Tsezou, A. (2012). Bone morphogenetic protein-2-induced Wnt/β-catenin signaling pathway activation through enhanced low-density-lipoprotein receptor-related protein 5 catabolic activity contributes to hypertrophy in osteoarthritic chondrocytes. *Arthritis Res Ther* **14**, R82.

Piston, D. W. (1999). Imaging living cells and tissues by two-photon excitation microscopy. *Trends Cell Biol* **9**, 66-9.

Pizette, S. and Niswander, L. (2000). BMPs are required at two steps of limb chondrogenesis: formation of prechondrogenic condensations and their differentiation into chondrocytes. *Dev Biol* **219**, 237-49.

Poliard, A., Ronzière, M. C., Freyria, A. M., Lamblin, D., Herbage, D. and Kellermann, O. (1999). Lineage-dependent collagen expression and assembly during osteogenic or chondrogenic differentiation of a mesoblastic cell line. *Exp Cell Res* **253**, 385-95.

Poole, A. R., Kobayashi, M., Yasuda, T., Laverty, S., Mwale, F., Kojima, T., Sakai, T., Wahl, C., El-Maadawy, S., Webb, G. et al. (2002). Type II collagen degradation and its regulation in articular cartilage in osteoarthritis. *Ann Rheum Dis* **61 Suppl 2**, ii78-81.

Poole, A. R., Rizkalla, G., Ionescu, M., Reiner, A., Brooks, E., Rorabeck, C., Bourne, R. and Bogoch, E. (1993). Osteoarthritis in the human knee: a dynamic process of cartilage matrix degradation, synthesis and reorganization. *Agents Actions Suppl* **39**, 3-13.

Poole, C. A. (1997). Articular cartilage chondrons: form, function and failure. *J Anat* **191 (Pt 1)**, 1-13.

Price, J. S., Oyajobi, B. O. and Russell, R. G. (1994). The cell biology of bone growth. *Eur J Clin Nutr* **48 Suppl 1**, S131-49.

Proff, P. and Romer, P. (2009). The molecular mechanism behind bone remodelling: a review. *Clin Oral Investig* **13**, 355-62.

Rainbow, R. S., Won, H. K. and Zeng, L. (2014). The role of Nkx3.2 in chondrogenesis. *Front Biol (Beijing)* **9**, 376-381.

Raisz, L. G. (2005). Pathogenesis of osteoporosis: concepts, conflicts, and prospects. *J Clin Invest* **115**, 3318-25.

Reddi, A. H. (2005). BMPs: from bone morphogenetic proteins to body morphogenetic proteins. *Cytokine Growth Factor Rev* **16**, 249-50.

Remst, D. F., Blaney Davidson, E. N. and van der Kraan, P. M. (2015). Unravelling osteoarthritis-related synovial fibrosis: a step closer to solving joint stiffness. *Rheumatology (Oxford)* **54**, 1954-63.

Retting, K. N., Song, B., Yoon, B. S. and Lyons, K. M. (2009). BMP canonical Smad signaling through Smad1 and Smad5 is required for endochondral bone formation. *Development* **136**, 1093-104.

Richette, P. and Roux, C. (2012). Impact of treatments for osteoporosis on cartilage biomarkers in humans. *Osteoporos Int* **23 Suppl 8**, S877-80.

Rigoglou, S. and Papavassiliou, A. G. (2013). The NF-κB signalling pathway in osteoarthritis. *Int J Biochem Cell Biol* **45**, 2580-4.

Roodman, G. D. (2006). Regulation of osteoclast differentiation. *Ann N Y Acad Sci* **1068**, 100-9.

Rosen, H. (2008). Review of comparative effectiveness of treatments to prevent fractures. *Ann Intern Med* **148**, 884; author reply 887.

Roughley, P. J. and Lee, E. R. (1994). Cartilage proteoglycans: structure and potential functions. *Microsc Res Tech* **28**, 385-97.

Roy, R., Kudryashov, V., Doty, S. B., Binderman, I. and Boskey, A. L. (2010). Differentiation and mineralization of murine mesenchymal C3H10T1/2 cells in micromass culture. *Differentiation* **79**, 211-7.

Rubart, M. (2004). Two-photon microscopy of cells and tissue. *Circ Res* **95**, 1154-66.

Ryoo, H. M., Lee, M. H. and Kim, Y. J. (2006). Critical molecular switches involved in BMP-2-induced osteogenic differentiation of mesenchymal cells. *Gene* **366**, 51-7.

Sacks, J. J., Luo, Y. H. and Helmick, C. G. (2010). Prevalence of specific types of arthritis and other rheumatic conditions in the ambulatory health care system in the United States, 2001-2005. *Arthritis Care Res (Hoboken)* **62**, 460-4.

Sahoo, S., Chung, C., Khetan, S. and Burdick, J. A. (2008). Hydrolytically degradable hyaluronic acid hydrogels with controlled temporal structures. *Biomacromolecules* **9**, 1088-92.

Saito, T., Fukai, A., Mabuchi, A., Ikeda, T., Yano, F., Ohba, S., Nishida, N., Akune, T., Yoshimura, N., Nakagawa, T. et al. (2010). Transcriptional regulation of endochondral ossification by HIF-2alpha during skeletal growth and osteoarthritis development. *Nat Med* **16**, 678-86.

Sandell, L. J. and Aigner, T. (2001). Articular cartilage and changes in arthritis. An introduction: cell biology of osteoarthritis. *Arthritis Res* **3**, 107-13.

Sapkota, G., Alarcon, C., Spagnoli, F. M., Brivanlou, A. H. and Massague, J. (2007). Balancing BMP signaling through integrated inputs into the Smad1 linker. *Mol Cell* **25**, 441-54.

Scarfi, S. (2016). Use of bone morphogenetic proteins in mesenchymal stem cell stimulation of cartilage and bone repair. *World J Stem Cells* **8**, 1-12.

SCHENK, R. (1965). [ON THE HISTOLOGICAL PROCESSING OF UNDECALCIFIED BONE]. *Acta Anat (Basel)* **60**, 3-19.

Schilcher, J., Koeppen, V., Aspenberg, P. and Michaelsson, K. (2014). Risk of atypical femoral fracture during and after bisphosphonate use. *N Engl J Med* **371**, 974-6.

Schmidt, C., Priemel, M., Kohler, T., Weusten, A., Müller, R., Amling, M. and Eckstein, F. (2003). Precision and accuracy of peripheral quantitative computed tomography (pQCT) in the mouse skeleton compared with histology and microcomputed tomography (microCT). *J Bone Miner Res* **18**, 1486-96.

Schmitt, B., Ringe, J., Häupl, T., Notter, M., Manz, R., Burmester, G. R., Sittinger, M. and Kaps, C. (2003). BMP2 initiates chondrogenic lineage

development of adult human mesenchymal stem cells in high-density culture. *Differentiation* **71**, 567-77.

Schmittgen, T. D. and Livak, K. J. (2008). Analyzing real-time PCR data by the comparative C(T) method. *Nat Protoc* **3**, 1101-8.

Schwappacher, R., Weiske, J., Heining, E., Ezerski, V., Marom, B., Henis, Y. I., Huber, O. and Knaus, P. (2009). Novel crosstalk to BMP signalling: cGMP-dependent kinase I modulates BMP receptor and Smad activity. *EMBO J* **28**, 1537-50.

Sengle, G., Charbonneau, N. L., Ono, R. N., Sasaki, T., Alvarez, J., Keene, D. R., Bachinger, H. P. and Sakai, L. Y. (2008). Targeting of bone morphogenetic protein growth factor complexes to fibrillin. *J Biol Chem* **283**, 13874-88.

Senta, H., Park, H., Bergeron, E., Drevelle, O., Fong, D., Leblanc, E., Cabana, F., Roux, S., Grenier, G. and Faucheux, N. (2009). Cell responses to bone morphogenetic proteins and peptides derived from them: biomedical applications and limitations. *Cytokine Growth Factor Rev* **20**, 213-22.

Sharma, A. R., Jagga, S., Lee, S. S. and Nam, J. S. (2013). Interplay between cartilage and subchondral bone contributing to pathogenesis of osteoarthritis. *Int J Mol Sci* **14**, 19805-30.

Shea, C. M., Edgar, C. M., Einhorn, T. A. and Gerstenfeld, L. C. (2003). BMP treatment of C3H10T1/2 mesenchymal stem cells induces both chondrogenesis and osteogenesis. *J Cell Biochem* **90**, 1112-27.

Sheehan, D. C. and Hrapchak, B. B. (1980). Theory and practice of Histotechnology: Battelle Press.

Shi, S., Mercer, S., Eckert, G. J. and Trippel, S. B. (2009). Growth factor regulation of growth factors in articular chondrocytes. *J Biol Chem* **284**, 6697-704.

Shi, S. R., Cote, R. J. and Taylor, C. R. (1997). Antigen retrieval immunohistochemistry: past, present, and future. *J Histochem Cytochem* **45**, 327-43.

Shi, S. R., Shi, Y. and Taylor, C. R. (2011). Antigen retrieval immunohistochemistry: review and future prospects in research and diagnosis over two decades. *J Histochem Cytochem* **59**, 13-32.

Shibuya, H., Iwata, H., Masuyama, N., Gotoh, Y., Yamaguchi, K., Irie, K., Matsumoto, K., Nishida, E. and Ueno, N. (1998). Role of TAK1 and TAB1 in BMP signaling in early Xenopus development. *EMBO J* **17**, 1019-28.

Shintani, N., Siebenrock, K. A. and Hunziker, E. B. (2013). TGF-ß1 enhances the BMP-2-induced chondrogenesis of bovine synovial explants and arrests downstream differentiation at an early stage of hypertrophy. *PLoS One* **8**, e53086.

Shu, B., Zhang, M., Xie, R., Wang, M., Jin, H., Hou, W., Tang, D., Harris, S. E., Mishina, Y., O'Keefe, R. J. et al. (2011). BMP2, but not BMP4, is crucial for chondrocyte proliferation and maturation during endochondral bone development. *J Cell Sci* **124**, 3428-40.

Sieber, C., Kopf, J., Hiepen, C. and Knaus, P. (2009). Recent advances in BMP receptor signaling. *Cytokine Growth Factor Rev* **20**, 343-55.

Simonet, W. S., Lacey, D. L., Dunstan, C. R., Kelley, M., Chang, M. S., Luthy, R., Nguyen, H. Q., Wooden, S., Bennett, L., Boone, T. et al. (1997).

Osteoprotegerin: a novel secreted protein involved in the regulation of bone density. *Cell* **89**, 309-19.

Song, B., Estrada, K. D. and Lyons, K. M. (2009). Smad signaling in skeletal development and regeneration. *Cytokine Growth Factor Rev* **20**, 379-88.

Sophia Fox, A. J., Bedi, A. and Rodeo, S. A. (2009). The basic science of articular cartilage: structure, composition, and function. *Sports Health* **1**, 461-8.

Srinivasan, P. P., McCoy, S. Y., Jha, A. K., Yang, W., Jia, X., Farach-Carson, M. C. and Kirn-Safran, C. B. (2012). Injectable perlecan domain 1-hyaluronan microgels potentiate the cartilage repair effect of BMP2 in a murine model of early osteoarthritis. *Biomed Mater* **7**, 024109.

Stannus, O., Jones, G., Cicuttini, F., Parameswaran, V., Quinn, S., Burgess, J. and Ding, C. (2010). Circulating levels of IL-6 and TNF-α are associated with knee radiographic osteoarthritis and knee cartilage loss in older adults. *Osteoarthritis Cartilage* **18**, 1441-7.

Su, N., Sun, Q., Li, C., Lu, X., Qi, H., Chen, S., Yang, J., Du, X., Zhao, L., He, Q. et al. (2010). Gain-of-function mutation in FGFR3 in mice leads to decreased bone mass by affecting both osteoblastogenesis and osteoclastogenesis. *Hum Mol Genet* **19**, 1199-210.

Suda, T., Takahashi, N., Udagawa, N., Jimi, E., Gillespie, M. T. and Martin, T. J. (1999). Modulation of osteoclast differentiation and function by the new members of the tumor necrosis factor receptor and ligand families. *Endocr Rev* **20**, 345-57.

Suetterlin, R., Baschong, W. and Laeng, R. H. (2004). Immunofluorescence and confocal laser scanning microscopy of chronic myeloproliferative disorders on archival formaldehyde-fixed bone marrow. *J Histochem Cytochem* **52**, 347-54.

Sugimori, K., Matsui, K., Motomura, H., Tokoro, T., Wang, J., Higa, S., Kimura, T. and Kitajima, I. (2005). BMP-2 prevents apoptosis of the N1511 chondrocytic cell line through PI3K/Akt-mediated NF-kappaB activation. *J Bone Miner Metab* **23**, 411-9.

Takada, I., Yogiashi, Y. and Kato, S. (2012). Signaling Crosstalk between PPARgamma and BMP2 in Mesenchymal Stem Cells. *PPAR Res* **2012**, 607141.

Takahashi, N., Udagawa, N. and Suda, T. (1999). A new member of tumor necrosis factor ligand family, ODF/OPGL/TRANCE/RANKL, regulates osteoclast differentiation and function. *Biochem Biophys Res Commun* **256**, 449-55.

Teitelbaum, S. L. (2000). Bone resorption by osteoclasts. *Science* **289**, 1504-8.

Thériault, G., Cottet, M., Castonguay, A., McCarthy, N. and De Koninck, Y. (2014). Extended two-photon microscopy in live samples with Bessel beams: steadier focus, faster volume scans, and simpler stereoscopic imaging. *Front Cell Neurosci* **8**, 139.

Troeberg, L. and Nagase, H. (2012). Proteases involved in cartilage matrix degradation in osteoarthritis. *Biochim Biophys Acta* **1824**, 133-45.

Tsuda, H., Wada, T., Ito, Y., Uchida, H., Dehari, H., Nakamura, K., Sasaki, K., Kobune, M., Yamashita, T. and Hamada, H. (2003). Efficient BMP2 gene transfer and bone formation of mesenchymal stem cells by a fiber-mutant adenoviral vector. *Mol Ther* **7**, 354-65.

Tsumaki, N., Nakase, T., Miyaji, T., Kakiuchi, M., Kimura, T., Ochi, T. and Yoshikawa, H. (2002). Bone morphogenetic protein signals are required for cartilage formation and differently regulate joint development during skeletogenesis. *J Bone Miner Res* **17**, 898-906.

Turgeman, G., Zilberman, Y., Zhou, S., Kelly, P., Moutsatsos, I. K., Kharode, Y. P., Borella, L. E., Bex, F. J., Komm, B. S., Bodine, P. V. et al. (2002). Systemically administered rhBMP-2 promotes MSC activity and reverses bone and cartilage loss in osteopenic mice. *J Cell Biochem* **86**, 461-74.

Uchino, M., Izumi, T., Tominaga, T., Wakita, R., Minehara, H., Sekiguchi, M. and Itoman, M. (2000). Growth factor expression in the osteophytes of the human femoral head in osteoarthritis. *Clin Orthop Relat Res*, 119-25.

Udagawa, N., Takahashi, N., Jimi, E., Matsuzaki, K., Tsurukai, T., Itoh, K., Nakagawa, N., Yasuda, H., Goto, M., Tsuda, E. et al. (1999). Osteoblasts/stromal cells stimulate osteoclast activation through expression of osteoclast differentiation factor/RANKL but not macrophage colony-stimulating factor: receptor activator of NF-kappa B ligand. *Bone* **25**, 517-23.

Uusitalo, H., Hiltunen, A., Ahonen, M., Gao, T. J., Lefebvre, V., Harley, V., Kahari, V. M. and Vuorio, E. (2001). Accelerated up-regulation of L-Sox5, Sox6, and Sox9 by BMP-2 gene transfer during murine fracture healing. *J Bone Miner Res* **16**, 1837-45.

Vaananen, H. K. and Laitala-Leinonen, T. (2008). Osteoclast lineage and function. *Arch Biochem Biophys* **473**, 132-8.

van Beuningen, H. M., Glansbeek, H. L., van der Kraan, P. M. and van den Berg, W. B. (1998). Differential effects of local application of BMP-2 or TGF-beta 1 on both articular cartilage composition and osteophyte formation. *Osteoarthritis Cartilage* **6**, 306-17.

van de Loo, F. A., Joosten, L. A., van Lent, P. L., Arntz, O. J. and van den Berg, W. B. (1995). Role of interleukin-1, tumor necrosis factor alpha, and interleukin-6 in cartilage proteoglycan metabolism and destruction. Effect of in situ blocking in murine antigen- and zymosan-induced arthritis. *Arthritis Rheum* **38**, 164-72.

van der Kraan, P. M., Blaney Davidson, E. N., Blom, A. and van den Berg, W. B. (2009). TGF-beta signaling in chondrocyte terminal differentiation and osteoarthritis: modulation and integration of signaling pathways through receptor-Smads. *Osteoarthritis Cartilage* **17**, 1539-45.

van der Kraan, P. M., Blaney Davidson, E. N. and van den Berg, W. B. Bone morphogenetic proteins and articular cartilage: To serve and protect or a wolf in sheep clothing's? *Osteoarthritis Cartilage* **18**, 735-41.

van der Kraan, P. M., Blaney Davidson, E. N. and van den Berg, W. B. (2010). Bone morphogenetic proteins and articular cartilage: To serve and protect or a wolf in sheep clothing's? *Osteoarthritis Cartilage* **18**, 735-41.

van der Kraan, P. M. and van den Berg, W. B. (2012). Chondrocyte hypertrophy and osteoarthritis: role in initiation and progression of cartilage degeneration? *Osteoarthritis Cartilage* **20**, 223-32.

Vandesompele, J., De Preter, K., Pattyn, F., Poppe, B., Van Roy, N., De Paepe, A. and Speleman, F. (2002). Accurate normalization of real-time quantitative RT-PCR data by geometric averaging of multiple internal control genes. *Genome Biol* **3**, RESEARCH0034.

Vane, J. R. and Botting, R. M. (1997). Mechanism of action of aspirin-like drugs. *Semin Arthritis Rheum* **26**, 2-10.

Varkey, M., Kucharski, C., Haque, T., Sebald, W. and Uludag, H. (2006). In vitro osteogenic response of rat bone marrow cells to bFGF and BMP-2 treatments. *Clin Orthop Relat Res* **443**, 113-23.

Veronesi, F., Torricelli, P., Borsari, V., Tschon, M., Rimondini, L. and Fini, M. (2011). Mesenchymal stem cells in the aging and osteoporotic population. *Crit Rev Eukaryot Gene Expr* **21**, 363-77.

Verzijl, N., DeGroot, J., Thorpe, S. R., Bank, R. A., Shaw, J. N., Lyons, T. J., Bijlsma, J. W., Lafeber, F. P., Baynes, J. W. and TeKoppele, J. M. (2000). Effect of collagen turnover on the accumulation of advanced glycation end products. *J Biol Chem* **275**, 39027-31.

Villanueva, A. R. and Lundin, K. D. (1989). A versatile new mineralized bone stain for simultaneous assessment of tetracycline and osteoid seams. *Stain Technol* **64**, 129-38.

von Bubnoff, A. and Cho, K. W. (2001). Intracellular BMP signaling regulation in vertebrates: pathway or network? *Dev Biol* **239**, 1-14.

Wada, T., Nakashima, T., Hiroshi, N. and Penninger, J. M. (2006). RANKL-RANK signaling in osteoclastogenesis and bone disease. *Trends Mol Med* **12**, 17-25.

Wagner, D. O., Sieber, C., Bhushan, R., Borgermann, J. H., Graf, D. and Knaus, P. (2010). BMPs: from bone to body morphogenetic proteins. *Sci Signal* **3**, mr1.

Wang, R. N., Green, J., Wang, Z., Deng, Y., Qiao, M., Peabody, M., Zhang, Q., Ye, J., Yan, Z., Denduluri, S. et al. (2014). Bone Morphogenetic Protein (BMP) signaling in development and human diseases. *Genes Dis* **1**, 87-105.

Wang, X., Manner, P. A., Horner, A., Shum, L., Tuan, R. S. and Nuckolls, G. H. (2004). Regulation of MMP-13 expression by RUNX2 and FGF2 in osteoarthritic cartilage. *Osteoarthritis Cartilage* **12**, 963-73.

Wehling, N., Palmer, G. D., Pilapil, C., Liu, F., Wells, J. W., Müller, P. E., Evans, C. H. and Porter, R. M. (2009). Interleukin-1beta and tumor necrosis factor alpha inhibit chondrogenesis by human mesenchymal stem cells through NF-kappaB-dependent pathways. *Arthritis Rheum* **60**, 801-12.

Weitzmann, M. N., Cenci, S., Rifas, L., Haug, J., Dipersio, J. and Pacifici, R. (2001). T cell activation induces human osteoclast formation via receptor activator of nuclear factor kappaB ligand-dependent and -independent mechanisms. *J Bone Miner Res* **16**, 328-37.

Wennberg, C., Hessle, L., Lundberg, P., Mauro, S., Narisawa, S., Lerner, U. H. and Millan, J. L. (2000). Functional characterization of osteoblasts and osteoclasts from alkaline phosphatase knockout mice. *J Bone Miner Res* **15**, 1879-88.

Wertz, J. W. and Bauer, P. M. (2008). Caveolin-1 regulates BMPRII localization and signaling in vascular smooth muscle cells. *Biochem Biophys Res Commun* **375**, 557-61.

Wiater, E., Harrison, C. A., Lewis, K. A., Gray, P. C. and Vale, W. W. (2006). Identification of distinct inhibin and transforming growth factor beta-binding sites on betaglycan: functional separation of betaglycan co-receptor actions. *J Biol Chem* **281**, 17011-22.

Willbold, E. and Witte, F. (2010). Histology and research at the hard tissue-implant interface using Technovit 9100 New embedding technique. *Acta Biomater* **6**, 4447-55.

Wittenburg, G., Volkel, C., Mai, R. and Lauer, G. (2009). Immunohistochemical comparison of differentiation markers on paraffin and plastic embedded human bone samples. *J Physiol Pharmacol* **60 Suppl 8**, 43-9.

Wong, S. P., Rowley, J. E., Redpath, A. N., Tilman, J. D., Fellous, T. G. and Johnson, J. R. (2015). Pericytes, mesenchymal stem cells and their contributions to tissue repair. *Pharmacol Ther* **151**, 107-20.

Wong, W. K., Knowles, J. A. and Morse, J. H. (2005). Bone morphogenetic protein receptor type II C-terminus interacts with c-Src: implication for a role in pulmonary arterial hypertension. *Am J Respir Cell Mol Biol* **33**, 438-46.

Wright, E., Hargrave, M. R., Christiansen, J., Cooper, L., Kun, J., Evans, T., Gangadharan, U., Greenfield, A. and Koopman, P. (1995). The Sry-related gene Sox9 is expressed during chondrogenesis in mouse embryos. *Nat Genet* **9**, 15-20.

Wu, J. J., Lark, M. W., Chun, L. E. and Eyre, D. R. (1991). Sites of stromelysin cleavage in collagen types II, IX, X, and XI of cartilage. *J Biol Chem* **266**, 5625-8.

Xiao, L., Tong, Z., Chen, Y., Pochan, D. J., Sabanayagam, C. R. and Jia, X. (2013). Hyaluronic acid-based hydrogels containing covalently integrated drug depots: implication for controlling inflammation in mechanically stressed tissues. *Biomacromolecules* **14**, 3808-19.

Xu, X., Jha, A. K., Harrington, D. A., Farach-Carson, M. C. and Jia, X. (2012). Hyaluronic Acid-Based Hydrogels: from a Natural Polysaccharide to Complex Networks. *Soft Matter* **8**, 3280-3294.

Yamaguchi, A., Ishizuya, T., Kintou, N., Wada, Y., Katagiri, T., Wozney, J. M., Rosen, V. and Yoshiki, S. (1996). Effects of BMP-2, BMP-4, and BMP-6 on osteoblastic differentiation of bone marrow-derived stromal cell lines, ST2 and MC3T3-G2/PA6. *Biochem Biophys Res Commun* **220**, 366-71.

Yamaguchi, D. T., Hahn, T. J., Iida-Klein, A., Kleeman, C. R. and Muallem, S. (1987). Parathyroid hormone-activated calcium channels in an osteoblast-like clonal osteosarcoma cell line. cAMP-dependent and cAMP-independent calcium channels. *J Biol Chem* **262**, 7711-8.

Yamaguchi, K., Nagai, S., Ninomiya-Tsuji, J., Nishita, M., Tamai, K., Irie, K., Ueno, N., Nishida, E., Shibuya, H. and Matsumoto, K. (1999). XIAP, a cellular member of the inhibitor of apoptosis protein family, links the receptors to TAB1-TAK1 in the BMP signaling pathway. *EMBO J* **18**, 179-87.

Yamaguchi, Y., Wada, T., Suzuki, F., Takagi, T., Hasegawa, J. and Handa, H. (1998). Casein kinase II interacts with the bZIP domains of several transcription factors. *Nucleic Acids Res* **26**, 3854-61.

Yamashita, H., Ten Dijke, P., Heldin, C. H. and Miyazono, K. (1996). Bone morphogenetic protein receptors. *Bone* **19**, 569-74.

Yan, D., Chen, D., Cool, S. M., van Wijnen, A. J., Mikecz, K., Murphy, G. and Im, H. J. (2011). Fibroblast growth factor receptor 1 is principally responsible for fibroblast growth factor 2-induced catabolic activities in human articular chondrocytes. *Arthritis Res Ther* **13**, R130.

Yang, R., Davies, C. M., Archer, C. W. and Richards, R. G. (2003). Immunohistochemistry of matrix markers in Technovit 9100 New-embedded undecalcified bone sections. *Eur Cell Mater* **6**, 57-71; discussion 71.

Yasuda, H., Shima, N., Nakagawa, N., Yamaguchi, K., Kinosaki, M., Mochizuki, S., Tomoyasu, A., Yano, K., Goto, M., Murakami, A. et al. (1998). Osteoclast differentiation factor is a ligand for osteoprotegerin/osteoclastogenesis-inhibitory factor and is identical to TRANCE/RANKL. *Proc Natl Acad Sci U S A* **95**, 3597-602.

Yeung, D. K., Griffith, J. F., Antonio, G. E., Lee, F. K., Woo, J. and Leung, P. C. (2005). Osteoporosis is associated with increased marrow fat content and decreased marrow fat unsaturation: a proton MR spectroscopy study. *J Magn Reson Imaging* **22**, 279-85.

Yoon, B. S. and Lyons, K. M. (2004). Multiple functions of BMPs in chondrogenesis. *J Cell Biochem* **93**, 93-103.

Yoshida, C. A., Yamamoto, H., Fujita, T., Furuichi, T., Ito, K., Inoue, K., Yamana, K., Zanma, A., Takada, K., Ito, Y. et al. (2004). Runx2 and Runx3 are essential for chondrocyte maturation, and Runx2 regulates limb growth through induction of Indian hedgehog. *Genes Dev* **18**, 952-63.

Yuehuei H. An, K. L. M. (2003). Histological techniques for decalcified bone and cartilage Handbook of Histology Methods for Bone and Cartilage.

Zappitelli, T., Chen, F. and Aubin, J. E. (2015). Up-regulation of BMP2/4 signaling increases both osteoblast-specific marker expression and bone marrow adipogenesis in Gja1Jrt/+ stromal cell cultures. *Mol Biol Cell* **26**, 832-42.

Zaucke, F., Dinser, R., Maurer, P. and Paulsson, M. (2001). Cartilage oligomeric matrix protein (COMP) and collagen IX are sensitive markers for the differentiation state of articular primary chondrocytes. *Biochem J* **358**, 17-24.

Zhang, F., Qiu, T., Wu, X., Wan, C., Shi, W., Wang, Y., Chen, J. G., Wan, M., Clemens, T. L. and Cao, X. (2009). Sustained BMP signaling in osteoblasts stimulates bone formation by promoting angiogenesis and osteoblast differentiation. *J Bone Miner Res* **24**, 1224-33.

Zheng, Q., Zhou, G., Morello, R., Chen, Y., Garcia-Rojas, X. and Lee, B. (2003). Type X collagen gene regulation by Runx2 contributes directly to its hypertrophic chondrocyte-specific expression in vivo. *J Cell Biol* **162**, 833-42.

Zoricic, S., Maric, I., Bobinac, D. and Vukicevic, S. (2003). Expression of bone morphogenetic proteins and cartilage-derived morphogenetic proteins during osteophyte formation in humans. *J Anat* **202**, 269-77.

Appendix A

REPRINT PERMISSION

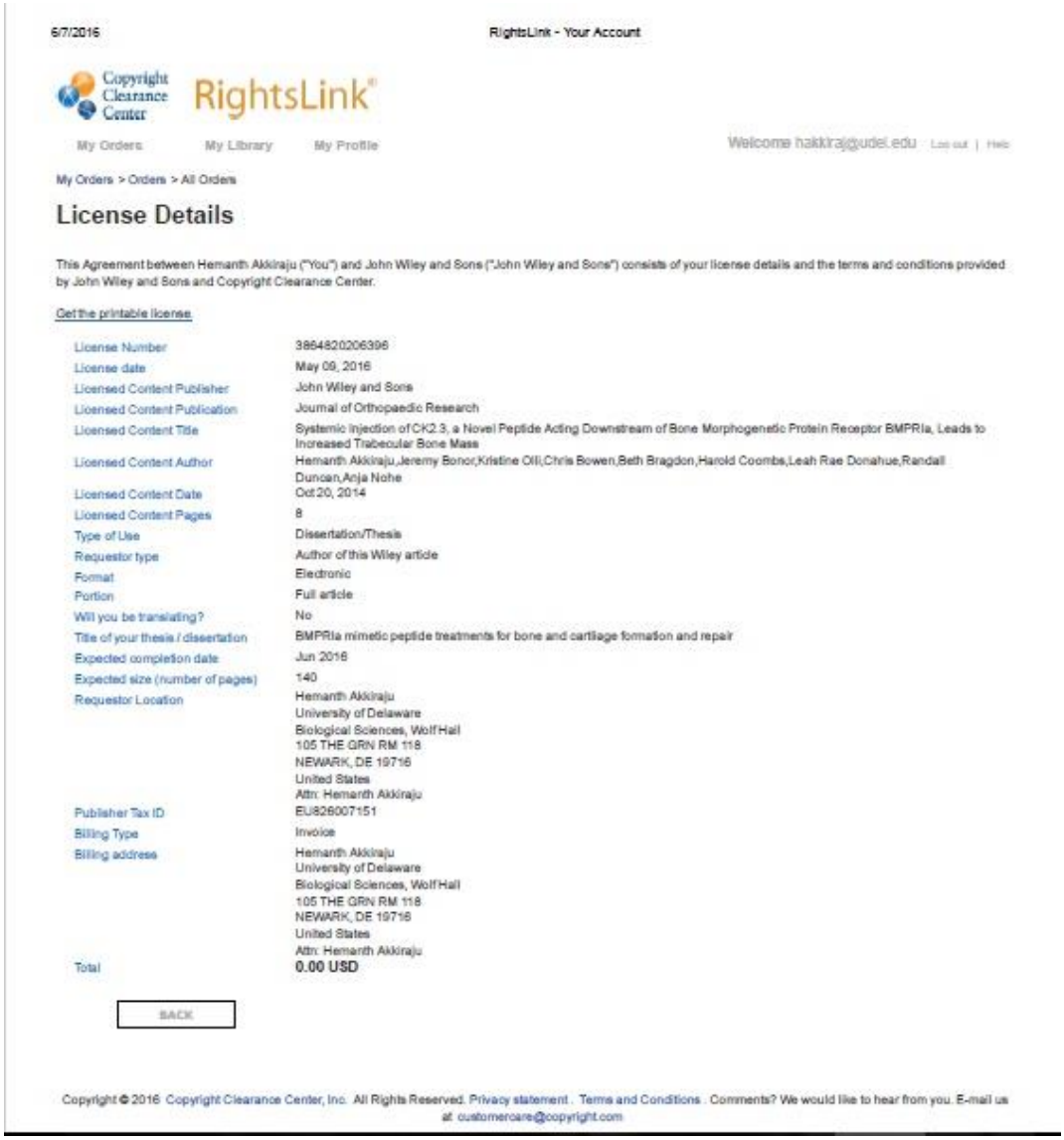

6/7/2016 RightsLink - Your Account

Copyright Clearance Center RightsLink®

My Orders My Library My Profile Welcome hakkiraj@udel.edu Log out | Help

My Orders > Orders > All Orders

License Details

This Agreement between Hemanth Akkiraju ("You") and John Wiley and Sons ("John Wiley and Sons") consists of your license details and the terms and conditions provided by John Wiley and Sons and Copyright Clearance Center.

Get the printable license.

License Number	3864820206396
License date	May 09, 2016
Licensed Content Publisher	John Wiley and Sons
Licensed Content Publication	Journal of Orthopaedic Research
Licensed Content Title	Systemic Injection of CK2.3, a Novel Peptide Acting Downstream of Bone Morphogenetic Protein Receptor BMPRIa, Leads to Increased Trabecular Bone Mass
Licensed Content Author	Hemanth Akkiraju,Jeremy Bonor,Kristine Olli,Chris Bowen,Beth Bragdon,Harold Coombs,Leah Rae Donahue,Randall Duncan,Anja Nohe
Licensed Content Date	Oct 20, 2014
Licensed Content Pages	8
Type of Use	Dissertation/Thesis
Requestor type	Author of this Wiley article
Format	Electronic
Portion	Full article
Will you be translating?	No
Title of your thesis / dissertation	BMPRIa mimetic peptide treatments for bone and cartilage formation and repair
Expected completion date	Jun 2016
Expected size (number of pages)	140
Requestor Location	Hemanth Akkiraju University of Delaware Biological Sciences, Wolf Hall 105 THE GRN RM 118 NEWARK, DE 19716 United States Attn: Hemanth Akkiraju
Publisher Tax ID	EU826007151
Billing Type	Invoice
Billing address	Hemanth Akkiraju University of Delaware Biological Sciences, Wolf Hall 105 THE GRN RM 118 NEWARK, DE 19716 United States Attn: Hemanth Akkiraju
Total	0.00 USD

BACK

Copyright © 2016 Copyright Clearance Center, Inc. All Rights Reserved. Privacy statement . Terms and Conditions . Comments? We would like to hear from you. E-mail us at customercare@copyright.com

ELSEVIER LICENSE
TERMS AND CONDITIONS

Jul 02, 2016

This Agreement between Hemanth Akkiraju ("You") and Elsevier ("Elsevier") consists of your license details and the terms and conditions provided by Elsevier and Copyright Clearance Center.

License Number	3901010415002
License date	Jul 02, 2016
Licensed Content Publisher	Elsevier
Licensed Content Publication	The International Journal of Biochemistry & Cell Biology
Licensed Content Title	Endochondral ossification: How cartilage is converted into bone in the developing skeleton
Licensed Content Author	E.J. Mackie,Y.A. Ahmed,L. Tatarczuch,K.-S. Chen,M. Mirams
Licensed Content Date	2008
Licensed Content Volume Number	40
Licensed Content Issue Number	1
Licensed Content Pages	17
Start Page	46
End Page	62
Type of Use	reuse in a thesis/dissertation
Portion	figures/tables/illustrations
Number of figures/tables/illustrations	1
Format	electronic
Are you the author of this Elsevier article?	No
Will you be translating?	No
Order reference number	
Original figure numbers	Figure 1
Title of your thesis/dissertation	BMPRIa mimetic peptide treatments for bone and cartilage formation and repair
Expected completion date	Jun 2016
Estimated size (number of pages)	140
Elsevier VAT number	GB 494 6272 12
Requestor Location	Hemanth Akkiraju University of Delaware Biological Sciences, Wolf Hall 105 THE GRN RM 118 NEWARK, DE 19716 United States Attn: Hemanth Akkiraju

Appendix B

IACUC PROTOCOL APPROVAL

RECEIVED
AUG 11 2014
IACUC

University of Delaware
Institutional Animal Care and Use Committee
Application to Use Animals in Research and Teaching

Title of Protocol: Determine the *in-vivo* Effects of Blocking Peptide and Understanding the Role of Membrane Domains on Bone Formation

AUP Number: 1194-2015-0 ← **(4 digits only — if new, leave blank)**

Principal Investigator: Dr.Anja Nohe

Common Name: Mouse

Genus Species: *Mus domesticus*

Pain Category: ***(please mark one)***

USDA PAIN CATEGORY: *(Note change of categories from previous form)*

Category	Description
☐ B	Breeding or holding where NO research is conducted
☒ C	Procedure involving momentary or no pain or distress
☐ D	Procedure where pain or distress is alleviated by appropriate means (analgesics, tranquilizers, euthanasia etc.)
☐ E	Procedure where pain or distress cannot be alleviated, as this would adversely affect the procedures, results or interpretation

Official Use Only

IACUC Approval Signature: Glenn Tallia, DVM

Date of Approval: 10/1/2014

RECEIVED
AUG 20 2012
IACUC

University of Delaware
Institutional Animal Care and Use Committee
Request to Amend An Animal Use Protocol
AMENDMENT TO ADD/DELETE PERSONNEL

(Please complete below using Arial, size 12 Font.)

Title of Protocol: Generation of mouse models with Cartilage/Bone Defects

AUP Number: 1170-2013-AP ← (4 digits only)

Principal Investigator: Catherine Kirn-Safran

Common Name: Mice

Genus Species: *Mus musculus*

Pain Category: ***(please mark one)***

USDA PAIN CATEGORY: *(Note change of categories from previous form)*

Category	Description
☐ B	Breeding or holding where NO research is conducted
☐ C	Procedure involving momentary or no pain or distress
× D	Procedure where pain or distress is alleviated by appropriate means (analgesics, tranquilizers, euthanasia etc.)
☐ E	Procedure where pain or distress cannot be alleviated, as this would adversely affect the procedures, results or interpretation

IACUC approval of major changes to an animal protocol must be reviewed and approved prior to initiating the work.

Official Use Only

IACUC Approval Signature: _____

Date of Approval: 8/27/12

Appendix C

AN IMPROVED IMMUNOSTAINING AND IMAGING METHODOLOGY TO DETERMINE CELL AND PROTEIN DISTRIBUTIONS WITHIN THE BONE ENVIRONMENT.

Abstract

Bone is a dynamic tissue that undergoes multiple changes throughout its life time. Its maintenance requires a tight regulation between the cells embedded within the bone matrix and an imbalance between these cells may lead to bone diseases such as osteoporosis. Identifying cell populations and their proteins within the bones is necessary for understanding bone biology.

Immunolabelling is one approach used to visualize proteins in tissues. Efficient immunolabelling of bone samples often requires decalcification, which may lead to changes in the structural morphology of the bone. Recently Methyl-methacrylate embedding of non-decalcified tissue followed by heat induced antigen retrieval was used to process bone sections for immunolabelling. However, this technique is applicable for bone slices below 50μM thickness while fixed on slides. Additionally, enhancing epitope exposure for immunolabelling is still a challenge. Moreover, imaging bone cells within the bone environment using standard confocal microscopy is difficult. Here we demonstrate for the first time an improved methodology for immunolabelling of non-decalcified bone using a testicular hyaluronidase enzyme based antigen retrieval technique followed by two photon fluorescence laser microscopy (TPLM) imaging.

This allowed us to image key intracellular proteins in bone cells while preserving the structural morphology of the cells and the bone.

Introduction

Bone formation is a tightly regulated process that requires coordination between osteoclasts and osteoblasts in the bone. The interaction and communication between different cell types within the bone environment leads to a densely packed rigid structure comprised of inorganic minerals, collagenous and non-collagenous matrix (Clarke, 2008). These cells are embedded within this mineralized matrix that is crucial for the proper functioning of bone (Clarke, 2008). In progressive bone disorders like osteoporosis, bone structures are weakened due to an imbalance between bone formation and bone resorption leading to bone fractures. Studying the bone composition, especially the localization of cells within the bone matrix and their protein regulation is important to better understand bone turnover. However, to achieve this goal, cells must be preserved in their native calcified structures.

Immunohistochemistry (IHC) is an attractive tool to determine cell localization and protein expression within tissues. However, application of this technique to bone is limited due to several drawbacks (Matos et al., 2010). Common practices of sample preparation for IHC involve paraffin embedding of the decalcified bone tissue (Yuehuei H. An, 2003). However, decalcifying bone leads to the loss of trabecular integrity, causing changes in the overall morphology, and makes it difficult to maintain the same bone cell environment compared to the native mineralized bone. Alternatively, Methyl

methacrylate (MMA) embedding of non-decalcified bone can be used to preserve the bone structure with the inorganic phosphates (Erben, 1997). However, sectioning of these MMA embedded bone samples is difficult. Following MMA embedding conventional IHC is performed using heat induced antigen retrieval. However, heat induced antigen retrieval is a complicated process that requires extreme precision in controlling the temperature to save the sample from destruction (Merchant et al., 2006). Microwave based heat induced retrieval is another approach to this technique (Blythe et al., 1997). However, controlling the correct temperature is a very important aspect of this technique (Yang et al., 2003). Heat induced antigen retrieval is commonly utilized for sections under 10µM thickness for IHC. The samples are then mounted on slides and the structural defects and changes in protein activity at the subcellular level are analyzed by confocal microscopy (Wittenburg et al., 2009). However, the number of fluorophores that can be used are severely limited and the technique still requires other alternatives to improve antigen availability (Yang et al., 2003). Additionally, the quality of the images obtained is limited due to low fluorescent intensity from the samples. Moreover, only small areas can be analyzed that are around 0.18 mm^2 compared to the large area covered by the tile scan around 1.62 mm^2.

Here we demonstrate for the first time the application of a testicular hyaluronidase based antigen retrieval method on non-decalcified tissues followed by TPLM imaging. Testicular hyaluronidase successfully exposes the antigen epitopes in multiple tissue types (Jurukovski et al., 2005; Suetterlin et al., 2004). However, it was not applied to

MMA embedded bone samples until now. Our method used testicular hyaluronidase without heating of the sample for a milder antigen retrieval. This prevented morphing of the sample without the necessity of fixation on a slide. Furthermore, we used TPLM imaging to penetrate deeper into the bone. We demonstrate here the imaging of a larger area and obtain higher quality images. Using a combination of these techniques allowed us to identify intracellular proteins without altering the gross morphology of the bone. Additionally the anatomical distinctions between different cell populations was also clearly resolved.

Materials and Methods

Mice

All C57BL/6J mice were obtained from The Jackson Laboratory (Bar Harbor, Me) and maintained under conventional conditions. The animal protocol was approved by IUCAC at the University of Delaware and The Jackson Laboratory. At eight weeks of age, female C57BL/6J mice (n = 7/group) were injected in the tail vein with 50 µl of PBS for 5 days. This protocol was a part of the previous study (Akkiraju et al., 2015). Mice were sacrificed four week after the last PBS injection and femurs were isolated and fixed using 10% neutral buffered formalin for 48 hours at 4^{o}C before processing. For this work we used mice samples n = 3 (out of n = 7/group) as other samples were used for previous work (Akkiraju et al., 2015).

Histology

Bones fixed in 10% Neutral Buffered Formalin (NBF) were embedded using modified protocol according to O'Brien (O'Brien et al., 2000). Chemicals purchased for infiltration and embedding were Methyl Methacrylate (MMA) (Acros, New Jersey, USA), N- Butyl Pthalate, and Benzoyl Peroxide (Wet) (Fisher Scientific, Fair Lawn, New Jersey, USA) dried carefully. Fixed bones were washed with PBS thoroughly at room temperature. Subsequently, bones were dehydrated using serial changes of ethanol gradients at 70% (8 to 16 hours), 90% (8 to 16 hours), 95% (8 to 16 hours), 100% (8 to 16 hours), 100% (8 to 16 hours), 2 changes of 2-propanol (8 to 16 hours each rinse) and 2 changes of clearing solution methyl salicylate (4 hours each). After complete dehydration, samples were infiltrated first with MMA I (765ml MMA + 140ml n-Butyl Pthalate) solution at room temperature for 48 hours, next MMA II (765ml MMA + 140ml n-Butyl Pthalate + 9.0g Dry Benzoyl Peroxide) solution at 4℃ for 48 hours, and last in MMA III (765ml MMA + 140ml n-Butyl Pthalate + 17.75g Dry Benzoyl Peroxide) solution at 4C for 48 hours. MMA III thickened is polymerized in glass vials where the infiltrated samples were placed on the polymerized layer of plastic and allowed to polymerize for 7 days in 40^{o}C oven. Polymerized blocks were trimmed and sectioned at 200μm using (10.2cm X 0.3mm) using IsoMet Low Speed Saw (Buehler, Illinois, USA) with diamond wafering blade (Buehler, Illinois, USA) and sanded down to even the surface using CarbiMet Abrasive Discs MicroCut PSA 12in 1200[P2500] (Buehler, Illinois, USA)\ grade sand paper to thin surfaces.

Morphological Staining

MMA embedded samples cut and sanded were stained using Villanueva Osteochrome bone stain according to the manufacturer protocol (Polysciences, Inc. Warrington, PA). Phase contrast images of MMA sections were taken using Nikon TMS (model TMS-F #211153).

Testicular Hyaluronidase induced Antigen Retrieval

MMA embedded samples at 200µm thickness were sanded down using CarbiMet Abrasive Discs MicroCut PSA 12in 1200[P2500] (Beuhler, Illinois, USA). Sanded sections were incubated in xylene for 1 minute to dissolve the top layer of the MMA section. These samples were then kept in pre-warmed testicular hyaluronidase solution, that was prepared accordingly; 47ml of 0.1M Potassium Phosphate + 3ml of 0.1M Sodium phosphate with 0.025gms of testicular hyaluronidase (Sigma H3884, St. Louis, MO) (Bancroft and Stevens, 1982; Luna, 1968; Sheehan and Hrapchak, 1980). Samples were incubated in the pre-warmed solution at 37°C for 30 minutes. Post incubation samples were washed with 1X PBS 3 times 5 minutes each to remove all remnants of testicular hyaluronidase solution before immunostaining.

Heat Induced Antigen Retrieval

Samples cut and sanded were treated with xylene for 1 minute as mentioned above and were placed in 400ml of 0.01M sodium citrate buffer (pH 6.0) that was brought to boiling using electric rice cooker. Sections were placed in a ceramic coverslip holder in the pre heated sodium citrate buffer for 30 minutes and taken out and allowed to cool

on ice. Samples were then washed using 1X PBS for 3 times 5 minutes each. This heat induced antigen retrieval method was adopted and modified to use electric rice cooker instead of microwave to control the temperature of the solution (Blythe et al., 1997).

Immunostaining

Immunostaining of plastic embedded samples were performed by modification and optimization of the protocols described by (O'Brien et al., 2000; Su et al., 2010) using non decalcified MMA embedded bone sections. Samples labelled for Smad1/5/ 8, pERK1/2, Osteocalcin, and Alkaline Phosphatase (ALP) MMA sections were pretreated in testicular hyaluronidase (Sigma H3884, St.Louis, MO) for 30 minutes at 37°C followed by blocking with 3% BSA for one hour. Blocked samples were labeled for with either rabbit polyclonal Smad 1/5/8 IgG (Santa Cruz Biotech, CA, USA) diluted 1:500 in 3% BSA overnight at 4°C followed by a 1:500 dilution of Alexa 546 goat anti rabbit (Invitrogen, Eugene, OR, USA) for 1 hour at room temperature (RT) or Mouse monoclonal p44/p42 MAPK (ERK1/2) antibody (cell signaling, MA, USA) preconjugated with Alexa 633 goat anti mouse IgG (Invitrogen, Eugene, OR, USA) diluted 1:500 in 3% BSA for 1 hour or rabbit polyclonal Osteocalcin (Santa Cruz, Biotech, CA, USA) diluted 1:500 in 3% BSA overnight at 4°C followed by a 1:500 dilution of Alexa 488 donkey anti rabbit (Invitrogen, Eugene, OR, USA) for 1 hour at RT or goat polyclonal ALP (Santa Cruz, Biotech, CA, USA) diluted 1:500 in 3% BSA overnight at 4°C followed by a 1:500 dilution of Alexa 568 donkey anti goat (Invitrogen, Eugene, OR, USA) for 1 hour at RT . Nuclear stain Hoechst

(Bisbenzinamide 33342, Sigma Aldrich, St.Louis, MO) was administered for 10 minutes and washed using PBS.

Confocal Imaging

Samples were imaged (n=3 mice) using Zeiss LSM 780 NLO; with 20X EC Plan Apochromat- 0.6 HD DIC M27. Two photon excitation was used to penetrate deeper into the plastic sections. Titanium:Sapphire ($Ti:Al_2O_3$) laser was tuned to 780 nm with a laser power of 3.5% and Helium Neon ($HeNe_2$) laser set at excitation 633 nm at 7% laser power equipped with 20X, 0.6NA HD M27 air objective corrected for samples without coverslips. The Main Beam Splitter (MBS) of the confocal was set to 488/561/633, MBS 760+, with the filters set to measure Alexa 488, Alexa 546, Alexa 568, Alexa 633, and Hoechst (405 nm excitation). Using the 780 as conventional confocal, the main beam splitter was set to and MBS 488/561/633 and MBS 405. Fluorophores were detected utilizing Argon laser tuned to 488 nm at 2% laser power, diode pumped solid state (DPSS) laser tuned to 561 nm at 7% laser power, HeNe laser tuned to 633 at 2% laser power, and diode 405-30 tuned to 405 nm wit 2% laser power with the filters set to measure Alexa 488, Alexa 546, Alexa 568, Alexa 633, and Hoechst (405 nm excitation). Objective comparison was done between 20X, 0.6NA HD M27 EC Epiplan Apochromat corrected for samples without coverslips and 20X, 0.75NA Plan Apochromat corrected for 0.17 mm coverslip. All images were processed using ImageJ.

Results

MMA embedding preserved gross morphology of bone

Examination of bone histomorphometry is essential for the measurement of localized bone turnover and remodeling using histological sections of bone (Compston, 2004). However, bone remodeling still remains a poorly understood process due to its many technical limitations in the histology and imaging field.

The conventional techniques used to identify the signaling events in calcified tissue are limited, and require decalcification of the tissue for thin sections (Yuehuei H. An, 2003). However, in this process the gross morphology of the bone is lost. Respectively bone cells like osteoblasts that traverse the bone in its calcified regions are lost. Therefore, we embedded the non-decalcified bone in MMA. Conventional MMA embedding has been around for many decades now and due to its simplicity (O'Brien et al., 2000; SCHENK, 1965). Utilizing this technique we embedded the trabecular head of the femurs to study the trabecular architecture and its cellular activity. Following embedding, our samples were sectioned and sanded to thin even areas for further processing. To understand the base morphology of the trabecular bone makeup (Clarke, 2008) we used Villanueva Osteochrome stain to mark the regions of new bone formation by osteoblasts and the calcified regions of the tissue (Villanueva and Lundin, 1989) as demonstrated in Fig 1 .

Antigen retrieval of calcified tissue by testicular hyaluronidase digestion

In order to gain more insight into bone homeostasis it is crucial to determine changes in cell distribution and protein expression within bone. Imaging cells and proteins in their

native environment can provide an accurate evaluation of bone remodeling. Osteoblasts preserved in the calcified regions are responsible for the overall bone formation. Smad1/5/8 and ERK1/2 signaling activity is required for osteoblast mediated bone formation (Matsushita et al., 2009; Retting et al., 2009; Song et al., 2009). In addition common biomarkers of osteoblasts include alkaline phosphatase (ALP) and osteocalcin determining the osteoblast activity in bone formation (Christenson, 1997). Therefore we chose these proteins for IHC of our bone sections.

We used a testicular hyaluronidase based antigen retrieval to expose the cells from the tissue ECM. This allowed us to immunostain proteins as Smad, p-ERK , osteocalcin and ALP. Immunostaining was performed by pretreatment of bone sections with testicular hyaluronidase. Samples were then incubated with primary antibodies overnight followed by secondary antibodies at RT for an hour. As controls we used heat induced antigen retrieval as described earlier (Jiao et al., 1999). (Fig. 2A) shows non-treated bone samples as a comparison. We observed excellent antigen retrieval using testicular hyaluronidase using our method compared to non-treated samples (Fig. 2B, 2C). Heat induced antigen retrieval led to the disfiguring of the sample making the imaging process an arduous task as it was hard to obtain a flat image surface (Fig. 2D). Additionally the images obtained by this technique showed low quality staining (Fig. 2E).

Two photon fluorescence laser microscopy (TPLM) imaging of thick MMA embedded sections

To view the patterns of bone tissue sections conventional confocal microscopy is not the ideal source of imaging. This is due to its limited capability in penetration of thicker bone tissue samples for the acquisition of large bone areas. To penetrate deeper into these thick samples we used two photon fluorescence laser microscopy (TPLM) (Fig 2). It is the preferred technique to resolve any microscopic structures with uneven ridges on an optically thick specimen (Piston, 1999). To determine the protein expression in osteoblasts in MMA embedded samples we immunolabelled sections for signaling factors as Smad1/5/8 and pERK1/2 and osteoblast biomarkers like ALP and osteocalcin. Sections were imaged using two photon excitation microscopy. We compared the TPLM obtained image quality to conventional confocal microscopy. Using a tile scan we stitched the images together to visualize the overall structure of the trabecular portion (Fig. 3). As can be seen two photon excitation microscopy surpassed the ability of conventional confocal microscopy allowing for deeper penetration and greater signal to noise ratio. This also allowed us to focus at cellular levels using high resolution imaging to identify the cells expressing proteins of interest as demonstrated in Figure 4.

Selection of Objective used for TLPM imaging of bone

Thick bone samples were imaged without a coverslips using 20X 0.6NA HD M27 (EC Epiplan Apochromat) objective designed for samples without coverslips (Fig. 5A). For comparison we also imaged the sample using 20X 0.75NA (Plan Apochromat) corrected for 0.17mm coverslips (Fig. 5B). It is important to notice that the working distance of the objective effects the penetration of the laser beam into the sample (Piston, 1999).

Working distance of the 20X 0.6NA HD M27 objective is 1.7mm, while the objective 20X 0.75NA working distance only 0.61mm. This greater working distance allowed for the deeper penetration of the sample and compensate for the loss in NA to obtain larger area of information (Fig. 5).

Troubleshooting

Understanding the proper parameters is important in order to obtain the perfect sample. Table 1 summarizes potential problems and their solutions during the process. This allowed us to visualize the signaling proteins within the osteoblasts, the lining cells and the osteocytes.

Discussion

Bone is a dynamic tissue that undergoes continuous bone formation and resorption. This is regulated by bone cells such as osteoblasts and osteoclast. In progressive degenerative bone disorders like osteoporosis or osteomalacia an imbalance between cellular activities is responsible for these bone defects. The majority of the changes within the bone occur on the cancellous bone or the trabecular surface of the bone (Brandi, 2009). Therefore, it is imperative to understand the cellular signaling activity that causes such major imbalances between the bone cells. We can better understand cellular activity in bone formation by identifying osteoblast activity using intracellular signaling cascades.. For example, previous work demonstrated Smad1/5/8 and ERK1/2 activity in osteoblast

differentiation and their activity in bone formation (Matsushita et al., 2009; Retting et al., 2009; Song et al., 2009). Also we can identify osteoblast activity using biomarkers such as ALP and osteocalcin (Christenson, 1997).However, direct labelling of these proteins in bone samples is challenging. Indeed labelling proteins in general in cells within the bone environment is difficult. The current practice of decalcifying the bone tissue may not be the best method to identify the changes in these proteins and their dynamics in bone turnover or bone remodeling.

We demonstrated for the first time the imaging of intracellular signaling proteins in calcified bone tissue using testicular hyaluronidase based antigen retrieval methodology. We optimized the methodology for immunostaining of multiple fluorophores and utilized two photon microscopy for imaging sample specimens with maximal resolution. For decades non decalcified bone tissue was commonly preserved and embedded in a resin type material for hard tissue sections. Previously described cold processing of MMA for hard tissue embedding like the technovit 9100 shows greater preservation of antigenicity. (Erben, 1997; Willbold and Witte, 2010; Yuehuei H. An, 2003). While the authors agree on its superiority in preservation, we focussed here only on the conventional MMA technique and remedial process for retrieving antigenicity to the tissue samples. We therefore, utilize the conventional MMA embedding for our experimental study. Moreover, due to chemical alterations during fixation and processing in conventional MMA embedding the samples require harsh treatments of antigen retrieval. In general there are two types of antigen retrieval methods; heat

induced epitope retrieval and enzyme induced epitope retrieval (Mueller et al., 2000; Shi et al., 1997; Shi et al., 2011; Willbold and Witte, 2010). However, only heat induced antigen retrieval was successfully demonstrated in MMA embedded samples. However, trauma induced to the sample due to high temperature conditions and disruption to its morphology is a notable concern (Merchant et al., 2006). Developing a process that uses a milder enzyme based antigen retrieval could be advantageous over heat induced antigen retrieval. This may allow labelling of sections thicker than 10µM thickness that are not mounted on permanent slide fixtures. Furthermore, reducing the number of steps required for sample processing ensures the sample health and improves labelling of the intracellular proteins. A pragmatic approach utilizing enzyme based antigen retrieval can help preserve the tissue in its present form without adverse changes to the surrounding proteins and to the sample structure. As an enzyme based antigen retrieval, testicular hyaluronidase is known to successfully expose the antigen epitopes in multiple tissue types (Jurukovski et al., 2005; Suetterlin et al., 2004). However, this was not demonstrated in MMA embedded samples until now.

Advances in confocal microscopy avails us the opportunity to visualize the micro-anatomical components of bone. To image these immunostained samples, TPLM based imaging best suits to obtain the resolution without the interference of the background noise generated by the surrounding ECM and the uneven ridges present on the surface of the calcified tissue. Moreover, TPLM allows for the penetration of thick specimens to image at deeper depths compared to conventional confocal microscopy (Gerritsen

and De Grauw, 1999; Thériault et al., 2014). Two photon excitation imaging permits the imaging of sensitive proteins with a reduced loss of fluorophore activity. Utilizing the microscopes focal volume but not confocal pinhole allows for a higher signal. Moreover, usage of an emission pinhole in conventional confocal microscopy leads to inevitable scattering of fluorescent photons. Two photon microscopy however requires no pinhole, thus this particular method can be exploited for exciting multiple fluorescent molecules by simultaneous absorption (Gerritsen and De Grauw, 1999). Furthermore, photo damage and photo bleaching of fluorophores are limited in two-photon excitation imaging compared to conventional confocal (Rubart, 2004). These advances in two photon excitation microscopy allowed us high resolution imaging of decalcified bone samples without the interference of background noise. Also we used an objective that is corrected for samples without coverslip and that covers a greater working distance for the enhancement of overall depth penetration and information acquired. While the NA of the objectives can provide greater brightness it is also important to recognize the objectives capability for it best working distance from the sample to obtain more information. This becomes a crucial aspect while imaging thick samples allowing for the deeper penetration into the tissue (Piston, 1999).

The protocol presented here is straight forward, however multiple problems can occur during the embedding process. We highlighted most common mistakes and their solution in Table 1.

The methodology described by us has multiple applications that are not only limited to bone diseases. It can be applied to identify multiple problems related to bone cancer metastasis by visualizing metastatic nature of cancer cells (Hanna et al., 2012). It may help to determine the protein expressions that may be involved in controlling the surrounding tissue and much more. In conclusion our improved methodology allows for the first time for the identification of multiple protein targets within the intact bone environment.

Acknowledgements

This work has been supported by NIH grant R01AR064243. Also we would like to thank Michael Moore of the Delaware Biotechnology Institute for aiding us with the image setup on the Zeiss 780. We would also like to thank Dr. Liyun Wang of University of Delaware for allowing us to utilize the Buehler Isomet saw for our experiments.

Conflicts of Interest

The authors declare no conflict of interest.

Authors Contribution

Hemanth Akkiraju has performed all experiments and wrote the manuscript. Jeremy Bonor extracted the animal tissue and helped in the embedding process. Anja Nohe, analyzed the images and oversaw the writing of this manuscript.

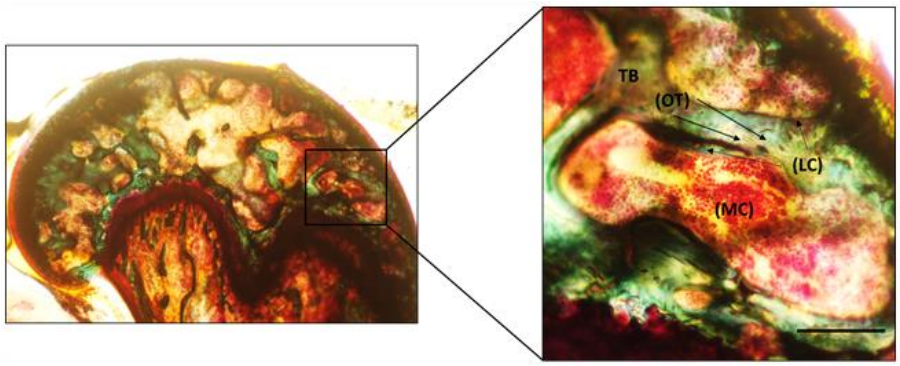

Figure 1. Trabecular morphology of the MMA embedded femur sample. Femurs from mice were processed in MMA and stained byVillanueva Osteochrome. Phase contrast images of the samples show Osteocytes (OT) represented in dark brownish color, dense osteoid seams of trabecular bone (TB) in green and osteoblasts or lining cells (LC) of the marrow cavity (MC) in light red color. Sections were imaged in the cancellous or TB of the mouse femur around MC where the LC or the active osteoblasts reside alongside of OT indicated by arrows. Images were taken using 20X magnification with scale bar representing 50 µm using a Nikon TMS (model TMS-F #211153)

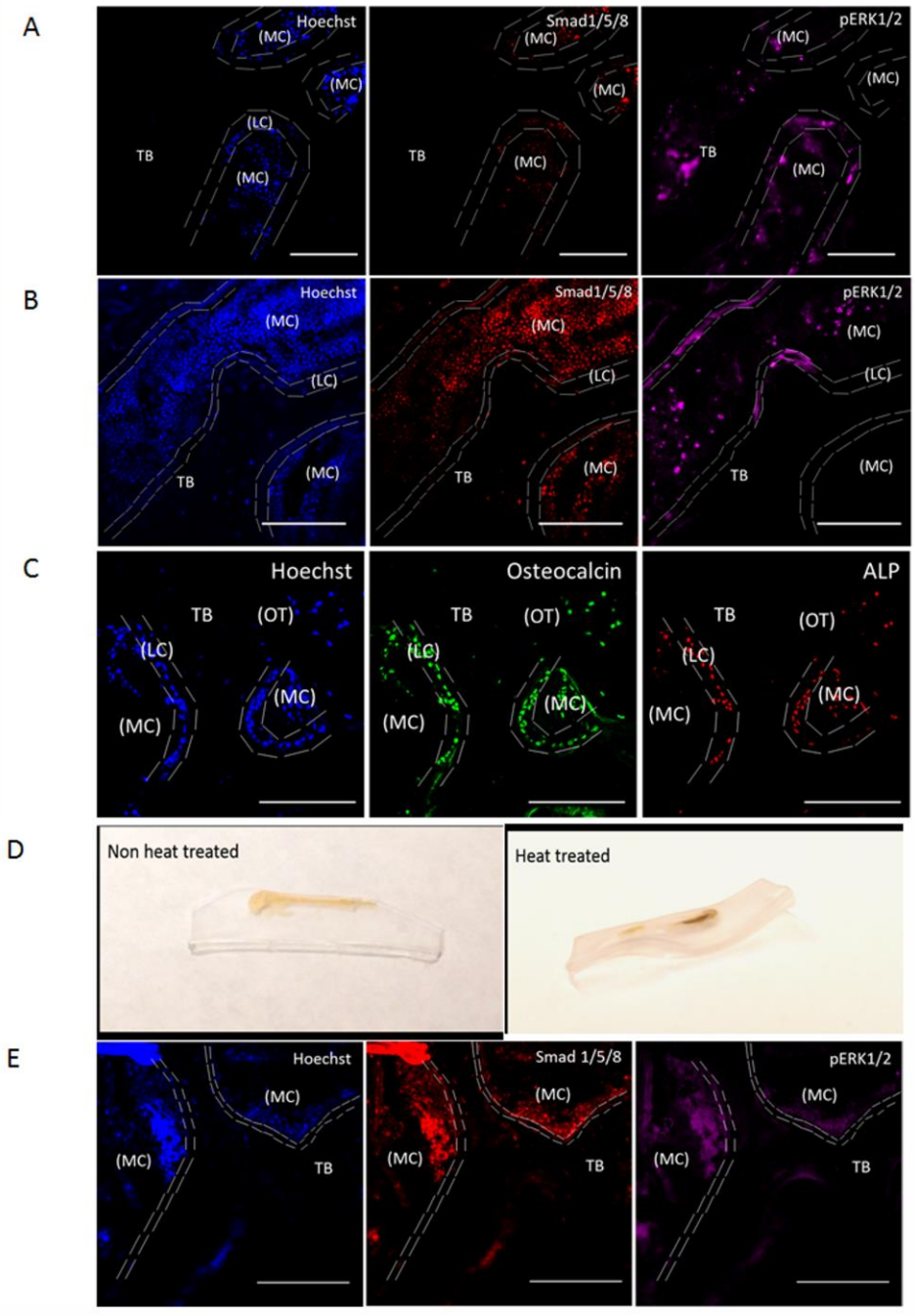
A
Hoechst
Smad1/5/8
pERK1/2
(MC)
(LC)
TB
B
C
Hoechst
Osteocalcin
ALP
(OT)
D
Non heat treated
Heat treated
E
Hoechst
Smad 1/5/8
pERK1/2

Figure 2 Testicular Hyaluronidase based antigen retrieval of MMA embedded femur slices. MMA embedded samples were immunostained for Smad 1/5/8, pERK1/2, osteocalcin and ALP. Hoechst staining was used to identify cells within the bone (blue). Heat induced antigen retrieval was used as a comparison. Sections were imaged in the cancellous or the trabecular bone (TB) of the mouse femur around the marrow cavity (MC) where the lining cells (LC) or the active osteoblasts reside alongside of osteocytes (OT). **2A)** MMA embedded samples not treated with testicular hyaluronidase imaged using TPLM. Tissue sections were stained with Hoechst (blue), regions of bone growth, and proteins associated with bone cell activity Smad 1/5/8 (red) and pERK1/2 (magenta). **2B)** MMA Samples treated with Testicular Hyaluronidase and stained as in **2A)** were imaged using TPLM **2C)** MMA samples treated with Testicular Hyaluronidase and stained for Osteocalcin (green), and ALP (red). **2D)** Heat induced antigen retrieval caused morphing of the thick MMA embedded bone sample if not mounted on to a permanent slide fixture. **2E)** MMA Samples heat treated were imaged using TPLM. Images were stained with Hoechst (blue), Smad 1/5/8 (red) and pERK1/2 (magenta). All images were taken using 20X magnification with scale bar representing 100 μM.

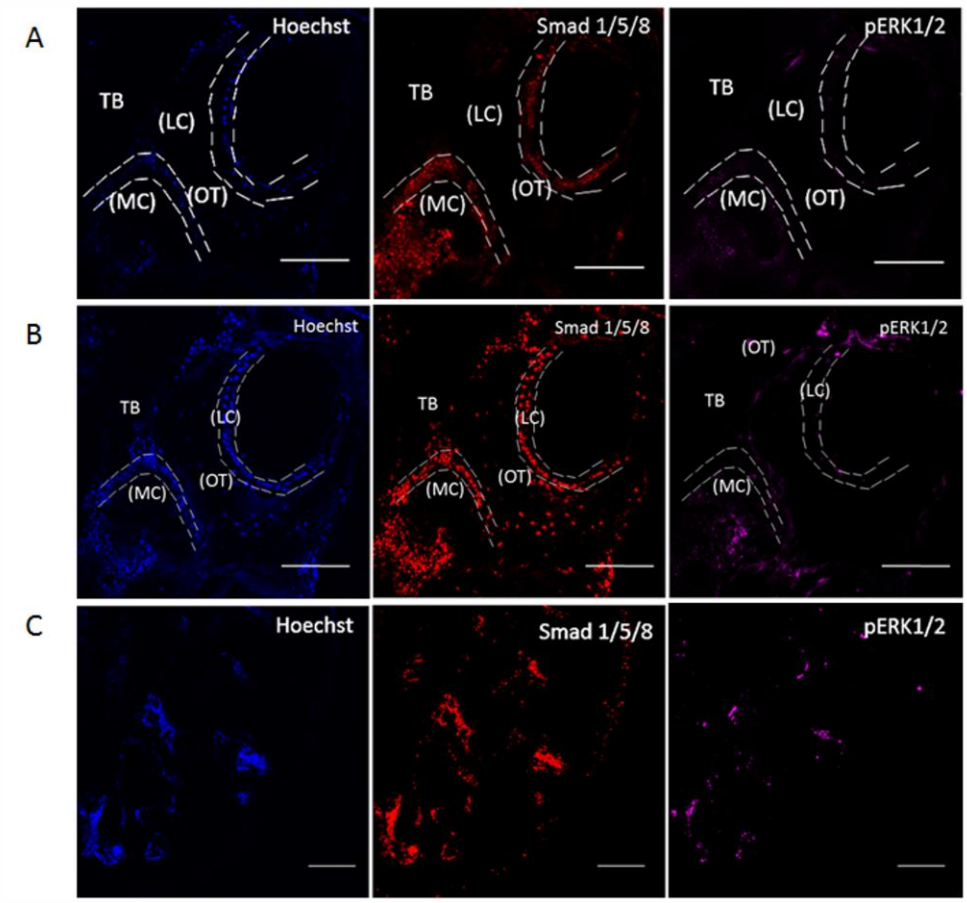

Figure 3 Two photon excitation laser microscopy imaging of MMA embedded samples. Imaging of MMA embedded samples stained with Hoechst (blue), Smad 1/5/8 (red) and pERK1/2 (magenta). **3A)** Conventional confocal setup. The collected images sow low resolution and high auto fluorescence. Images taken at 20X magnification with scale bar representing 100 μm **3B)** Two photon excitation laser microscopy imaging. Images show nuclei and labeling for proteins. Images taken at 20X magnification with scale bar representing 100 μm. **3C)** Representative tile scan image that was used obtain the entire

sample section. Sections were imaged in the cancellous or the trabecular bone (TB) of the mouse femur around marrow cavity (MC) where the lining cells (LC) or the active osteoblasts reside alongside of osteocytes (OT). Images taken at 20X magnification with scale bar representing 200 μm.

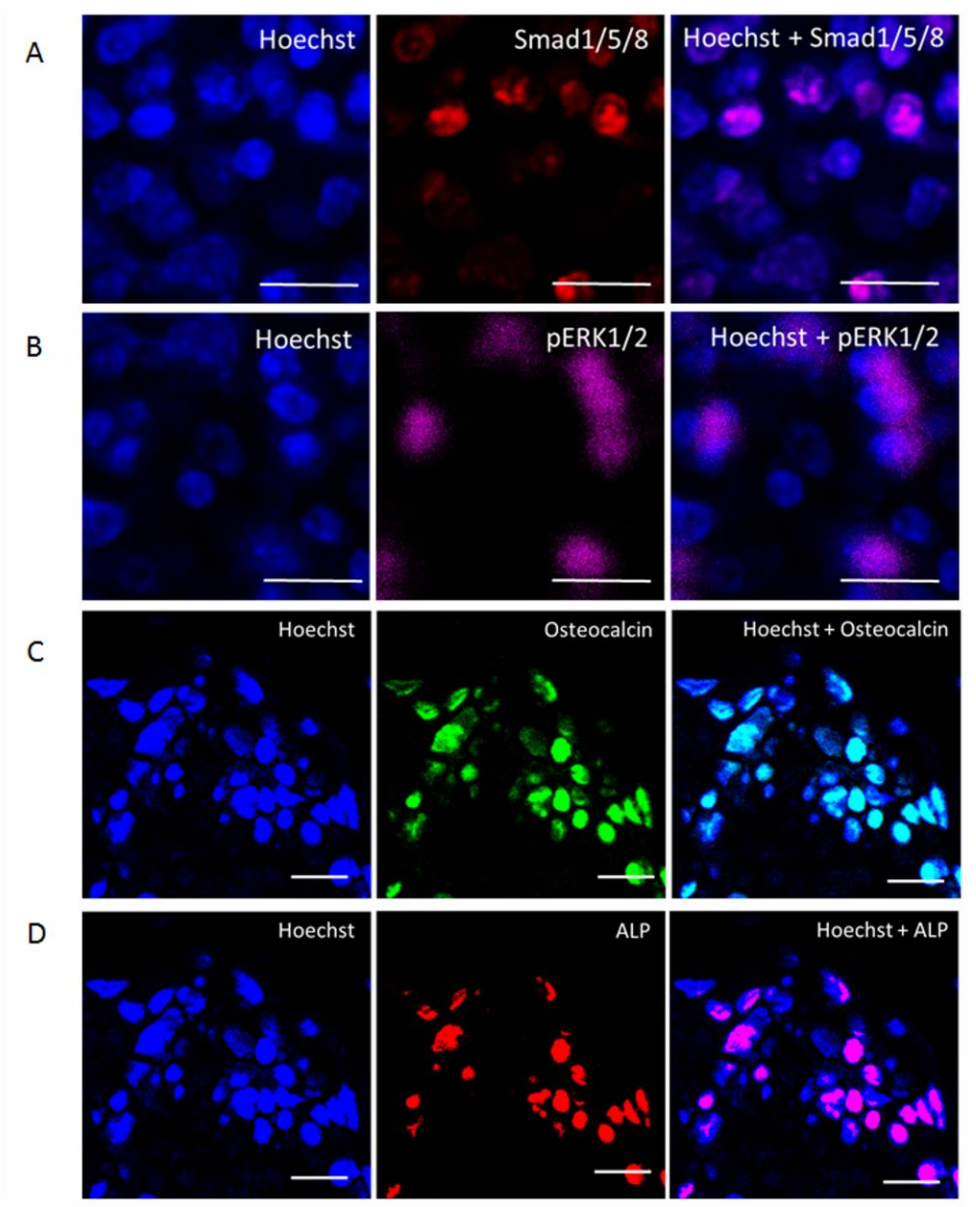

Figure 4. High resolution imaging of cells expressing Smad1,5,8, p-ERK, Osteocalcin and ALP. Magnified regions of the images was taken using 20X objective with 2X magnification at 4096X4096 pixels **4A)** Smad1/5/8 (red), Hoechst (blue) and **4B)** pERK1/2 (magenta) **4C)** Osteocalcin (green) and **4D)** ALP (red) and Hoechst. Overlay at high resolutions clearly distinguishes different expression of these proteins within different cells. Scale bar representing 10 µm.

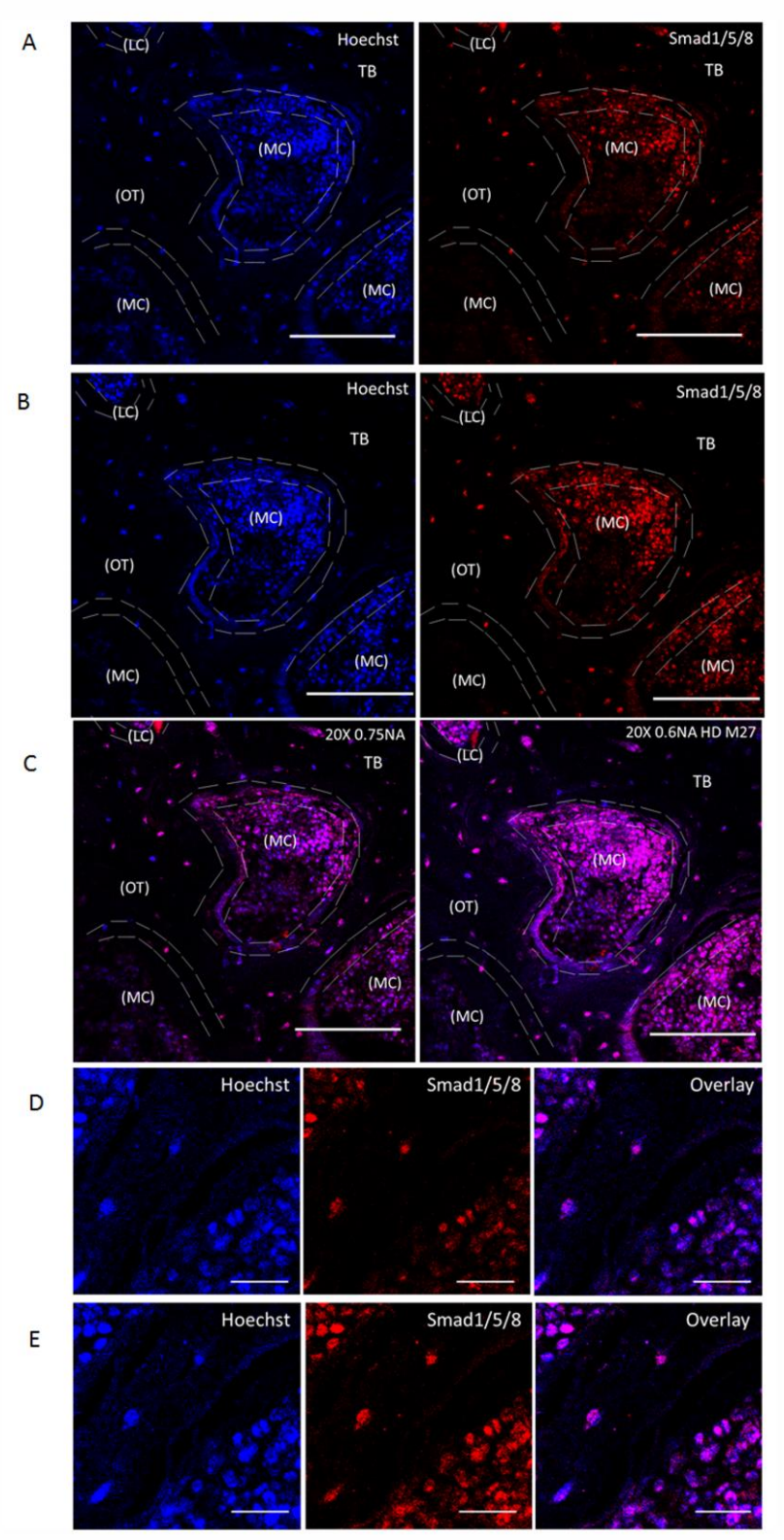
A
Hoechst
Smad1/5/8
(LC)
TB
(MC)
(OT)
B
C
20X 0.75NA
20X 0.6NA HD M27
D
Overlay
E

Figure 5. Objective differences and their impact on sample brightness. MMA embedded bone samples were TPLM imaged on an inverted microscope zeiss 780 using **5A)** 20X NA 0.75 designed to be imaged with coverslips. **5B)** 20X NA 0.6 HD M27 for samples without coverslips. The minor differences in spatial resolution is compared based on working distances of each objective. For the samples without coverslips objective 20X NA 0.6 HD M27 having working distance capability of 1.7mm suited best for the imaging providing a better field of view as shown in the **5C)** Overlay image. Sections were imaged in the cancellous or the trabecular bone (TB) of the mouse femur around marrow cavity (MC) where the lining cells (LC) or the active osteoblasts reside alongside of osteocytes (OT) labelled for smad1/5/8 (red) and hoechst (blue). Images taken at 20X magnification with scale bar representing 100 µm. High magnified images clearly distinguish objective differences in the staining of Smad (red) and hoechst (blue) with overlay in images taken using **5D)** 20X 0.75NA, and **5E)** 20X 0.6NA HD M27. Images taken at 20X magnification with scale bar representing 20 µm.

Table 1 Trouble shooting of TPLM imaging of non-decalcified testicular hyaluronidase antigen retrieved bones embedded in MMA.

Problem	**Possible Reasons**	**Solution**
Casting of MMA with bubbles as a consequence.	Moisture retention in the MMA mixture.	No moisture should be introduced to the thickened MMA solution.
Improper penetration of MMA into the sample	Improper dehydration of sample	Adequate time for alcohol changes must be given

Uneven surface planes of cut sections	Uneven sanding of tissue samples. Usage of non-diamond based wafered saws/ or without water	Use 1200 grade sand paper with water flow to sand the tissue sample. It is imperative to use even pressure throughout the sample for even sanding
Softened tissue sample	Long xylene washes of samples	Start with 1 minute to clear the surface plastic taking care not to completely clear the sample of plastic. If needed continue for 30 sec at a time to test the correct timing required for the plastic clearance
Unspecific staining of antibodies	Incorrect blocking buffer	Antibodies raised in the host tissue requires prior blocking of either Goat serum or Horse serum to impede unspecific binding. Pre-conjugation of the primary and secondary antibodies aid in staining without non-specific binding
Improper resolution of sample	Usage of wrong objective	Using proper objectives designed for tissue sample imaging with or without coverslip and matched NA for air will allow for the best resolution of the sample